Università degli Studi di Napoli

"Federico II"

DOTTORATO IN SCIENZE CHIMICHE

XXIV CICLO

SYNTHESIS AND CHARACTERIZATION OF PNA BASED MOLECULES ABLE TO INTERFERE IN GENE REGULATION

Tutore:

Dott.ssa

Stefania Galdiero

Relatore:

Ch.ma Prof.ssa

Lucia Falcigno

Candidata:

Dott.ssa

Concetta Avitabile

INDEX

ABBREVIATIONS

A	Adenine
AMO	AntimicroRNA oligonucleotide
ASO	Antisense oligonucleotide
Bhoc	Benzhydryloxycarbonyl
Bn	Benzyl
Boc	tert-Butyloxycarbonyl
C	Citosine
CD	Circular Dichroism
CPP	Cell penetrating peptide
DCM	Dichloromethane
Dde	1-(4,4-dimethyl-2,6-dioxocyclohexylidene)ethyl
DIPEA	*N*,*N*-Diisopropylethylamine
DMAP	4-Dimethylaminopyridine
DMF	*N*,*N*-Dimethylformamide
DMSO	Dimethyl sulfoxide
DNA	Deoxyribonucleic acid
EDC	*N*-(3-Dimethylaminopropyl)-*N′*-ethylcarbodiimide hydrochloride
ESI	Electrospray Ionization
Et_2O	Diethyl Ether
FACS	Flow Activated Cell Sorting
Fmoc	9-Fluorenylmethyloxycarbonyl
Fmoc-OSu	*N*-(9-Fluorenylmethoxycarbonyloxy)succinimide
G	Guanine
g^{OH}	Guanine-OH monomer

g^s	Guanine sulphate monomer
HATU	*O*-(7-Azabenzotriazol-1-yl)-*N*,*N*,*N'*,*N'*-tetramethyluronium hexafluorophosphate
HAx	Amino hexanoic acid
HBTU	*O*-(Benzotriazol-1-yl)-*N*,*N*,*N'*,*N'*-tetramethyluronium hexafluorophosphate
HOBt	1-Hydroxybenzotriazole
HPLC	High Performance Liquid Chromatography
i-Bu	Isobutyrril
LC-MS	Liquid Chromatography-Mass Spectrometry
LNA	Locked Nucleic Acid
Maldi-Tof	Matrix Assisted Laser Desorption Ionizzation-Time Of Flight
Me	Methyl
miRNA	microRNA
Mmt	Monomethoxytrityl
Mtt	4-Methyltrityl
NMM	*N*-Methylmorpholine
NMR	Nuclear Magnetic Resonance
NOESY	Nuclear Overhauser Effect Spectroscopy
NVOC	Nitroveratryloxycarbonyl
piRNA	Piwi-interacting RNA
PNA	Peptide Nucleic Acid
ppm	Part per million
qPCR	Real-Time Quantitative Polymerase Chain Reaction
RBP	RNA-binding-protein
RISC	RNA-induced silencing complex
RNA	Ribonucleic acid
RNAi	RNA interference

RNasi	Ribonuclease
Ser	L-Serine
siRNA	Small-interfering RNA
T	Timine
TBA	Tetrabutylammonium
TEA	Triethylamine
TFA	Trifluoroacetic Acid
THF	Tetrahydrofuran
TIS	Triisopropylsilane
Tm	Melting Temperature
TOCSY	Total Correlation Spectroscopy
UV	Ultraviolet Ray
Z	Benzyloxy-carbonyl

SUMMARY

The control of gene expression is a fundamental process to bring the genome to life, and it pervades most of biology, from cell proliferation and differentiation to development. It is well recognized that gene expression is regulated at several levels. Cells need to integrate intrinsic and environmental information and coordinate multiple regulatory mechanisms of gene expression to properly exert biological functions.

Mis-regulation of gene expression at any level can lead to disease. The various steps in the pathway from DNA sequence to proteins seem to be connected and coordinated with each other. Post-transcriptional control is mediated by various combinations of RNA-binding proteins (RBPs) that determine the fate of the tagged transcripts and that seem to regulate specific subsets of mRNAs.

Small interfering RNAs and microRNAs, together with protein effector complexes, can also control the degradation and translation of target transcripts;

MicroRNAs (miRNAs) are single-stranded RNAs (ssRNAs) of 19–25 nucleotides in length that are generated from endogenous hairpin-shaped transcripts[1] and they function as guide molecules in post-transcriptional gene silencing by base pairing with target mRNAs, which leads to mRNA cleavage or translational repression. There is a growing number of reports that link miRNAs to the regulation of pathways associated with human diseases such as cancer, neurological diseases and most recently also with viral and metabolic diseases.

Modified synthetic anti-miRNA oligonucleotides (AMOs) are useful tools in specifically inhibiting individual miRNAs, thereby helping to unravel the function of miRNAs and their targets. Similar to antisense-based oligonu-

cleotides (ASOs), AMOs may contribute to the prioritization of pharmaceutical targets and have the potential to eventually progress into a new class of therapeutic agents. Among these, the peptide nucleic acids (PNAs) show a great potential as therapeutic and diagnostic reagents, due to their higher affinity and specificity for complementary nucleobase sequences and to their higher resistance to enzymatic degradation than the corresponding natural nucleic acids.

PNAs are compounds that are analogous to oligonucleotides, but differ in composition. In PNAs, in fact, the deoxyribose backbone of oligonucleotide is replaced by subunits of peptide backbone, constituted by repeating units of N-(2- aminoethyl)glycine and attached to a nucleobase through a methylene carbonyl linker. As PNAs bind selectively and effectively to both DNA and RNA, they can target mRNA, miRNA or DNA, interfering in transcription and translation.

In this work PNA based molecules designed to interfere in the maturation of miRNA and gene expression were obtained.

To achieve these goals, firstly a new, efficient and inexpensive protocol to obtain PNA by Fmoc solid-phase synthesis was developed.

The new protocol involves the PNA monomer activation with HOBt and HBTU in place of HATU, a more expensive activators, and NMM in pyridine as a base, in place of DIPEA and Lutidine (standard bases). Furthermore a comparison between standard and new protocol revealed that yields using the new coupling conditions were significantly improved.

To interfere in the miRNA function PNA anti-premiR were obtained. PNA sequences targeting the "sense region" (PNA 5) and the " 5’ end region" (PNA 6) of the pre-miR210 were designed.

To improve PNA delivery in cells, conjugation to cell-penetrating peptides, such as Tat peptide, and nuclear localization signal (NLS and biNLS) peptides was carried out. Furthermore, in order to demonstrate that the de-

signed PNAs were able to bind to the pre-miRNA210 a Thiazole Orange (TO) modified PNA for fluorescence studies was obtained. Finally, with the aim to verify whether these molecules were capable of entering the cells some FITC modified PNAs for FACS experiments were synthesized too.

Fluorescence studies indicated that PNA 5 is able to hybridize efficiently with target RNA sequences, but FACS experiments revealed in a qualitative manner that a low cellular uptake limits the potentialities of designed oligomers.

A further aim of this project was the synthesis and the characterization of new modified PNA monomers. Several PNA analogues with modification on the backbone and bases have been obtained so far in the attempt to overcome solubility, uptake and aggregation issues and a recently investigated family of PNA analogues is represented by gamma Peptide Nucleic Acid (γ PNA), PNA derivatives bearing a substituent, usually corresponding to the side chain of a natural amino acid, in the gamma position of the backbone.

Several analogues have been explored so far, having methyl, hydroxymethyl, thiomethyl, aminobutyl and guanidinium groups attached and studies showed that the introduction in gamma position of a functional group leads to an improvement of PNA oligomer features, such as a high preorganization as well as a better ability to invade a mixed sequence DNA double helix.

In this work γ sulphate PNAs were investigated. Protocols for the synthesis of the four PNA monomers having the sulphate group in the gamma position of the backbone and of oligomers containing sulphate monomers were set up. The conformational preferences of the PNA monomers were investigated by NMR. Studies on the secondary structure of a polypirimidine oligomer were carried out by CD. The ability of the modified oligomer to interact with DNA, the specificity and affinity of binding were investigated by UV and CD.

Finally, the ability of the sulphate PNA to interfere with the transcription of the *ErbB2* gene on a human cell line overexpressing ErbB2 (SKBR3), by FACS and qPCR was explored.

CHAPTER 1

INTRODUCTION

1. *GENE REGULATION*

Regulation of gene expression is fundamental for the coordinate synthesis, assembly and localization of the macromolecular structures of cells[2]. This is achieved by a multi-step program that is highly interconnected and regulated at diverse levels (Figure 1).

Gene regulation can occur at three possible places in the production of an active gene product[3]. First, the transcription of the gene can be regulated. This is known as **transcriptional regulation**[4]. When the gene is transcribed and how much it is transcribed influences the amount of gene product that is produced. Second, if the gene encodes a protein, it can be regulated at the translational level. This is known as **translational regulation**. How often the mRNA is translated influences the amount of gene product that is obtained. Third, gene products can be regulated after they are completely synthesized by either **post-transcriptional** or **post-translational regulation** mechanisms[5]. Both RNA and protein can be regulated by degradation to control how much active gene product is present[6]. Both can also be subjected to modifications such as the methylation of nucleosides in rRNA, the extensive modifications made to tRNAs (over 80 modified nucleosides have been described), or the phosphorylation of response-regulator proteins[7].

These modifications can play a major role in the function of the gene product. In general, every step that is required to make an active gene product can be the focus of a regulatory event. In practice, most bacterial regulation occurs at the transcriptional level. Transcriptional regulation is thought

to be more frequent because it would be a waste to make the RNA if neither the RNA nor its encoded protein is needed.

Gene regulation starts in the nucleus, where transcription factors bind to specific DNA sequences proximal to the genes they regulate and recruit RNA polymerases for RNA synthesis. As soon as RNA precursors are formed, they get covered by a host of proteins forming ribonucleoprotein complexes[8]. Messenger RNA-binding proteins (mRBPs) associate with nascent mRNA precursors and mediate diverse RNA processing reactions including end capping, splicing, editing, end cleavage and polyadenylation. The transcripts are subsequently exported through nuclear pores to the cytoplasm where they may undergo localization to subcellular regions by complexes consisting of motor proteins and RBPs or by the signal recognition particle[9].

The transcripts assemble with translation factors and ribosomes for protein synthesis, which is controlled by global or transcript-specific mechanisms[10].

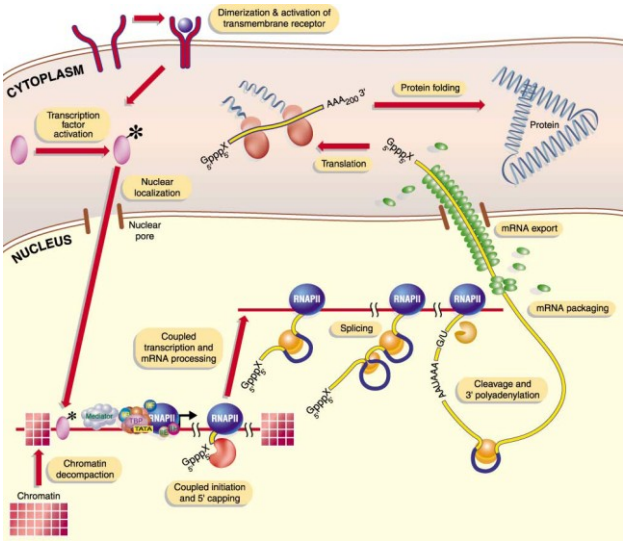

Figure 1: Gene expression is controlled at multiple steps: Transcriptional control (DNA binding proteins); Post-Transcriptional control (RNA binding proteins); Post-Translational control;

Finally, mRNAs undergo exonuclease-mediated degradation by diverse decay pathways[11]. The fate and location of proteins can be further controlled through modification of specific amino acids, cleavage by site-specific proteases and degradation through the proteasome. The majority of studies to date have focused on transcriptional control mechanisms, but the importance of post-transcriptional mechanisms in regulating gene expression in eukaryotes is becoming increasingly clear.

Post-transcriptional regulation of gene expression plays important roles in diverse cellular processes such as development, metabolism and cancer progression[6]. Whereas many classical studies explored the mechanistics and physiological impact on specific mRNA substrates, the recent development of genome-wide analysis tools enables the study of post-transcriptional gene regulation on a global scale. Importantly, these studies revealed distinct programs of RNA regulation, suggesting a complex and versatile post-transcriptional regulatory network[12]. This network is controlled by specific RNA-binding proteins and/or non-coding RNAs, which bind to specific sequence or structural elements in the RNAs and thereby regulate subsets of mRNAs that partly encode functionally related proteins.

Over the past decade, small RNAs emerged as a new class of key regulators of eukaryotic biology, helping to control cellular metabolism, growth and differentiation, to maintain genome integrity and to combat viruses and mobile genetic elements[13].

This diverse class of RNAs includes small interfering RNAs (siRNAs), microRNA (miRNAs) and PIWI-interacting RNAs (piRNAs)[14], all of which associate with multiple protein components within a complex to regulate partially or perfectly complementary transcripts[15]. The common feature of RNAi and all related small-RNA-mediated silencing pathways is the association of a small silencing RNA (also known as a guide RNA in this context) with a protein of the Argonaute family. The resultant protein–RNA complex forms

the minimal core of the effector complex known as the RISC. Within the RISC, the small RNA functions as a sequence-specific guide that recruits an Argonaute protein to complementary target transcripts through base-pairing interactions[16]. The target transcripts, typically mRNAs, are then either cleaved or prevented from being translated by ribosomes, leading to their degradation. Throughout evolution, the Argonaute family has diverged into specialized clades (or subfamilies) that recognize different small RNA types and confer the specific effects of the various small-RNA silencing pathways.

Both siRNAs and miRNAs associate with members of the AGO clade of Argonaute proteins, whereas piRNAs bind to those of the PIWI clade. In classic RNAi, which is elicited by siRNAs, Argonaute proteins silence targeted mRNAs by catalysing their endo nucleolytic cleavage, a process known as slicing. The PIWI clade of the Argonaute protein family is thought to use slicing in piRNA-mediated silencing of mobile genetic elements in the germ line[17] (Figure 2).

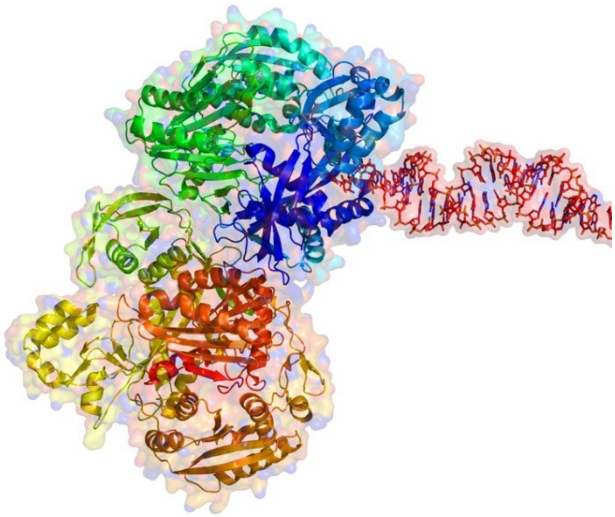

Figure 2. Double-stranded RNA (siRNA) entering the Argonaute Complex.

To function as an effector of small-RNA-mediated silencing, the Argonaute protein must bind to the guide RNA strand, eject the non-guide (passenger) strand of the siRNA or miRNA–miRNA* duplex (where miRNA* is the passenger strand) during loading, and subsequently recognize the target RNA.

1.1. MICRORNAS

MicroRNAs are a class of 20-25 nucleotide-long non coding RNAs that modulate gene expression through canonical base pairing between the seed sequence of miRNA (nucleotides 2-8- at its 5' end) and its complementary seed match sequence (which is present in the 3' UTR of target mRNAs)[18].
miRNAs have a peculiar biogenesis: First, they are transcribed as primary (pri-miRNAs) by RNA polymerase II. Each pri-miRNA contains one or more hairpin structures that is recognized and processed by the microprocessor complex, which consists of the RNase III type endonuclease Drosha and its partner, DGCR8 (Figure 3) .

The microprocessor complex generates a 70-nucleotide stem loop known as the precursor miRNA (pre-miRNA), which is actively exported to the cytoplasm by exportin 5. In the cytoplasm, the pre-miRNA is recognized by Dicer, another RNase III type endonuclease, and TAR RNA-binding protein (TRBP; also known as TARBP2). Dicer cleaves this precursor, generating a 20-nucleotide mature miRNA duplex[19]. Generally, only one strand is selected as the biologically active mature miRNA and the other strand is degraded.

The mature miRNA is loaded into the RNA-induced silencing complex (RISC), which contains Argonaute (Ago) proteins and the single-stranded miRNA[20].

Mature miRNA allows the RISC to recognize target mRNAs through partial sequence complementarity with its target. In particular, perfect base pairing

between the seed sequence of the miRNA (from the second to the eighth nucleotide) and the seed match sequences in the mRNA 3′ UTR is crucial[21].

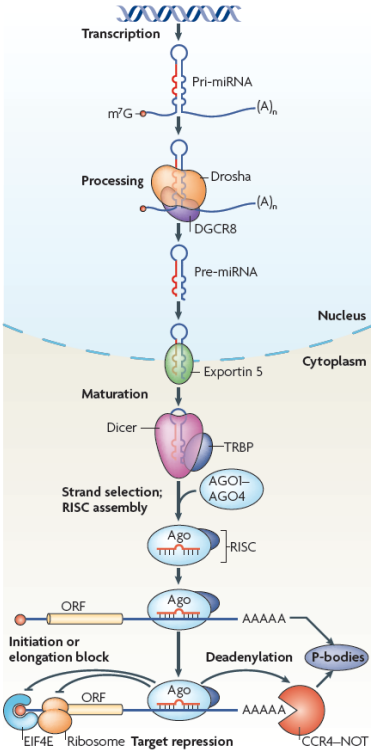

Figure 3: miRNAs biogenesis and mechanisms of action

The RISC can inhibit the expression of the target mRNA through two main mechanisms that have several variations: removal of the polyA tail (deadenylation) by fostering the activity of deadenylases (such as CCR4–NOT), followed by mRNA degradation and blockade of translation at the initiation step or at the elongation;

Therefore RISCs use the small RNAs as guides for the sequence-specific silencing of messenger RNAs that contain complementary sequence through inducing the degradation of the mRNAs or repressing their translation. In addition, in certain organisms, a specialized nuclear Argonaute-containing complex, known as the RNA-induced transcriptional silencing complex

(RITS), mediates transcriptional gene silencing by inducing heterochromatin formation[14].

The first glimpse into the new world of small RNAs came with seminal papers from Ambros, Ruvkun and colleagues: they reported that *lin-4* and *let-7*, the first miRNA genes identified, control developmental timing in nematodes by modulating the expression of other genes at the post-transcriptional level[22].

The first discovery providing evidence that gene regulation mediated by small RNAs of 22-nt may exist in species beyond worms came from Pasquinelli et al.[23]. They found that let-7 RNA expression can be detected in a wide range of animal species, including vertebrate, ascidians, hemichordate, mollusc, annelid and arthropod. Other 3 members of the let-7 family were identified in *C. elegans* and at least 15 in human, but only one in *Drosophila*[24]. This extensive conservation strongly indicated a more general role of small RNAs in developmental regulation, as supported by the recent characterization of miRNA functions in metazoan organisms.

The second discovery, suggesting the widespread existence of miRNAs was the finding that small interfering RNAs of about 22nt lenght (siRNAs) are central to RNA interference (RNAi)[25].

Generally, each miRNA is thought to regulate multiple genes, hundreds of miRNA genes were predicted (Lim et al. 2003b) and several hundreds have been already cloned and sequenced from *C.elegans, Drosophila, Arabidopsis,* mice and human[26]. The large number of miRNAs and homologous sequences of many miRNAs among organisms suggest that these RNAs might constitute an abundant and conserved component of the gene regulatory machinery[27].

Several studies have indicated that the 5' end of the miRNA is crucial for the stability and proper loading of the miRNA into the miRISC complex, and this end is also important for biological function.

Recent studies have revealed that miRNAs have key roles in diverse regulatory pathways, including control of developmental timing, haematopoietic cell differentiation, apoptosis, cell proliferation and organ development[28].

MicroiRNAs and their targets seem to form complex regulatory networks. For example, a single miRNA can bind to and regulate many different mRNA targets and, conversely, several different miRNAs can bind to and cooperatively control a single mRNA target.

Recent work by the Bartel and Burge laboratories predicted that over one third of all human genes are targeted by miRNAs.

Consequently, the unique combination of miRNAs that are expressed in each cell type might affect or 'dampen' the utilization of thousands of mRNAs[1].

Because miRNAs potentially have a broad influence over several diverse genetic pathways, the deletion or misexpression of these small RNAs is likely to be pleotropic and contribute to disease, including cancer.

They function as post-transcriptional repressors of their target genes when bound to the specific sites in the 3′ untranslated region (UTR) of the target mRNA[29]. To date, only a small number of miRNAs are known for their biological functions. For example, *bantam* RNA from *Drosophila melanogaster* suppresses apoptosis and stimulates cell proliferation. Being expressed in a temporal and tissue-specific manner, *bantam* RNA regulates tissue formation during development. Another nematode miRNA, *lsy-6*RNA, was identified in a genetic screen for left–right asymmetry of neuronal chemoreceptor expression. *Lsy-6*RNA targets *cog-1*, which encodes a transcription factor[30].

In mammals, *miR-181* is involved in the control of haematopoiesis through as-yet-unknown targets. More recently, *miR-196* miRNAs were shown to repress the expression of the *HoxB8*, which encodes a transcription factor that is important in developmental regulation[31]; miR-196 family

RNAs are the first examples of animal miRNAs that cause target mRNA cleavage rather than translational repression (Table 1).

miRNA	Function	Known targets	Species
Lin-4	Developmental timing	*lin-14, lin-28*	*Ce*
Let-7	Developmental timing	*lin-41, hbl-1*	*Ce*
Lsy-6	Neuronal patterning	*cog-1*	*Ce*
miR-273	Neuronal patterning	*die-1*	*Ce*
bantam	Cell death, proliferation	*hid*	*Dm*
miR-14	Cell death, fat storage	Caspase?	*Dm*
miR-181	Haematopoiesis	?	*Mm*
miR-196	Devevelopment	*HoxB8, HoxC8, HoxD8, HoxA7*	*Mm*
miR-143	Adipocyte differentiation	?	*Hs*
miR-375	Insulin secretation	Myotrophin	*Mm*

Table 1: microRNAs functions

Another *D. melanogaster* miRNA, miR-14, is a strong suppressor of apoptosis[32]. In addition, miR-14 also seems to have unrelated functions in the *D. melanogaster* stress-response pathway and in regulating fat metabolism. Other characterized miRNAs have essential functions during development and direct the proper differentiation of cells into various tissues. Examples include miR-273, which is involved in patterning the *C. elegans* nervous system[33]; miR-430 in *Danio rerio* brain development; miR-375 in mammalian pancreatic islet-cell development and the regulation of insulin secretion[34]; miR-143 during mammalian adipocyte differentiation[35]; miR-196 in mammalian limb patterning[36]; and the miR-1 genes during mammalian heart development[37].

In small-sized viral genomes, miRNAs offer an efficient means to specifically inactivate host cell defense factors compared to virally encoded proteins. Several recent reports describe miRNAs cloned from a variety of viruses such as herpes viruses and human immunodeficiency virus 1 (HIV-

1)[38]. Pfeffer et al. identified five miRNAs in Epstein-Barr virus (EBV) and nine miRNAs encoded by human cytomegalovirus (HCMV)[39], while, simultaneously, Cai et al. found eleven miRNAs from Kaposi's sarcoma-associated virus (KSHV)[40]. Finally, recent evidence indicates that miRNAs might also function as tumour suppressors and oncogenes (Figure 4).

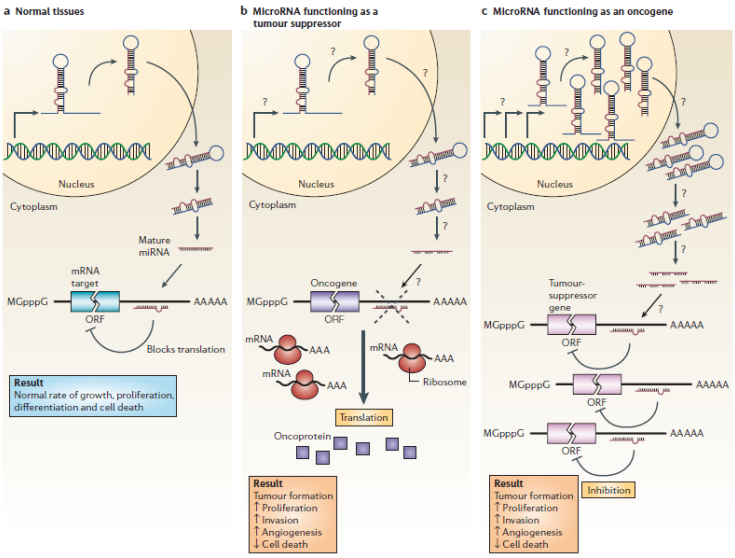

Figure 4: MicroRNAs can function as tumour suppressors or oncogenes.

The first indication that miRNAs could function as tumour suppressors came from a report by Calin *et al.* that showed that patients who were diagnosed with a common form of adult leukaemia, B-cell chronic lymphocytic leukemia (CLL), often have deletions or downregulation of two clustered miRNA genes, *mir-15a* and *mir-16-1*[41]. A recent report by Cimmino *et al.* showed that *miR-15a* and *miR-16-1* negatively regulate *BCL2*, which is an anti-apoptotic gene that is often overexpressed in many types of human cancers, including leukaemias and lymphomas[42].

Therefore, it is thought that the deletion or downregulation of *mir-15a* and *mir-16-1* results in increased expression of BCL2, promoting leukaemogeneis and lymphomagenesis in haematopoietic cells.

Additional studies have shown a strong correlation between abrogated expression of miRNAs and oncogenesis. For example, mature miRNA levels of miR-143 and miR-145 are significantly reduced in colorectal tumours[43]. Another report demonstrated that miR-21 is upregulated in glioblastoma (Table 2).

miRNA	Gene loci	Cancer association	Function
miR-15a, miR-16-1	Chromosome 13q14	Frequently deleted or downregulatedin B-cell chronic lymphocytic leukemia	TS
miR-143, miR-145	Chromosome Sq32-33	Dowregulated in breast, prostate, cervical and lymphoid cancer cell lines	TS
miR-21	Chromosome 17q23.2	Anti-apoptotic factor: upregulated in glioblastomas and breast cancer	OG
let-7 family members	Multiple loci	Negatively regulate the Ras oncogenes	TS
miR-142	Chromosome 17q22	Associate to Leukemia	N/A
BIC/miR-155	Chromosome 21q21	Upregulated in breast cancer	OG
miR-17-19b cluster	Chromosome 13q31-32	Found in Hepatocellular carcinoma	TS/OG

Table 2: MicroRNAs that are associated with human cancers

Therefore, in a global sense, miRNAs might function to drive cells into a more differentiated state, and the expression profiles of miRNAs in tumours compared with normal tissues might represent the degree of differentiation in those cells. These studies implied that abnormalities in miRNA expression might directly result in the de-differentiation of cells, allowing tumour formation to occur.

1.1.1. ANTAGOMIR

With the identification of a vast number of miRNAs, each carrying a long list of putative targets, the challenge is now to understand their biological function. Much of the progress in understanding miRNA function to date derives from inhibition studies with antisense oligonucletides (ASOs)[44]. The importance of such reagents also is that microRNA targeting represents a novel and undeveloped approach toward potential therapeutic applications. Where a deletion or a mutation is present in the miRNA gene itself, a therapeutic approach could entail exogenous delivery of corrective synthetic miRNAs in the form of (siRNA-like) dsRNA. This principle was first demonstrated in vitro by Zeng et al., who showed in a model system that partially complementary siRNAs can inhibit target mRNAs by miRNA-like translational inhibition[45].

Oligonucletides (ON) or analogs that inhibit miRNAs were called *antagomir* and they function essentially by a steric block, RNase H-independent and RISC-independent, antisense mechanism through complementary binding to the microRNA sequence (Figure 5).

The cellular outcome of such binding is still unclear, with reports arguing either in favor of a mechanism based on simple sequestration by stoichiometric complex formation between the mature microRNA and the ON inhibitor[46], or in favor of a yet unknown mechanism by which complex formation leads to degradation of the target microRNA[47]. The result of these mechanisms is marked by the inhibition of microRNA-mRNA complex and consequently by the interference of the gene transcription process.

Over the past decade, however, microRNAs inhibition by ON has not proven to be a robust or generally reliable technology. In fact, natural oligonucleotides have some unfavorable features:

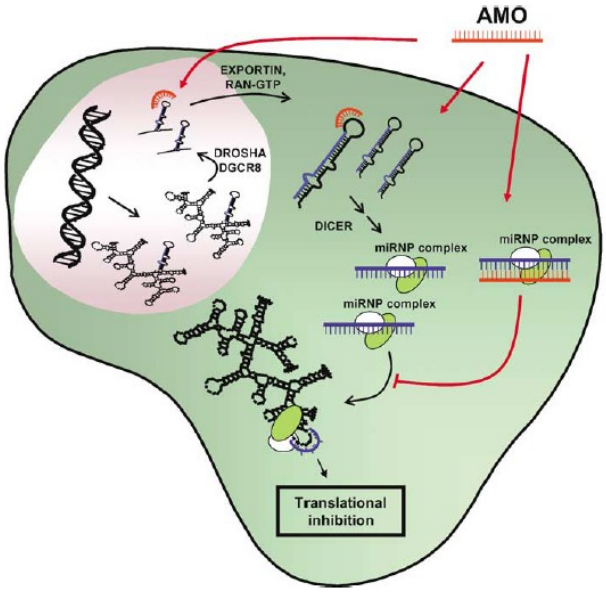

Figure 5: Interference with the miRNA pathway using synthetic oligonucleotides. Inhibition of miRNA activity may be achieved by introducing anti-miRNA oligonucleotides (AMOs) fully complementary to the pri-miRNA, the pre-miRNA or the mature miRNA.

First of all, as they are, they cannot penetrate spontaneously into the cell (it is usually necessary to employ a commercially available cationic lipid or other transfection reagent) , and even if they were to succeed, they would be immediately subjected to enzymatic cleavage of the endonuclease and exonuclease.

Furthermore, it has been difficult to identify oligonucleotides that act as potent inhibitors of miRNAs in particular and of gene expression in general because of the difficulties in predicting the secondary structures of RNA. Due to the secondary structures of RNA there is a limited number of freely accessible regions, therefore a high number of oligomers need to be screened to identify those (or the one) which efficiently work[48].

For these reasons the need for antisense oligomers that are more potent and more selective has been widely recognized and has led to the development of chemical modifications to improve binding and selectivity (Figure 6).

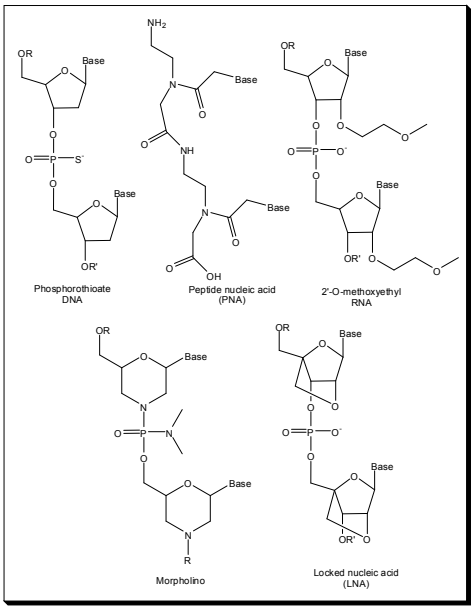

Figure 6: Nucleic acid analogues (phosphorothioate DNA, 2'-*O*-methoxy-ethyl RNA, morpholino, PNA and LNA).

The introduction of **phosphorothioate linkages** (PS), for example, profoundly influences the proprieties of antisense oligonucleotides. PS linkage not only enhance the nuclease resistance but also improve pharmacokinetic properties by promoting binding to serum proteins, greatly increasing in vivo half-life, thereby facilitating the development of oligonucleotide drugs[49]. Another strategy for improving the efficiency of antisense oligonucleotides is to increase the difference between their affinity for their intended targets and their propensity to bind to nontargeted molecules.

The **2'-*O*-methyl-group** (OMe) is one of the oldest, simplest and most often used modifications to oligonucleotides. The methyl group decreases the susceptibility to nuclease degradation, and improves binding affinity to RNA compared to unmodified sequences. Fully-modified OMe oligonucleotides have been used to correct aberrant exon splicing in cells[50], and mixed backbone OMe/DNA hybrid antisense oligonucleotides are also being pursued in clinical studies. Hutvàgner et al. successfully demonstrated inhibition of let-

7 function in HeLa cells, as well as C. elegans larvae, using 31-mer OMe-AMOs[51].

2'-*O*-Methoxyethyl (MOE)-modified oligonucleotides have higher affinity and specificity to RNA than their OMe-analogs[52]. Concerning their application in miRNA research, Esau et al. transfected separately MOE-AMOs targeting 86 human miRNA into cultured human preadipocytes to address the role of miRNAs in adipocyte differentiation. By following gene expression profiles of five marker genes, they found miR-143 to be involved in this process through regulation of ERK5 protein levels. Treatment of adipocytes with a MOE AMO complementary to miR-143 effectively inhibited the differentiation process, whereas negative controls were inactive.

Locked nucleic acid (LNA)-modified oligonucleotides are distinctive 2'-*O*-modified RNA in which the 2'-*O*-oxygen is bridged to the 4'-*O*-position via a methylene linker to form a rigid bicycle, locked into a C3'-endo (RNA) sugar conformation. The LNA modification leads to the thermodynamically strongest duplex formation with complementary RNA known and consequently, a biological activity is often attained with very short LNA oligomers. Furthermore, LNAs display excellent mismatch discrimination, resistance to enzymes and they show a serum decay and a tissue distribution similar to that of phosphorothioate oligonucleotides[53].

Mixed LNA/DNA AMOs potently abolished miR-32 function in PFV-1 infected HeLa cells and led to the accumulation of viral mRNA, resulting in increased production of viral progeny[54]. Recently, Chan et al. have successfully applied 2'-*O*-methyl- and DNA/LNA-mixed oligonucleotides to specifically knockdown miR-21 in order to investigate the potential contribution of this miRNA in the regulation of apoptosis-associated genes in glioblastoma cell lines[46].

Synthetic ONs with electrically neutral backbones have also shown great promise as steric block antisense agents. For example phosphorodiamidate morpholino oligonucletides (PMOs) or their conjugates with a cell-penetrating peptide (CPP) have been applied very effectively for inhibition of RNA function by blocking mRNA translation[55], redirection of splicing[56] and more recently as microRNA antagomiR[57]. Due to the neutral backbone, morpholino oligomers are less likely to form undesired interactions with cellular proteins, especially when used at high concentration. Recent reports indicate that morpholino oligonucleotides allow a selective control of gene expression; for example, MOs microinjected into a zebrafish, sea urchin or xenopus embryos block gene expression and exert effects during the early stages of development[57].

Other synthetic oligonucleotides are **Peptide Nucleic Acids**, to which the next section is dedicated, as they have been the focus of these studies[58]. For inhibition of gene expressions they appear to be more effective than other antisense molecules, because of their neutral backbone, that allow the molecule to invade local RNA secondary structures more efficiently, making accessibility less of an obstacle than it is for other types of oligomer.

Recently, studies described in literature have proposed an alternative strategy for micro-RNAs inhibition. Such method involves targeting of miRNA precursors (pre-miRNA) using synthetic oligonucleotides or analogs with the following features[59]:

1) High binding affinity and binding specificity for RNA targets;
2) Complementary sequences to "sense" strand of pre-miR;
3) Excellent capacity to stably hybridize their targets;

Thus, the maturation of microRNAs and therefore the processing by nucleases are inhibited and the result of this leads to a net reduction of miRNAs in the cell[60].

It has been reported that single nucleotide polymorphism (SNPs) or mutation located in miRNAs regions might change the processing of miRNA as well as alter the target binding affinity and specificity[61]. Hoffman et al. reported that the risky *miR-196a2-C* allele led to more efficient processing of the miRNA precursor to its mature form as well as enhanced capacity to regulate target genes[62].

Several studies have reported that the sequence variations in pre-miRNA may affect the maturation process of miRNAs and binding activity to their target mRNAs. Jazdzewski et al. proposed that decreasing pri-miR-*146*a nuclear processing efficiency also mature miRNA production is reduced and this resulted in less efficient inhibition of target gene like *TRAF6, IRAK1* and *PTC1*[63].

Evidence suggests that miRNA expression may be regulated at the level of maturation. Some miRNAs in *D. melanogaster* appear to be processed inefficiently at early stages of embryonic development[64]. In the sea urchin *Strongylocentrotus purpuratus*, *Let-7* transcripts of about 100 nt are expressed throughout embryonic development, although mature *Let-7* appears to be only at a later stage[23].

In conclusion the regulation of miRNA expression may occur at multiple levels including the two processing steps and the nuclear export step.

1.2. PEPTIDE NUCLEIC ACID

Peptide nucleic acids (PNA) originated from efforts during the 1980 in organic chemist Prof. Ole Buchardt's laboratory in Copenhagen together with biochemist Peter Nielsen to develop new nucleic acid sequence-specific reagents. PNA are synthetic analogues of DNA and RNA, in which the naturally occurring sugar-phosphate backbone has been replaced by N-(2 -aminoethyl)-glycine units. A methylene carbonyl linker connects natural as well as unusual (in some cases) nucleotide bases to this backbone at the amino nitrogens[65] (Figure 7).

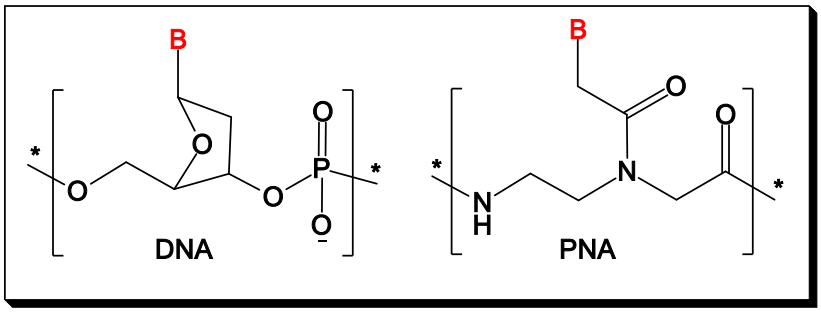

Figure 7 Chemical structure of PNA (right) and of DNA (left)

This simple and yet entirely new synthetic molecule has an interesting and non prototype chemistry. PNAs are non-ionic, achiral molecules and are not susceptible to hydrolytic (enzymatic) cleavage. Despite all these variations from natural nucleic acids, PNA is still capable of sequence- specific binding to DNA as well as RNA, obeying the Watson-Crick hydrogen bonding rules. Usually PNA is represented as a peptide, with the N-terminus side to the left (or upward) and the C-terminus side to the right (or down) and unlike DNA and RNA, PNA recognizes and binds complementary strands in both parallel and antiparallel orientations (Figure 8). In the antiparallel hybridization PNA's N-terminus binds to DNA's 3'end, while its C-terminus hy-

bridize to DNA's 5'end. In contrast, in the parallel hybridization PNA's N-terminus binds to DNA's 5'end, while its C-terminus hybridize to DNA's 3'end.

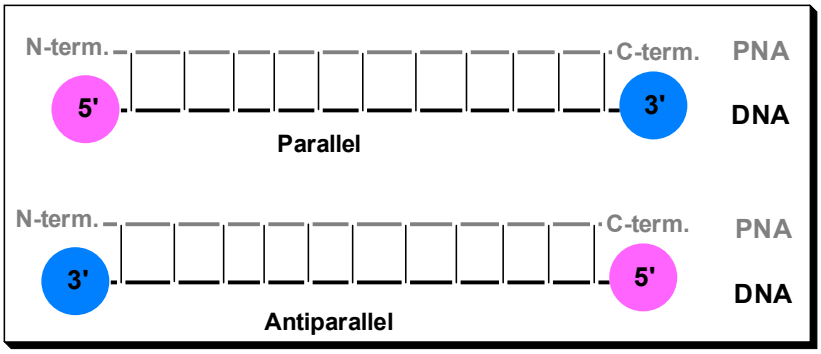

Figure 8: Parallel and anti parallel orientation of PNA:DNA duplexes

However, the antiparallel orientation illustrated in Figure 9 was found to be more stable. Although the PNA's chemical structure is totally different from that of natural nucleic acids, hybridization properties of PNAs are not only preserved, but improved.

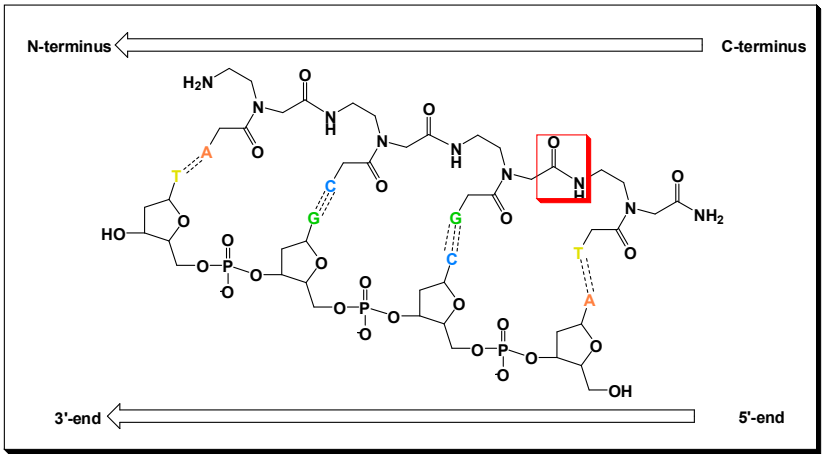

Figure 9: Preferred orientation of PNA:DNA duplexes

In fact, the uncharged nature of the PNA backbone is an important feature that renders the binding affinity between PNA/DNA strand much stronger

than that between DNA/DNA strands, just because of the absence of electrostatic repulsion.

The uncharged nature of PNA is responsible for an enhanced thermal stability of PNA–DNA duplexes compared with the DNA–DNA equivalents[66]. The neutral amide backbone also enables PNA to hybridize to DNA-molecules in low-salt conditions because no positive ions are necessary for counteracting the interstrand repulsion that hampers duplex formation between two negatively charged nucleic acids. Consequently, the abundance and stability of intramolecular folding structures in the DNA or RNA analytes are significantly reduced, making the molecules more accessible to complementary PNA oligomers.

Furthermore, PNA is stable across a wide range of temperatures and pHs, unlike DNA, which depurinates at acidic conditions[67]. However, under strong alkaline conditions (pH >11), a rearrangement of the PNA molecules might occur[68]. Additionally, PNA is resistant to nucleases and proteases.

A strong binding affinity together with the higher sequence specificity of PNA results in a superior activity of antisense PNAs compared with some oligonucleotide derivatives, such as morpholino and 2'-*O*-methoxyethyl modified derivatives.

Nevertheless, similar to regular oligonucleotides, the equilibrium mismatch discriminative ability of mixed-base PNAs rapidly declines with increasing length PNA oligomers because, in this case, sequence specificity also anticorrelates with an increase in affinity. It is worth noting that 8–15mer PNA probes carrying all four nucleobases show good selectivity for single-stranded DNA targets during PNA-based affinity electrophoresis and on PNA microarrays, whereas longer, 16mer mixed-base PNAs exhibit some problems with sequence specificity (15mer probes are required for targeting unique sites in entire genomes).

1.3. PNA: APPLICATIONS

Because of their high thermal stability and resistance to proteases and nucleases enzymes, PNA are ideal candidates for the artificial modulation of gene expression and currently they are used not only as potential therapeutic agents, but also as powerful tools in molecular biology and in diagnostics.

1.3.1. THERAPEUTIC APPLICATIONS

Peptide nucleic acids have promise as candidates for gene therapeutic drugs design.

In literature it was reported that the action of PNA on gene expression can occur through different mechanism: antigene, antisense and decoy (Figure 10).

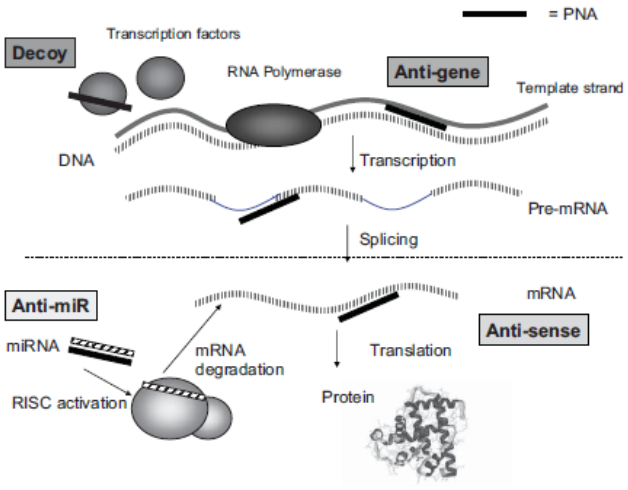

Figure 10: Different strategies for gene regulation using PNAs: antisense, blocking translation from mRNA into protein or regulating splicing of pre-mRNA; anti-gene, blocking transcription from DNA to mRNA; decoy, scavenging transcription factors; anti-miR, preventing micro- RNA activity.

- *Antisense strategy*

An antisense oligonucleotide binds specifically a region of mRNA through Watson-Crick base pairing, disrupting the translation in the corresponding protein. The mechanism used by ON to produce an antisense action has not yet been unequivocally defined, and data in literature show that the interference could be ascribed to two different mechanisms.

The first mechanism provides that the high binding affinity of ON with RNA target blocks the translation process because of steric hindrance. Therefore the ON/RNA complex would prevent the RNA interaction with ribosomes required in protein synthesis.

The second and most accredited antisense mechanism assumes the activation of an enzyme, Ribonuclease H, which specifically degrades only the mRNA strand of the ON/RNA duplex.

PNAs are a class of modified oligonucleotides that are not able to stimulate Ribonuclease H when they form a complex with RNA target[44]. Normally, the peptide nucleic acid antisense effect is based on the steric blocking of either RNA processing, transport into cytoplasm, or translation.

It has been concluded from the results of *in vitro* translation experiments involving rabbit reticulocyte lysates that both duplex- (mixed sequence) and triplex-forming (pyrimidine-rich) PNAs are capable of inhibiting translation at targets overlapping the AUG start codon. Triplex-forming PNAs are able to hinder the translation machinery at targets in the coding region of mRNA. However, translation elongation arrest requires a (PNA)–RNA triplex and thus needs a homopurine target of 10–15 bases. In contrast, duplex-forming PNAs are incapable of this.

Triplex-forming PNAs can inhibit translation at initiation codon targets and ribosome elongation at codon region targets.

It has been reported that antisense PNAs alter the pre-miRNA splicing of the murine interleukin receptor IL-5R, thus resulting potentially useful in inflamatory deseases's treatment such as eosinophilic syndromes[69].
Mologni et al. showed that antisense PNA directed against the gene of the retinoic acid receptor (RAR) carried out a 90% inhibition of the target gene's expression[70].

M.J. Gait et al. and others have shown that PNAs, especially when conjugated to CPPs, have high efficiency in many RNA targeting applications, for example in inhibition of bacterial mRNA translation, inhibition of HIV-1 Tat-dependent trans-activation and RNA reverse transcription and as splicing redirection agents[71].

PNA has also been used to inhibit gene expression in vivo, thus making possible their use as antibiotics[72].

- *Antigene strategy*

For what concerns the antigene strategies for laboratory experimentation, the gold standard is the gene knockout achieved by homologous recombination, whereas an alternative option is based on the use of synthetic oligodeoxynucleotides capable of hybridizing with double-stranded DNA to form a triple-stranded molecule. In this case the gene is not altered but its transcription is inhibited either by preventing unwinding of the duplex or by preventing the binding of transcription factors to the promoter of the gene.
Peptide nucleic acids are capable of arresting transcriptional processes by virtue of their ability to form a stable triplex structure or a strand-invaded or strand displacement complex with DNA (Figure 11)[73].

Such complexes can create a structural hindrance to block the stable function of RNA polymerase and thus are capable of working as antigene agents.

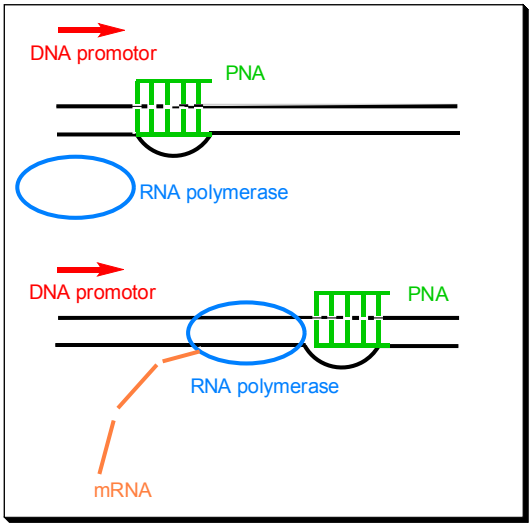

Figure 11: Transcription inhibition through triple-helix formation.

Transcriptional inhibition is accomplished by homopyrimidine PNAs that form invasion triplexes either at the promoter or the coding region of the gene. Evidence from *in vitro* studies supports the idea that such complexes are indeed capable of affecting the process of transcription involving both prokaryotic and eukaryotic RNA polymerases. PNA targeting the promoter region can form a stable PNA–DNA complex that restricts the DNA access of the corresponding polymerase. PNA strand displacement complexes, located far downstream from the promoter, can also efficiently block polymerase progression and transcription elongation and thereby produce truncated RNA transcripts;

Therefore it can be deduced that the PNA antigene application is restricted to the poly-purine parts of genome.

The PNA_2/DNA triplex arrests transcription *in vitro* and is capable of acting as an antigene agent. But one of the major obstacles to applying PNA as an antigene agent is that the strand invasion or the formation of strand displacement complex is rather slow at physiological salt concentrations.

Several modifications of PNA have shown improvement in terms of binding. Modifications of PNA by chemically linking the ends of the Watson-Crick and

Hoogsteen PNA strands to each other, introducing pH-independent pseudoisocytosines into the Hoogsteen strand, incorporating intercalators , or positively charged lysine residues) in PNA strand can drastically increase the association rates with dsDNA.

Using conjugation with a nuclear localization signal, a PNA directed against c-myc gene has been vehicled into the nucleus and an antigenic effect was observed[74]. It has also been shown that antigen PNAs directed against N-myc DNA can cause dramatic effect on cell proliferation of human tumor cells of neuroblastoma.

- *Decoy strategy:*

Transcription factors recognize exogenous oligonucleotide as target and bind to it, resulting in inability to reach the real DNA target. Few studies proved the success of PNA as decoy[75]. In fact PNA/PNA duplex or PNA/DNA duplex are not recognized by transcription factors because of their structural differences with the natural duplex.

To overcome the problem, the so-called DNA-PNA chimeras (PNA-DNA hybrid sequences linked covalently to each other) have demonstrated to be useful tools. In this case the PNA acts as a recognition sequence and the DNA acts as a substrate for proteins that interact with DNA (nucleases, transcription factors).

1.4. PNA DELIVERY

One of the most important problems about the use of PNA in therapy is related to their low uptake of these molecules in cells.

Because of the absence of charged groups in the backbone, PNAs have low solubility and strong tendency to aggregate. It has been observed that the solubility decreases with increasing in length of the PNA oligomer and the number of purines in the sequence[76].

To improve the solubility and therefore the delivery it is possible to conjugate charged molecules such as amino acids to one of two ends, or use modified PNA monomers in which the glycine unit is replaced by amino acids with charged side chains.

PNA-DNA chimeras were also designed both to improve the low cellular uptake and the low solubility of PNA and both to obtain molecules with structural and biological properties similar to DNA.

- *Unmodified PNA delivery*

A large variety of cellular transport systems have been developed and tested. These systems can be divided into two categories, those based on the PNA as they are and those using modified PNA, ie, conjugated to appropriate ligands, such as "carriers" peptides or "guide" sequences[77]. The first generation of vectors is represented by liposomes, colloidal vesicles generally composed of a double layer of phospholipids and cholesterol. Liposomes may be neutral or cationic, depending on the phospholipids nature. The nucleic acid can be easily encapsulated inside the liposome, which contains an aqueous compartment, or it can be anchored to the surface through electrostatic interactions. These carriers, because of their positive charge, have high affinity for cell membranes, which are negatively charged in physiological conditions.

These systems are internalized through endocytosis. For example, it is possible to internalize them by diffusion, creating transient pores in the membrane by electroporation[78] or by microinjection[79].
Some studies have also reported the direct transport of PNA in a cell without the use of any mentioned protocols. However, in this case, the high PNA concentrations that is required (20μM) increased greatly the risk of toxic effects.

➢ *Modified PNA delivery*

The conjugation of PNAs with molecules recognized by the cells appears as a simple and convenient alternative to the standard translocation techniques mentioned above.
In this context, mention should be made to the conjugation of PNA with guide ligands, which can interact with specific receptors and can carry PNA only in target cells, in order to reduce undesired side effects in normal cells, according to an endocytosis receptor-mediated mechanism.

This mechanism requires the existence of transmembrane proteins, defined receptors, that interact specifically with certain molecules in the extracellular fluid.
Although the transport receptor mediated is a highly specific process, however it is not always effective, probably because of the limited amount of available receptors on the cell surface and the entrapment in endosomes / lysosomes of the transported material[80].

An alternative strategy involves the use of "Trojan peptides", reported to have a general cell membrane-penetrating capacity and capable of transporting a conjugated cargo to the interior of the cells[81].
These peptides are suggested to work by a receptor independent mechanism, through a physical interaction with components of biologic mem-

branes, resulting in inverted micelles that allow the passage of water-soluble molecules to the interior of the cells. However, the exact mechanism underlying the membrane passage of these peptides is still largely unknown [82]. This class of peptides consists of a series of positively charged peptides, including certain domains of the HIV regulatory protein, Tat[83], and the *Drosophila* homeodomain transcription factor, Antennapedia[84]. For their ability to cross the cell membrane, these peptides have been called "cell-penetrating peptides" (CPP). Peptides are generally composed of about thirty or less amino acid residues and they have a net positive charge.

The first CPP shown to be capable of carrying PNA oligomers in cells is derived from the third helix of the Antennapedia protein's homodomain[85]. Since then, the number of peptides (or derivatives from proteins found in nature, both designed and synthesized) with this capacity is gradually increasing.

Interaction of CPP and cargo is either achieved by covalent attachment or by non-covalent complexation through mainly ionic interactions (Figure 12).

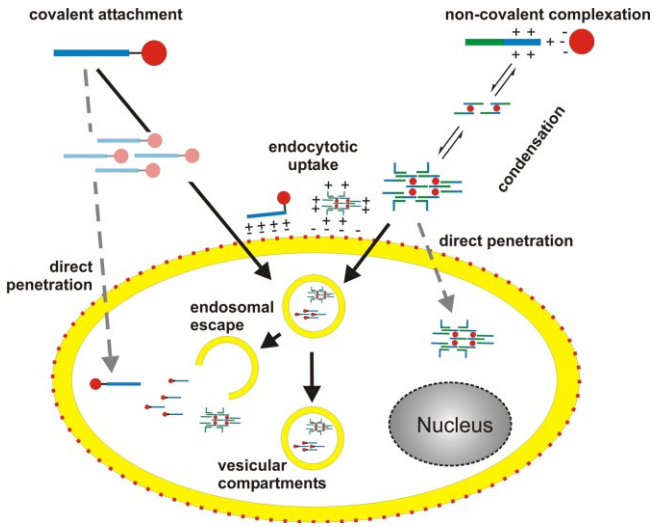

Figure 12: Principles of peptide-based nucleic acid delivery systems.

In case of non-covalent complex formation, a further assembly of cargo/carrier complexes occurs, leading to the formation of nanoparticles. In case of covalently joined molecules a similar scenario is less likely, yet cannot be excluded. Prior to the translocation process the particles attach to the cell surface by ionic interactions of positively charged CPP residues with negatively charged membrane components. Subsequently, complexes are taken up by directly penetrating the cell membrane or by an endocytotic pathway. Recent data suggest that the main uptake route is endocytosis.

Though, direct penetration cannot be excluded and may occur simultaneously (depicted by dashed, grey arrows). Once inside the cell, the cargo has to reach its target. Depending on the mechanism of uptake several scenarios like 'endosomal escape' are feasible.

PNAs conjugated to such peptides have been studied in several cell types (Figure 13). Corey's group found that a PNA conjugated to the Antennapedia peptide was internalized in human prostate tumor-derived DU145 cells, giving rise to vesicular staining of the cells. Vesicular staining of the cytoplasm is expected from a mechanism involving (receptor-mediated) endocytosis.

Other investigators have observed diffuse cytoplasmic and nuclear staining in Bowes cells after treatment of a PNA conjugated to penetratin (as well as transportan), as would be expected from the proposed mechanism of these peptides[86].

Peptide	Sequence
Tat^{48-60}	GRKKRRQRRRPPQ
penetratin ($Antp^{43-58}$)	RQIKIWFQNRRMKWKK
transportan	GWTLNSAGYLLGKINLKALAALAKKIL
TP10	AGYLLGKINLKALAALAKKIL
Oligoarginine (R_8)	RRRRRRRR
MAP	KLALKLALKALKAALKLA
MPG	GALFLGFLGAAGSTMGAWSQPKKKRKV
MPGα	GALFLAFLAAALSLMGLWSQPKKKRKV

Figure 13. Sequences of classical CPPs

It is also worth noting that the therapeutic potential of conjugated PNA-peptide may be limited by the fact that peptide motifs, although covalently linked to the PNA, have low stability in biological fluids and are inevitably subject to enzymatic degradation. Therefore, studies have shown that it is possible to improve the stability of peptides using D amino acids in order to make the peptide more resistant to protease degradation and therefore a better carrier of PNA. The use of D-amino acids, however, can cause a decrease in terms of biological activity.

This problem can be avoided by employing the so-called retro-inverse peptides, which, besides being more resistant to enzymatic degradation, maintain their biological activity intact. In fact Aldrian-Herrada et al. have claimed that neuronal cells readily take up PNAs conjugated to a retro-inverso derivative of the pAnt peptide, causing diffuse cytoplasmic as well as nuclear staining of the cells[87] .

- *PNA delivery in nucleus*

Two factors were identified as prerequisites for effective translocation to the nucleus: a) an efficient transport of cargo in the cytoplasm (discussed above);b) a nuclear localization sequence accessible and biologically active.
Regarding the second aspect, very useful for nuclear uptake proved to be the so-called topogenic sequences[88]. They are usually short and strongly basic peptide sequences, consisting of sequences of lysine or arginine interrupted by other amino acids, often neutral and hydrophobic.

These sequences are signals that are recognized and bound by receptors on the surface of the nuclear pores.

These pores play an important role to let pass freely ions and small molecules through the membrane and selectively control the transport of larger molecules.

After recognition and binding, ATP-dependent mechanism drives the molecule through the pore complex, inside the nucleus. The first of these sequences has been identified on the viral protein T antigen of SV40[89].

To simultaneously ensure an efficient passage through the plasma membrane and also an effective nuclear uptake, Braun and his team have synthesized a PNA conjugated to a peptide capable of passing the cell membrane (pAntp) and another PNA conjugated to an NLS peptide as a carrier system within the nucleus[90]. The efficiency of this complex has been successfully tested on human prostate cancer cells: the entry into the cytoplasm is visible after an hour and the entry into the nucleus becomes visible already after three hours.

The following table shows some examples of nuclear localization signal.

Protein	*Signal*
E1A adenovirus	KRPRP
Nuclear Protein of flu virus	PKKAREP
SV40 T antigene	PKKKRKV
UP1 of SV40	APTKRKGS
yeast ribosomal protein L3	PRKR

Table 3: Nuclear Localization Signal

In recent years a valid alternative to the approaches presented above involves chemical modification of the first generation PNA in order to improve those negative characteristics previously presented, such as cellular uptake.

AIMS OF THESIS WORK

The proposed thesis work was carried out pursuing the following objectives:

1) Development of a new strategy for the manual solid phase synthesis of Peptide Nucleic Acids.

2) Synthesis of oligomers consisting of peptide nucleic acid units and Peptide Nucleic Acids and Peptide conjugates to target pre-miRNA involved in human diseases such as Hsa-miR-210.

3) Design and synthesis of novel PNA analogues, in particular PNA with a sulfate group in γ position of the backbone, in order to evaluate if and how modifications in the structure may affect physical, chemical properties (i.e. in terms of improved affinity for the target, increased solubility in water, etc.) and biological activity of PNA.

CHAPTER 2

2. *DEVELOPMENT OF AN EFFICIENT AND LOW COST PROTOCOL FOR THE MANUAL PNA SYNTHESIS BY FMOC-CHEMISTRY.*

Due to the need of obtaining a large number of PNA oligomers in the course of these studies, the first significant aim of this thesis work has been the development of an efficient and low cost protocol for the manual PNA synthesis by Fmoc-chemistry. Generally, synthesis of PNA oligomers has been carried out using a variety of monomers and coupling conditions. Examples of protecting groups employed for the PNA monomers are represented by Boc/Z, Fmoc/Z, Fmoc/Boc, Mmt/acyl, Fmoc/acyl, Dde/Mmt, NVOC/acyl, azide/Bhoc and Fmoc/Bhoc[91]. So far, only two kinds of PNA monomers are commercially available, protected with the Boc/Z and the Fmoc/Bhoc (Figure 14).

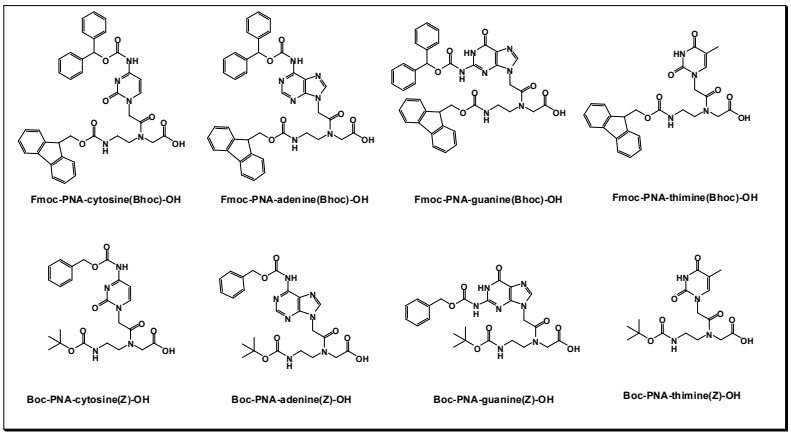

Figure 14: Commercially available PNA monomers for solid synthesis

Oligomerization conditions are usually set up considering the stability of the exocyclic amine protecting groups, the specific base sequences, the nature of the resin, other than the protecting group on the backbone amine.

The Fmoc/Bhoc combination of protecting groups is largely the most employed, due to the mild treatments for the cleavage of the oligomer from the resin and removal of Bhoc groups. Yields of oligomers depend on several factors, including the type of activator, the reaction time, the monomer excess, the pre-activation time, the times the coupling is repeated, the length of the oligomers, the temperature[92]. Syntheses of sequences with a high content of purines often give poor yields due to the difficulty of coupling very hindered monomers; furthermore expecially when using Fmoc protected monomers low yields may originate from aggregation of the peptide nucleic acid and stacking of the fluorenylmethoxycarbonyl with the nucleobases. Nowdays PNA syntheses are usually carried out on automated synthesizers, under controlled and standardized conditions.

Protocols for the manual synthesis are often an adaptation of protocols employed in automated synthesis. The synthesis by Fmoc chemistry of PNA oligomers relies on the protocol developed by Egholm and Casale for the automated synthesis of PNA oligomers using Fmoc/Bhoc protected PNA monomers. In this protocol 5 equivalents of PNA monomer are initially preactivated with HATU in the presence of the bases DIPEA and 2,6 lutidine and coupled for 20 minutes. Published protocols report manual synthesis with a number of PNA monomer equivalents for coupling ranging from 3 to 8[93].

When PNA monomers are coupled manually adapting the Egholm procedure, the coupling times are extended at least to 1 hour to increase the reaction yield. The coupling time is extended to 6 hours when 3 equivalents of PNA monomers are used, with HOBT/HBTU as activators and DIPEA as a base to get quantitative coupling. When polypurine stretches have to be synthesized couplings need to be repeated to obtain the desired oligomer. Overall, the combination of large excesses of PNA monomers, the use of HATU as activator, the increase in reaction times result in a very expensive and time consuming synthesis.

2.1. RESULTS AND DISCUSSIONS

With the aim of developing an efficient and low cost protocol for the manual synthesis of PNA oligomers by Fmoc chemistry, we have explored a new combination of activators and bases (Figure 15).

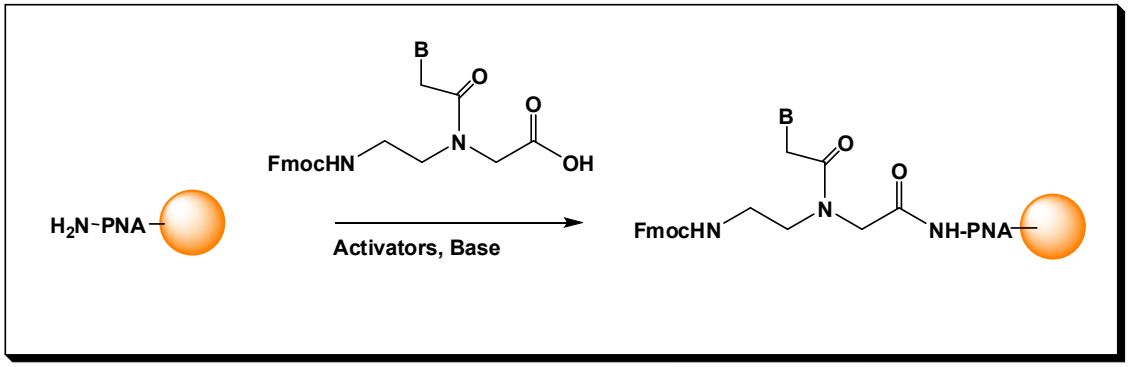

Figure 15: PNA synthesis

First of all, PNA oligomers were synthesised for reference by standard conditions, using 5 equivalents of PNA monomers activated with HATU (4 equivalents), in the presence of DIPEA (5 equivalents) and 2,6 lutidine (7.5 equivalents) for 1 minute and coupled for 20 minutes. The deprotection was carried out by treatment of the resin bound PNA with 20% piperidine in DMF, and capping steps were always carried out with a single treatment with a solution composed of 15/15/70 acetic anhydride/DIPEA/DMF v/v/v. Cleavage and deprotection were carried out with TFA/m-cresol 80/20 v/v, 90 minutes. Four PNA sequences with a length ranging from 9 to 12 bases were obtained, following the standard and the new protocols. (see Table 4 for sequences).

Sequence (name)	% purine	% Yields			
		Standard Protocol	Protocol 1	Protocol 2	Protocol 3
CACACTGTC (PNA 1)	33	19	75	18	45
ACGCACACTGTC (PNA 2)	42	0	45	<10	56
AGACGACCCA (PNA 3)	60	63	68	41	56
GGCCGGGACACA (PNA 4)	70	24	65	50	75

Table 4: Four PNA sequences choosen.

As sequences containing long stretches of purines are hard to synthesize, due to the toughness of coupling sterically hindred monomers such as adenine and guanine to each other, the protocols were tested on PNA oligomers having a purine content ranging from 30 to 67%. In all the cases only guanine monomers were double coupled.

These studies started checking protocols for Fmoc peptide and PNA synthesis, looking for conditions in which very little amounts of aminoacid/PNA and different combinations of bases and activators were employed. In this regard a rich font of information is represented by protocols for the coupling of modified PNAs, as those bearing side chains on the backbone. A protocol described by Le Chevalier Isaad et al reports the efficient synthesis of a peptide by manual coupling using only 2.5 equivalents of aminoacids activated with an equal amount of HOBT/TBTU, in the presence of N-methyl morpholine (NMM) as a base[94]. For the synthesis of PNAs, the protocol reported by Gogoi (3 equivalents of Fmoc/Bhoc monomers activated with HOBT/HBTU in the presence of DIPEA- coupling time 6 hours) was considered[93a]. Therefore investigations could reasonable begin changing the activator HATU for the combination HOBT/HBTU and improve the coupling conditions with the use of different bases. The first trials were carried out on two PNA sequences: one 9-mer and one 12 mer with a content of purines re-

spectively of 33% and 42% (Table 4, PNA 1 and PNA 2). The synthesis scale was 2 μmol; PNAs were elongated on the PAL-PEG PS resin (0.19 mmol/g).

The efforts were initially devoted to replace HATU using 5 equivalents of PNA monomers, activated with HOBT/HBTU. The PNA monomers (5 equivalents) were dissolved in a solution of HOBT/HBTU (5 equivalents) in DMF, adding as a base *N*-methyl morpholine (NMM) (5 equivalents) dissolved in DMF. (Pre-activation time: 1 minute) Oligomers were obtained using repetitive cycles of deprotection, coupling and capping. Coupling time was set at 20 minutes. Yields were judged at the end of the synthesis after analysis of the LC-MS profiles of the crudes. The results obtained with these protocols were unsatisfactory. The desired oligomers were not obtained, while we could see many deletes. NMM is a weak base, with a Kb around 10^{-7}, much lower as compared to the Kb for DIPEA. It was reasonable to think to combine it with a larger amount of another very weak base, pyridine (Kb 10^{-9}), which is also a good co-solvent for PNA monomers. So the combination of NMM with pyridine was investigated. Syntheses were carried out as described earlier, but coupling was carried out using a solution of NMM (5 equivalents) in pyridine.

The amount of pyridine in the coupling mixture is 25% (Protocol 1); this quantity does not cause cleavage of the N-terminal Fmoc. Interestingly the desired oligomers were obtained . A comparison of the LC-MS profiles of the crudes obtained with the new protocol (HOBT/HBTU/NMM/pyridine) and the standard protocol (HATU/DIPEA, 2,6 lutidine) revealed that yields using the new coupling conditions were significantly improved, as demonstrated by the LC profile in which the desired oligomer now corresponds to the major peak (for PNA 1 see Figure 16, compare panels A and B). Encouraged by these results we tasted the same protocol on two more sequences, a 10-mer and a 12-mer with a content of purines respectively of 60 and 67% (PNA 3 and 4),. The PNA oligomers were successfully obtained. The LC-MS profiles

in fact show a major peak, containing a single product with the mass corresponding to the desired oligomer. The LC profile for PNAs 3 and 4 are shown in Figure 16, (compare panel A with B). Next the synthesis of PNA oligomers reducing the amount of PNA equivalents, from 5 to 2.5, was explored. All oligomers were synthesized using 2.5 equivalents of PNA monomers, activated with an equal amount of HOBT/HBTU and 2.5 equivalents of NMM in pyridine as a base (Protocol 2). Syntheses yielded the desired products, although in reduced yields, as compared to those obtained using Protocol 1 (Table 4). Finally the effect of increasing the amount of bases was investigated. All PNAs were synthesised using 2.5 equivalents of PNA monomers, activated with an equal amount of HOBT/HBTU and 5 equivalents of NMM in pyridine (Protocol 3). The percentage of pyridine in the coupling mixture is now 40. The results showed that yields of PNAs doubling the amount of bases with 2.5 equivalents of PNA monomers (Protocol 3) were in average comparable to those obtained with 5 equivalents of PNA and lower content of bases (Protocol 1) (Table 4).

It is likely that doubling the NMM speeds up the formation of the intermediate active ester (as observed in peptide synthesis) and this effect counterbalances the decrease of the equivalents of PNA monomers.[17] The comparison of the LC profiles obtained with Protocol 3 is shown for three sequences, respectively in Figure 16, letter C.

Furthermore in all cases yields obtained using Protocol 3 were comparable or higher than to those obtained with the standard protocol, even for sequences with the higher content of purines (Figure 16, letter C and Table 4).

These results suggest that HATU is not necessary for the PNA coupling; the mixture HOBT/HBTU gives very good yields of coupling especially when combined with pyridine/NMM.

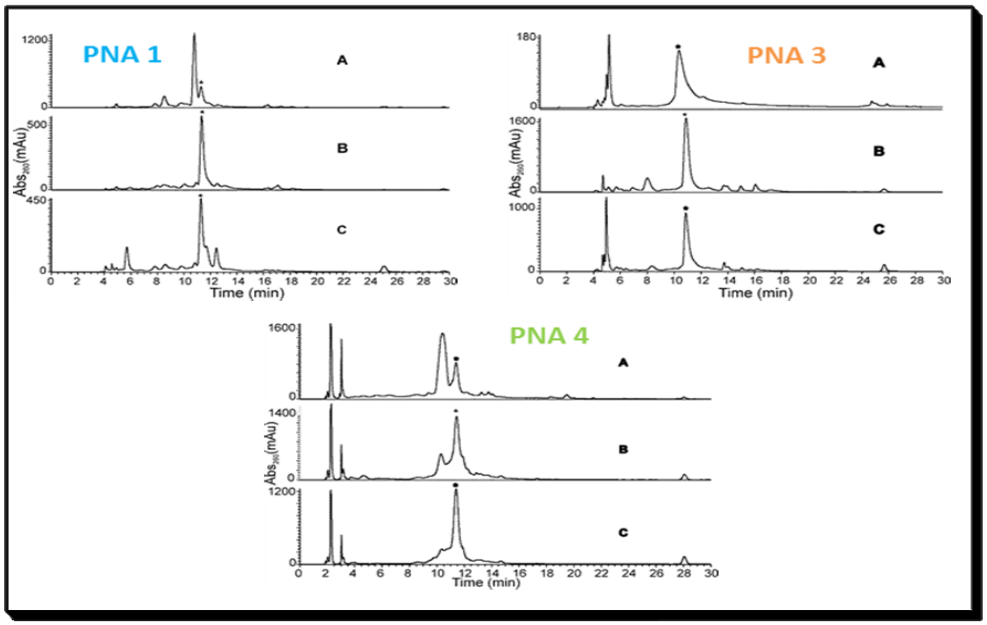

Figure 16: LC profile for the crudes obtained for PNA1, PNA3 and PNA4 with standard protocol (A), protocol 1 (B) and protocol 3 (C). The peak labelled with the asterisk corresponds to the desired product.

2.2. CONCLUSIONS

In conclusion it was demonstrated that the manual coupling of Fmoc/Bhoc PNA monomers is very efficient using HOBT/HBTU as activators in the presence of NMM/pyridine as bases. The protocol developed is robust and low cost and can be executed by an automated PNA synthesizer.

Interestingly the addition of large amounts of pyridine contributes to increase the yields of oligomers with high content of purines, as demonstrated for PNA 4 (content of purine 67%), in which very high yields are obtained even when the equivalents of monomer per coupling are halved.

Furthermore, the protocol developed will allow the obtainment with good yields of difficult sequences, avoiding expensive activators.

2.3. *MATERIALS AND METHODS*

Activators HBTU, HOBT and HATU were purchased at Inbios (Italy). Fmoc-PNA-cytosine(Bhoc)-OH, Fmoc-PNA-thymine-OH, Fmoc-PNA-guanine(Bhoc)-OH, Fmoc-PNA-adenine(Bhoc)-OH were obtained by Link Technologies. Acetonitrile (ACN) for LC-MS, N,N-dimethylformamide (DMF) for solid phase synthesis, DIPEA, Dichloromethane were from Romil Pure Chemistry, N-methylmorpholine from Fluka and piperidine from Biosolve. Fmoc-PAL-PEG-PS (0.19 mmol/g) resin was from Applied Biosystems.

All other chemicals were supplied by Sigma-Aldrich and were used without other purification. LC-MS analyses were performed on a LC-MS Thermo Finnigan with an electrospray source (MSQ) on a Phenomenex Jupiter 5μ C18 (300Å, 150x460 mm) column with a flow rate of 0.8 $mLmin^{-1}$ at 65°C.

Experimental

Each PNA oligomer was synthesized on a 2 μmol scale using both the standard PNA protocol and PNA new protocols. The syntheses were performed on a Fmoc-PAL-PEG-PS resin (0.19mmol/g). To improve the coupling efficiency double couplings were carried out on PNA-guanine monomers.

Standard protocol

Synthesis was carried out using repetitive cycles of deprotection, coupling and capping at room temperature. After each of these cycles two flow washes (25s) with DMF performed.

Deprotection: 20% piperidine in DMF, 7 minutes.

Coupling: 5 equivalents of PNA monomers were dissolved in DMF to a concentration of 0.22M; A solution of HATU in DMF 0.18M (4eq) and 50μL of a mixture of DIPEA 0.2M and 2,6-Lutidine 0.3M in DMF were added. (Pre-activation time: 1 minute- coupling time:20 minutes)

Capping: acetic anhydride/2,6 Lutidine/DMF (5/6/89 v/v/v/), 5 minutes.

At the end of the synthesis the resin was washed with DMF, DCM, diethyl ether and dried *in vacuo*. The PNA oligomers were cleaved from the resin and deprotected by a treatment with a solution of TFA/m-cresol (80/20) 90 minutes r.t.

The filtrate was flushed by a stream of nitrogen to remove the most of TFA and the PNA oligomers were precipitated by addition of cold diethyl ether, washed three times with diethyl ether and dried *in vacuo*.

Protocol 1 (5 eq PNA)

Synthesis was carried out using repetitive cycles of deprotection, coupling and capping at room temperature. After each of these cycles two flow washes (25s) with DMF were performed. Deprotection, and final cleavage were carried out as described in the Standard Protocol.

Coupling: 5 equivalents of PNA monomer were dissolved in DMF to a concentration of 0.22M; a solution of HOBT in DMF 0.20M (5 equivalents) and a solution of HBTU in DMF 0.20M (5 equivalents), were added. 50μL of a mixture of NMM 0.2M in pyridine were added. (Pre-activation time: 1 minute- coupling time:20 minutes).

Capping: acetic anhydride/2,6 lutidine/DMF (5/6/89 v/v/v/), 5 minutes

Protocol 2 (2.5 eq PNA)

Synthesis was carried out using repetitive cycles of deprotection, coupling and capping at room temperature. After each of these cycles two flow washes (25s) with DMF performed. Deprotection, and final cleavage were carried out as described in the Standard Protocol.

Coupling: 2.5 equivalents of PNA monomer were dissolved in DMF to a concentration of 0.22M; a solution of HOBT in DMF 0.20M (2.5 equivalents) and a solution of HBTU in DMF 0.20M (2.5 equivalents) were added. 25μL of a mixture of NMM 0.2M in pyridine were added. (Pre-activation time: 1 minute- coupling time:20 minutes)

Capping: acetic anhydride/2,6 lutidine/DMF (5/6/89 v/v/v/), 5 minutes

Protocol 3 (2.5 eq PNA + pyr)

Synthesis was carried out using repetitive cycles of deprotection, coupling and capping at room temperature. After each of these cycles two flow washes (25s) with DMF performed. Deprotection and final cleavage were carried out as described in the standard Protocol.

Coupling: 2.5 equivalents of PNA monomer were dissolved in DMF to a concentration of 0.22M; a solution of HOBT in DMF 0.20M (2.5 equivalents) and a solution of HBTU in DMF 0.20M (2.5 equivalents), was added. 50μL of

a mixture of NMM 0.2M in pyridine was added. (Pre-activation time: 1 minute- coupling time:20 minutes)

Capping: acetic anhydride/2,6 lutidine/DMF (5/6/89 v/v/v/), 5 minutes.
The following molecules were obtained (underlined bases were double coupled):

PNA 1 CACACTGTC

PNA 2 AGACGACCCA

PNA 3 ACGCACACTGTC

PNA 4 GGCCGGGACACA

All products were identified by electrospray mass analysis

PNA 1 (Da): Calculated: 2396.2; $[M+2H]^{2+}$: 1199.1; $[M+3H]^{3+}$: 799.6; $[M+4H]^{4+}$: 600.0.

Found: $[M+2H]^{2+}$: 1199.1; $[M+3H]^{3+}$: 799.8; $[M+4H]^{4+}$: 599.9.

PNA 2 (Da): Calculated: M=2705.6; $[M+2H]^{2+}$: 1353.8; $[M+3H]^{3+}$: 902.9; $[M+4H]^{4+}$: 677.0.

Found: $[M+2H]^{2+}$: 1352.7; $[M+3H]^{3+}$: 902.1; $[M+4H]^{4+}$: 676.8.

PNA 3 (Da): Calculated: M=3124.4; $[M+2H]^{2+}$: 1608.2; $[M+3H]^{3+}$: 1072.3; $[M+4H]^{4+}$: 804.5.

Found: $[M+2H]^{2+}$: 1606.8; $[M+3H]^{3+}$: 1071.4; $[M+4H]^{4+}$: 803.9.

PNA 4 (Da): Calculated: M=3304.4; $[M+2H]^{2+}$: 1653.2; $[M+3H]^{3+}$: 1102.5; $[M+4H]^{4+}$: 827.1.

Found: $[M+2H]^{2+}$: 1652.2; $[M+3H]^{3+}$: 1101.8; $[M+4H]^{4+}$: 826.6.

CHAPTER 3

3. *SYNTHESIS AND CHARACTERIZATION OF PNAS FOR TARGETING PRE-MIRNAS INVOLVED IN HUMAN DISEASES*

Another significant aim of this thesis work is the synthesis and characterization of PNAs which we will define since now on as **antago-premiR**, designed to inhibit the function of a target miR. This approach is actually completely new, and differs from the the antagomiR approach by the fact that PNAs will target the precursor of the mature miRNA, the pre-miRNA.

This strategy is aimed to inhibit maturation of the pre-miRNA into miRNA. For the experimental point of view one the advantages recognized by us in the present strategy is represented by the unique interpretation of the experimental results. When miRNA inhibition is achieved by antagomiRs, molecules complementary to the mature miRNA, and the amount of miRNA is quantified by RT-PCR, results are often doubtful: the PNA antagomiR, in fact, may bind to the primers and thus inhibit their amplification, resulting in low yield of amplificates, which is independent by the desired antagomiR function of the PNAs. Anti premiRNA are not fully complementary to the miRNA and are not expected to display interference. Furthermore, as pre-miRNAs are located both in the nucleus and in the cytoplasm there is in principle a dual possibility to reach them.

We designed PNA oligomers and PNA-peptide conjugates fully complementary to a specific region of the microRNA-210 precursor (pre-miR210). In fact, such molecules, pre-*antagomir*, should bind to the miRNA precursor

with high specificity and affinity, blocking the maturation process and so preventing the interaction of miR-210 with mRNA.

3.1. MIRNA210

In this work, the studies were focused on microRNA 210, a unique miRNA that is evolutionarily conserved and ubiquitously expressed in hypoxic cell and tissue types[95]. It directly represses multiple transcripts associated with diverse cellular functions and it has been mechanistically linked to the control of a wide range of cellular responses known to influence normal developmental physiology as well as a number of hypoxia-dependent disease states, including tissue ischemia, inflammation and tumorigenesis (Figure 17) [96]. Independent pieces of data now exist that link the dynamic regulation of miR-210 directly to low oxygen levels as opposed to other mechanisms that secondarily associated to hypoxia (i.e., oxidative stress, inflammation and others).

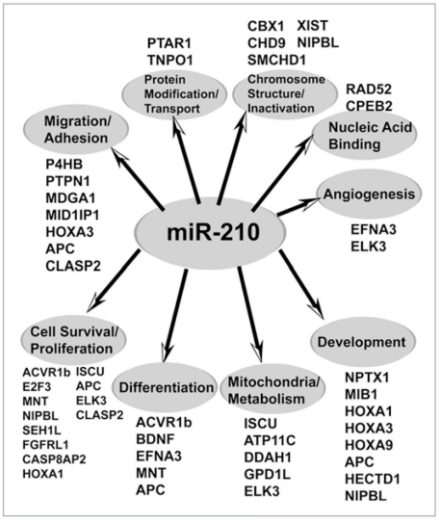

Figure 17: miR-210 controls diverse fundamental cellular preocesses

Multiple groups have found that miR-210 is specifically induced by HIF-1α and is unique in its wide distribution and robust upregulation in re-

sponse to hypoxia[97]. Furthermore, observational evidence suggests that levels of miR-210 are specifically regulated in a number of human disease states, indicating an important role for this miRNA in modulating hypoxia-induced pathogenesis[98]. miR-210 is also upregulated in a significant percentage of human samples derived from primary solid tumors, including head and neck cancer, melanoma, glioma, small cell and lung cancer, lung adenocarcinoma and adrenocortical carcinoma[99]. Genomic deletions of miR-210 have also been reported in human epithelial ovarian cancer samples, and these deletions are suggested as a possible trigger to tumorigenesis.

Correspondingly, Huang and colleagues have demonstrated that forced expression of miR-210 in implanted tumor tissue can repress tumor growth in immunodeficient mice[98]. However, upregulated levels of miR-210 in human breast cancer samples display an inverse correlation with disease-free and overall patient survival[97a] and, in a separate study, miR-210 levels correlate with breast cancer aggressiveness and metastatic potential[100]. While somewhat paradoxical, these findings taken together may indicate that miR-210 can play either adaptive or maladaptive roles in repressing or disease conditions, respectively, depending upon the specific in vivo context.

Finally, In addition to specialized endothelial functions, developing erythroid cells may also depend upon miR-210 to direct specific globin expression. Through miRNA profiling assays, Bianchi and colleagues have reported that miR-210 is overexpressed in thalassemic patients and is preferentially upregulated in human erythroid precursor cells displaying a hereditary persistence of fetal hemoglobin (HPFH)[101]. This upregulation is replicated by treatment of erythroid precursors in cell culture with mithramycin, which correlates with induction of fetal γ–globin expression. Hypoxia has previously been reported to alter progression of the erythroid program[102] and is certainly a driving stimulus in erythropoeisis[103]. Low O_2 might indeed modulate the relative amounts and types of hemoglobins produced by

erythroid cells, leading to increased HbF during stress erythropoiesis. However, it is unclear if this upregulation of miR-210 in HPFH erythroid cells is dependent upon HIF-1α or if miR210 and its direct targets are causatively responsible for this regulation.

Just because miR210 was found to be involved in all biological processes described above, in recent years the search for molecules capable of inhibiting its functions through an antisense approach was found desirable.

3.2. RESULTS AND DISCUSSION

3.2.1. SYNTHESIS OF THE PNA, PEPTIDE-PNA CONJUGATES

Two PNA sequences targeting the "sense region" (PNA 5) and the " 5' end region" (PNA 6) of the pre-miR210 were designed. (Figure 18).

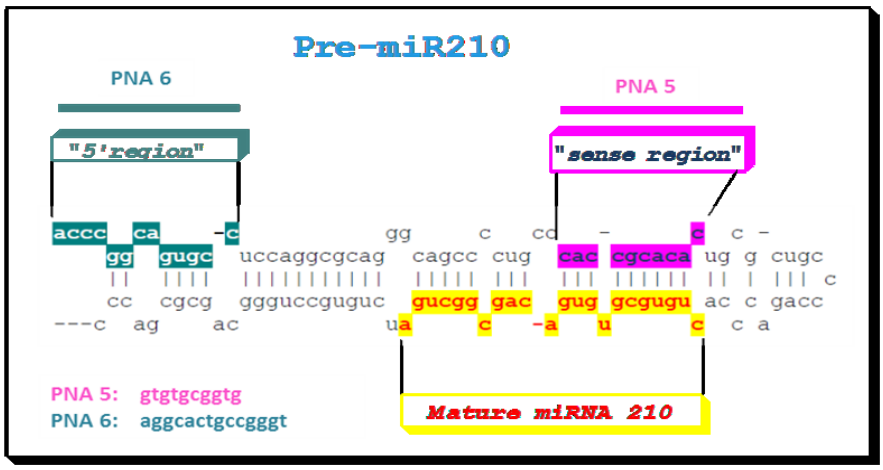

Figure 18: Pre-miRNA210 targeting by PNA 5 and PNA 6

These sequences differ by the corresponding tract of the mature miRNA by one or two bases: in the pre-miRNA, in fact, there is not fully complementarity between bases and PNAs were designed to be fully complementary to the pre-miRNA.

The high affinity and specificity of binding of PNA toward complementary RNA should in principle allow the interaction of the PNA with the desired RNA target, opening the RNA duplex and thus inhibiting the miRNA maturation (Figure 19).

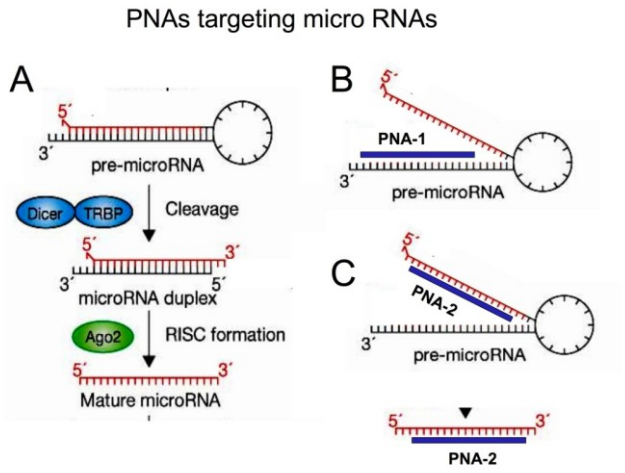

Figure 19: pre-microRNAs inhibition with PNAs antagomir

The chosen sequences are:

PNA 5: NH_2-gtgtgcggtg-H

PNA 6: NH_2-aggcactgccgggt-H

In order to improve the cellular uptake of the PNA oligomers and make sure the PNAs reach their target miR210, we obtained PNAs conjugated to carrier peptides. Since the pre-microRNA 210 is present both in the nucleus and in the cytoplasm, we choose different peptides for the delivery in both cellular compartments, TAT, NLS, combination of TAT and NLS and biNLS.

TAT is a small basic peptide derived from the HIV-1 Tat protein, that has been successfully shown to deliver a large variety of cargoes, from small particles to proteins, peptides and nucleic acids[104]. The transduction domain or region conveying the cell penetrating properties appears to be confined to a small (9 amino acids) stretch of basic amino acids, with the sequence RKKRRQRRR; the guanidinium groups of the arginine side chain seems to be responsible for the high transfection efficiency[83]. The TAT peptide has been reported to successfully deliver PNA in the cytoplasm in different cell types. Bendifallah *et al.* investigated the relative potency of different CPPs (Trans-

portan, oligo-arginine (R_{7-9}), pTat, Penetratin, KFF, SynB3, and NLS), as carriers of medicinally relevant cargo and employing a positive assay, showed that TAT peptide had a significantly transport capacity[105]. Diaz-Mochòn et al. synthesized PNA-peptides conjugates and tasted their intracellular delivery showing that conjugates bearing *hepta*-arginine peptide and TAT_{48-57} decapeptide were taken up by cells with high efficiency[106].

NLS, a Nuclear Localization Signal, is a short stretch of amino acids that mediates the transport of the nuclear proteins into the nucleus[107] (Figure 20).

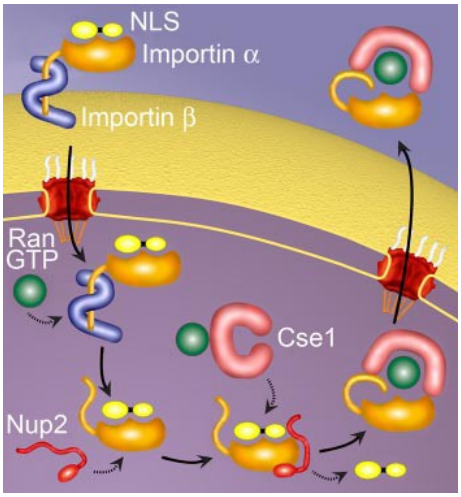

Figure 20: The classical nuclear import cycle.

In the cytoplasm, cargo containing a cNLS is bound by the heterodimeric import receptor, importin α/importin β. Importin α recognizes the cNLS, and importin β mediates interactions with the nuclear pore during translocation. Delivery of PNA conjugated to NLS into the nucleus has been demonstrated by several groups[108]. Tonelli et al., for example, developed an antigène peptide nucleic acid (PNA) for selective inhibition of MYCN transcription in neuroblastoma cells, linked at its amino terminus to a nuclear localization signal peptide and they showed through Fluorescence microscopy specific nuclear delivery of the PNA in six human neuroblastoma cell lines.

We also obtained a combination of TAT and NLS, in which NLS was anchored as a branch on the TAT peptide, after introducing a lysine residue at the C terminus position. We wish to verify whether the presence of a double cargo affects the delivery and the biological activity of the PNA.

Finally a new carrier, biNLS was also obtained and conjugated to our PNA. These peptide has been reported to bind to both arms of importin α and its uptake has been demonstrated to be very high in mammalian cells, yeast and plants. Kosugi et al. showed also that the length of the linker region between the two consensus sequences of the bi-NLS is a key factor. In fact, an effective length of the linker would be 10-12 residues, which would be equal to the distance between the major and the minor binding sites of importin α[109]. A long linker up to 20 residues makes a bi-NLS as two separate and classical monopartite NLSs.

Follow the sequences:

PNA 5-TAT	NH_2-gtgtgcggtg-GRKKRRQRRRPPQK-H
PNA 5-NLS	NH_2-gtgtgcggtg-PKKKRKV-H
PNA 5-TAT-NLS	NH_2-gtgtgcggtg-GRKKRRQRRRPPQK- PKKKRKV-H
NLS-PNA 5-TAT	NH_2PKKKRKV-gtgtgcggtg-GRKKRRQRRRPPQK-H
PNA 6-Bi-NLS	NH_2-aggcactgccgggt-RKRSADFERLYLVPSKK –H

A solid-phase synthesis strategy has been used to obtain the molecules. This strategy was originally introduced in 1963 by Merrifield for the synthesis of peptides and today is widely used for the synthesis of many organic polymers, such as oligonucleotides, peptides, peptide nucleic acids and oligosaccharides (Figure 21).

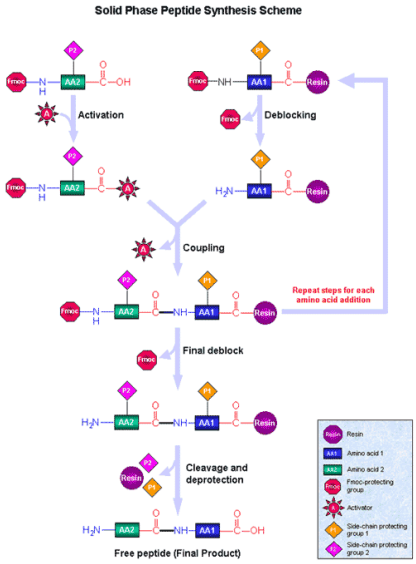

Figure 21: Solid Phase Synthesis Scheme

Each cycle of synthesis includes a number of consecutive steps:

- ✓ Removal of protecting group on the amino terminus;
- ✓ Accurate washing of the resin;
- ✓ Activation of the carboxyl of the residue that has to be coupled;
- ✓ Condensation reaction;
- ✓ Careful wash of the resin;
- ✓ Cleavage from the resin.

This strategy can be easily used for the synthesis of PNA oligomers and PNA-peptide conjugates.

PNA 5 was synthesized using a protocol for Fmoc solid-phase synthesis of PNA on a 2 μmol scale, previously described in chapter 2. To improve the synthesis yields double couplings were performed on purine monomers.

After purification by reverse phase HPLC on semi-preparative scale the product was analyzed by electrospray mass spectrometry and UV-visible spectroscopy. As expected the PNA is characterized by a maximum at 260 nm, due to the heterocyclic bases, and a maximum at 210 nm, due to peptide bonds (Figure 22).

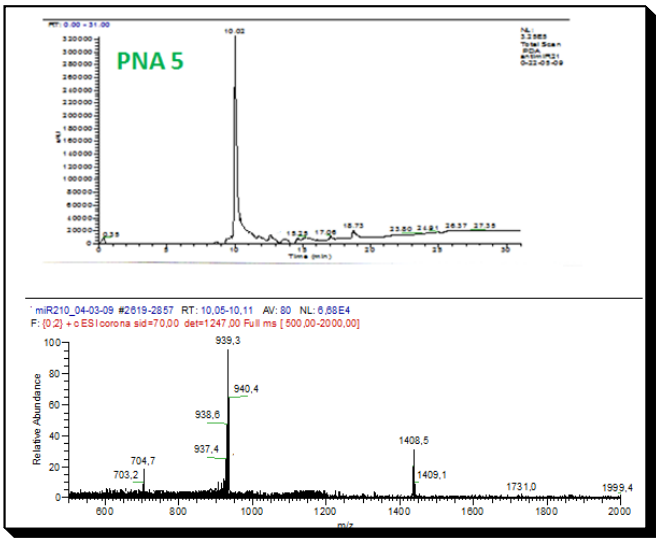

Figure 22: LC/MS spectrum of PNA 5

Instead, the PNA 6 oligomer was obtained with very low yields and for this reason, we decided to grow this PNA on a peptide to obtain directly the PNA-peptide conjugates.

The synthesis of PNA-peptide conjugates involved the solid-phase synthesis of the different peptides, then the growth of the PNAs chains on the support functionalized with the peptide (Figure 23).

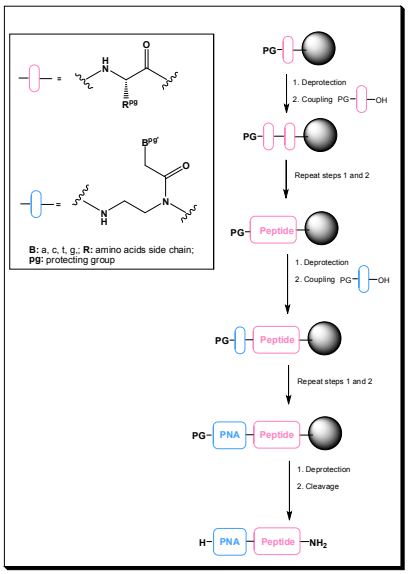

Figure 23: Conjugation strategy between petides and PNA.

The TAT peptide (GRKKRRQRRRPPQK) was anchored to a resin loaded with a Lys (Mtt); this residue is functional for the synthesis of the branched NLS-TAT. PNA5 is grown on the peptide loaded resin and the product, the PNA-peptide conjugate, is deprotected and cleaved off the resin after treatment with TFA / m-cresol / TIS (78/20/2) v / v / v. The PNA-peptide conjugate was analyzed by analytical reverse phase HPLC and purified by semi-preparative HPLC . The mass analysis of the crude revealed the presence of the desired PNA5- TAT conjugate (Figure 24).

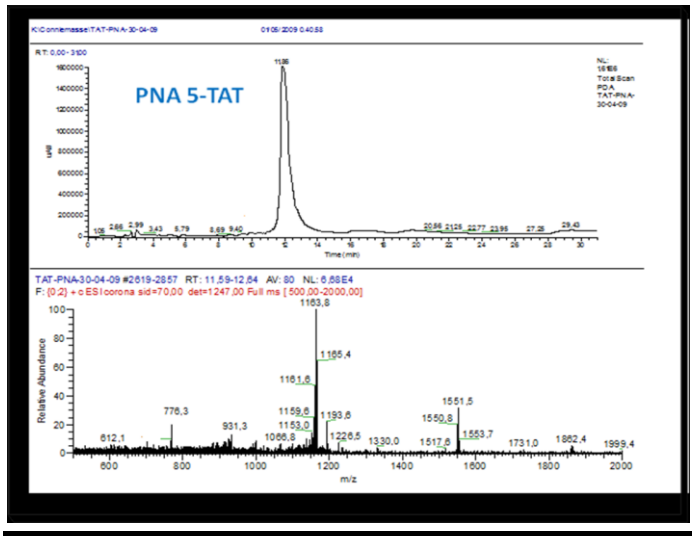

Figure 24: LC/MS spectrum of PNA 5-TAT crude

PNA5-NLS, NLS-PNA5-TAT, PNA6-Bi-NLS conjugates were obtained following the same strategy described for TAT-PNA 5. Below LC-MS profiles of the expected PNA5-NLS pure is reported as an example (Figure 25).

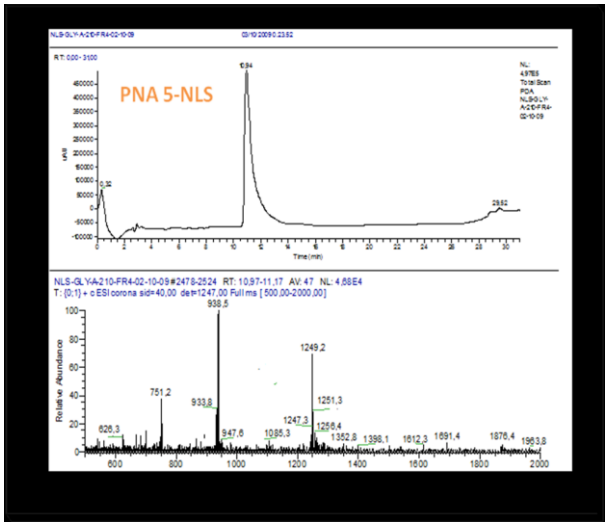

Figure 25: LC/MS spectrum of PNA 5-NLS

To obtain the branched TAT(NLS) PNA conjugate we first obtained the TAT-PNA, acetylated at the N-terminus. We next removed the Mtt from the side chain of the N-terminal lysine and on this we finally grow the NLS peptide. (Figure 26).

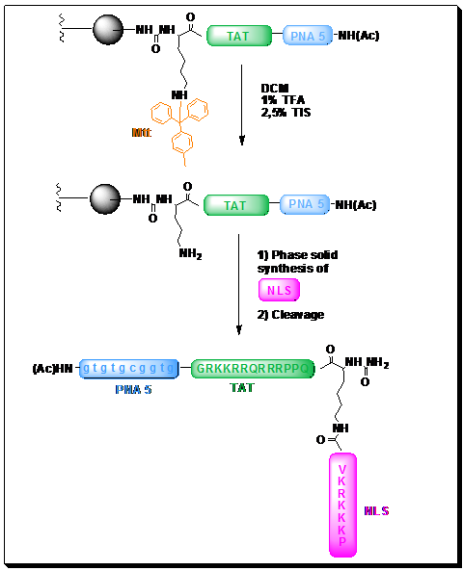

Figure 26: branched NLS-TAT synthesis

The MALDI-TOF mass spectrum of the sample obtained, however, has shown a construct whose molecular weight was found to be about 115 units less

than the expected weight. The product obtained is probably lacking the last proline of the peptide NLS (spectra not shown).

3.2.2. FLUORESCENCE STUDIES

In order to demonstrate that the PNA was able to bind to the pre-miRNA we obtained a Thiazole Orange (TO) modified PNA for fluorescence studies. Thiazole Orange (TO) is an asymmetric cyanine dye and a fluorescent DNA intercalator[110]. The functionalization of Peptide Nucleic Acid oligomers with Thiazole Orange has been extensively investigated and it has been shown to be one of the most effective fluorescence-based strategies for DNA detection involving modified PNA. This positively charged heterocycle, which provides a strong fluorescence enhancement upon DNA hybridization, combined with a well-known base stacking ability, has been successfully exploited for several PNA-based approaches. In previous works, Kubista's group constructed the so-called ''Light-Up'' probes, made by a TO molecule covalently linked to the N-terminus of the PNA oligomers by a linker[111]. These molecules showed a weak fluorescence signal as free probes and a high fluorescence enhancement upon DNA hybridization, revealing their suitability for specific detection of nucleic acids in homogeneous assays. This strategy was applied to detect post-PCR products with a single mismatch resolution and real time PCR detection assays[112]. TO-modified PNA oligomers have also been successfully applied in clinical diagnostic applications[113].

Tonelli et al. showed that TO–PNA probes had a good fluorescence enhancement upon hybridization with the target RNA sequence allowing the real time monitoring of the transcription-based amplification[114]. Moreover, even in the presence of remarkable amount of non-target RNA, the probe fluorescence emission remains low, compared to the free probes. So, the PNA probes conjugated with dyes like TO are appropriate tools for real time

isothermal assays that target RNA 'amplicons'[115]. TO is a florescence intercalator successfully employed for DNA detection, linked to synthetic conjugate through a linker attached to the quinoline nitrogen of the heterocycle[110] (Figure 27).

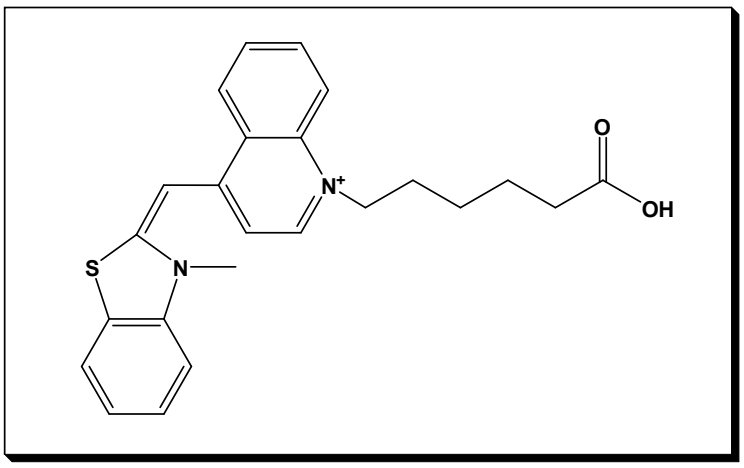

Figure 27: Thiazole Orange

The use of TO as fluorophore is compatible with the solid phase synthesis protocols commonly applied in the synthesis of PNA, since this molecule is stable under the strong acidic conditions used in the final step for cleaving the oligomer from the solid support.

A carboxy-functionalized TO derivative was prepared[116], employing Lepidine and 6-bromohexanoic acid (Figure 28).

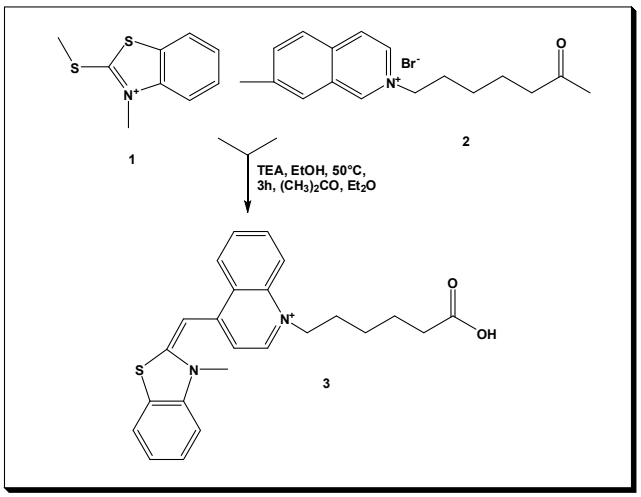

Figure 28: TO derivative synthetic strategy

The TO derivative was characterized by ^{1}H and ^{13}C NMR and employed for the derivatization of the PNA oligomers.

We derivatized the TAT-PNA 5 with TO. The peptide-PNA conjugate was prepared by solid synthesis, employing the same protocol discussed above for PNA-peptide conjugates synthesis. The probe was attached to the conjugate anchored on the solid support after reaction of 5 equivalents of TO dye activated by a mixture of HOBt/HBTU (4.9 eq.) in DMF and NMM (7 eq.). Double couplings of 60 minutes each were performed and the reaction was carried in the dark. After cleavage from the resin, the conjugate was analyzed by analytical reverse phase HPLC and purified by semi-preparative HPLC . The mass analysis of the crude revealed the presence of the desired TO-PNA5-TAT conjugate (Figure 29).

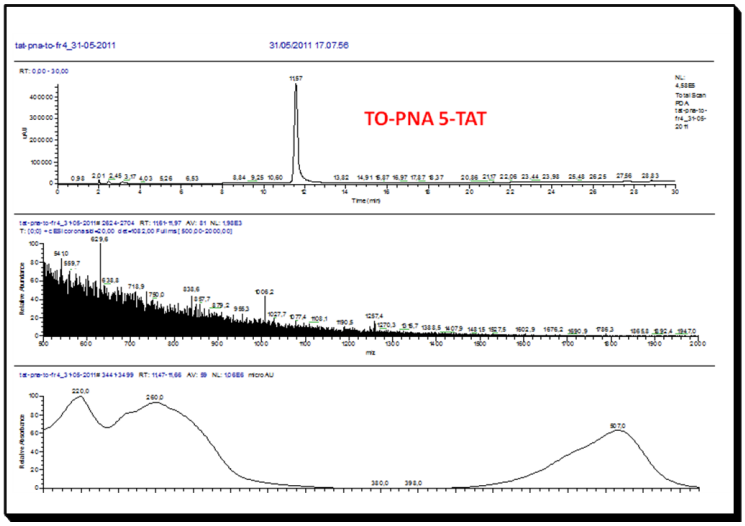

Figure 29: LC/MS spectrum of TO-PNA 5-TAT

For Fluorescence measurements DNA instead of RNA was employed, due to its higher stability. The sequence was a 42 mer DNA (DNA5) encompassing the tract complementary to PNA 5 and having additional bases at the 5'. It has been reported, in fact, that TO dye lights up only when binds to complementary sequences at least 28 bases long[111].

Follow the DNA sequences:

DNA5 CAGGGCAGCCCCTGCCCACCGCACACTGCGCTGCACGTACGT

DNA5c CCAGACCCACTGTGCGTGTGACAGCGGCTGATCTG

According to data reported in the literature, the fluorescence emission of free and hybridized probes is different. The TO-PNA was incubated with the DNA duplex (DNA5/DNA5c) and the variation in the fluorescence emission at 470nm was monitored. An increase in the fluorescence signal was observed, consistent with the hybridization of PNA to the DNA duplex, reasonably occurring after strand invasion (Figure 30).

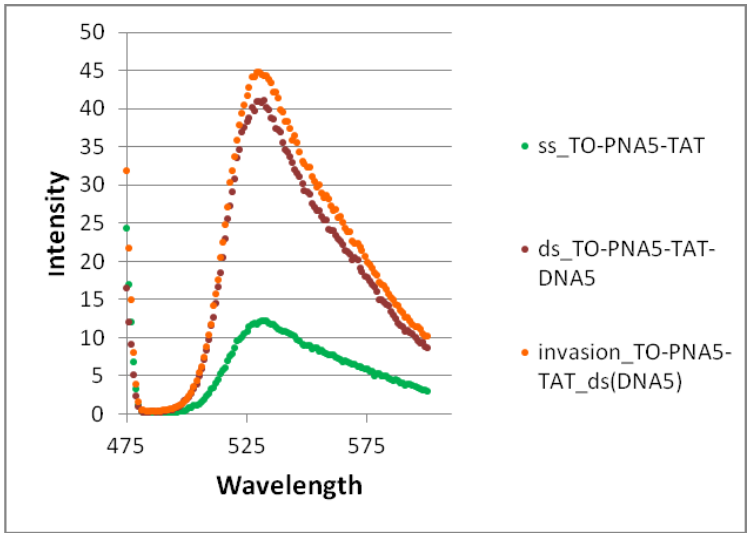

Figure 30: Fluorescence emission of free and hybridized probes.

Measurements of fluorescence were carried out also on the TO-PNA 5-TAT /DNA duplex to detect the fluorescence intensity displayed when all the PNA hybridize the DNA. Surprisingly the two spectra were found superimposable, demonstrating the efficiency in the binding of PNA5 to DNA duplex. Reasonably PNA 5 is able to invade the RNA duplex and disrupt it.

Next we had to test the effect of the molecules in cells, to verify either their uptake and their activity. With the aim to verify whether these molecules were capable of entering the cells some of these sequences were also derivatized with a fluorescent probe, FITC (Figure 31), in order to perform Fluorescence-activated cell sorting (FACS) experiments too.

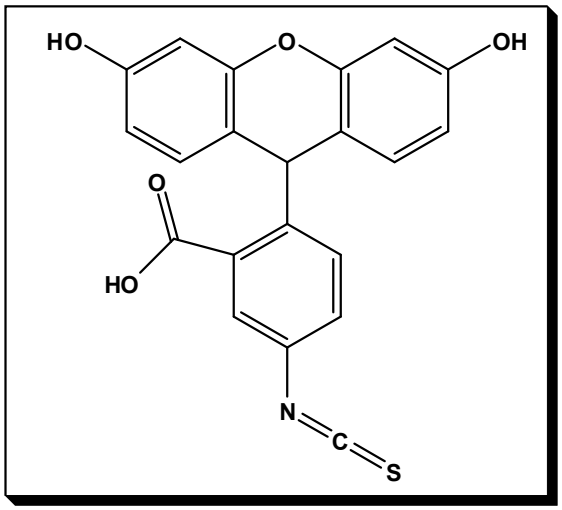

Figure 31: Fluorescein isothiocyanate

However, derivatization using the fluorescent probe requires, first of all, the introduction of an adequate linker, to avoid low yields of reaction, due to steric hindrance of the peptide-PNA conjugate. Amino hexanoic acid (HAx) was used as a spacer, and in particular the derivative Fmoc-HAx-OH was anchored to the PNA-peptides constructs already present on the resin, using the protocol described for the peptide solid phase synthesis. Derivatization of oligomers by FITC was carried out incubating the resin bound oligomer with a solution of FITC (5 eq.), NMM (7eq.) in DMF. (Figure 32). All products were cleaved off the resin as described earlier for PNA-peptide conjugates. Follow the products obtained:

FITC-PNA 5-TAT FITC-gtgtgcggtg-GRKKRRQRRRPPQK-H

FITC-NLS-PNA5-TAT FITC- PKKKRKV-gtgtgcggtg-GRKKRRQRRRPPQK-H

FITC-PNA 6-Bi-NLS FITC-aggcactgccgggt-RKRSADFERLYLVPSKK –H

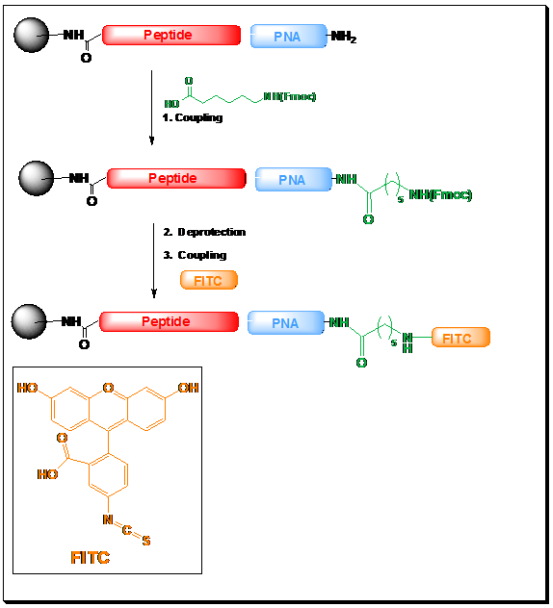

Figure 32: Synthesis Strategy for PNAs-Peptides derivatization with FITC

Conjugates **FITC-PNA5-TAT**, **FITC-NLS-PNA5-TAT**, **FITC-PNA6-Bi-NLS** were obtained after purification by reverse phase HPLC on semi-preparative scale and analyzed by electrospray mass spectrometry and UV-visible spectroscopy. As expected the molecules were characterized by a maximum at 495 nm, due precisely to the presence of fluorescein isothio-urea (Figure 33, Figure 34, Figure 35).

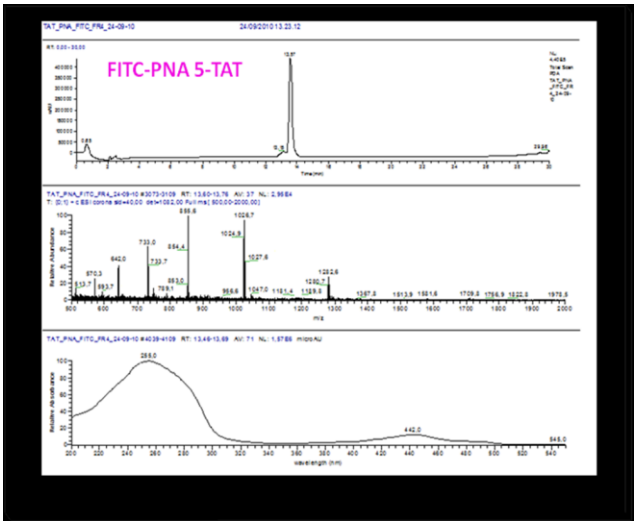

Figure 33: LC/MS spectrum of FITC-PNA 5-TAT

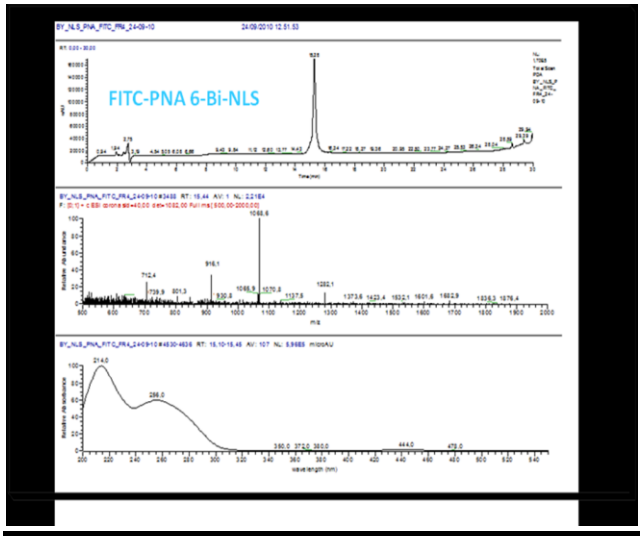

Figure 34: LC/MS spectrum of FITC-PNA 6-Bi-NLS

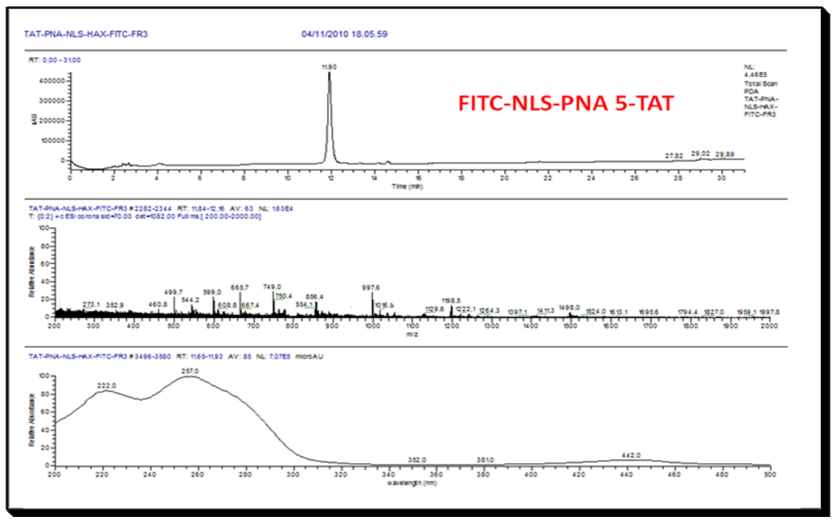

Figure 35: LC/MS spectrum of FITC-NLS-PNA 5-TAT

Some of these molecules were employed for FACS (Fluorescence Activated Cell Sorting) experiments, carried out in collaboration with the research team of Professor Roberto Gambari of University of Ferrara.

Preliminary investigations carried out on the three PNAs functionalized with FITC revealed that cells do incorporate FITC modified NLS (or TAT) PNAs, although in a lesser extent as compared to polyarginine conjugated PNA, as shown clearly in Figure 36.

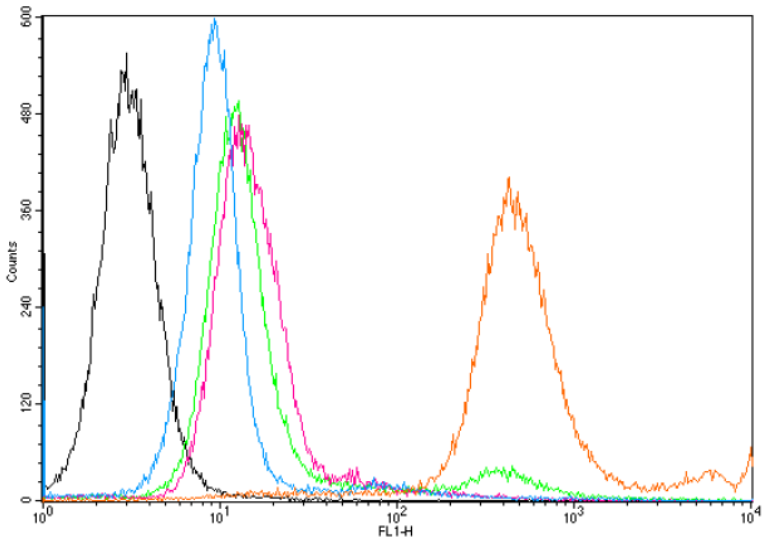

Figure 36: Fluorescence emission of: 1) FITC-PNA5-TAT (green curve); 2)FITC-NLS-PNA5-TAT (pink curve); 3)FITC-PNA6-BiNLS (light blue curve); Negative control and positive control are indicated respectively with a black curve and an orange curve.

3.3. CONCLUSIONS

One aim of this PhD project involved the synthesis of PNA oligomers to target microRNA 210 precursor and inhibit miRNA 210 functions, as it is involved in many diseases and many biological processes. We hypothesized that PNA hybridizing themiRNA precursor, could act as inhibitor already at the level of miRNA maturation process.

In particular two sequences were synthesized, respectively, complementary to the "sense region" (PNA5) and the 5' end region (PNA6) of the target precursor. Furthermore, in order to enhance the cellular uptake, PNAs were conjugated also to a carrier peptide (TAT) and to two nuclear localization signal peptides (NLS, Bi-NLS).

The ability of PNA oligomers to bind pre-miRNA was assessed by fluorescence. A DNA duplex, mimicking the pre-miRNA, was employed to demonstrate the ability of the PNA to give strand invasion opening the DNA duplex and forming a PNA/DNA duplex. After confirming the PNA ability of hybridizing the target sequence, the next step was to verify in a preliminary manner the cellular uptake with FACS experiments. The data show qualitatively that our conjugates are poorly taken up by cells and likely explains their low activity as miRNA nhibitors.

Future plans will focus precisely on the modification of PNA molecules to improve cellular uptake as well as on the synthesis of further sequences complementary to other regions of the miRNA precursor.

3.4. MATERIALS AND METHODS

Protected N-Fmoc-amino acid derivatives, acetic anhydride, coupling reagents and have been purchased from Novabiochem. Activators HBTU, HOBT and HATU were purchased at Inbios (Italy). Fmoc-PNA-cytosine(Bhoc)-OH, Fmoc-PNA-thymine-OH, Fmoc-PNA-guanine(Bhoc)-OH, Fmoc-PNA-adenine(Bhoc)-OH were obtained by Link Technologies.
Acetonitrile (ACN) for LC-MS, N,N-dimethylformamide (DMF) for solid phase synthesis, DIPEA, Dichloromethane were from Romil Pure Chemistry, N-methylmorpholine from Fluka and piperidine from Biosolve.

Fmoc-PAL-PEG-PS (0.18 mmol/g) resin was from Applied Biosystems. All other chemicals were supplied by Sigma-Aldrich and were used without other purification. Preparative purification was carried out on a Shimadzu LC-8A, equipped with a SPD-M10 AV diode array detector. Preparative HPLC was performed on a Phenomex Jupiter 10µm Proteo (90Å 250 x 10.00 mm) column with a flow rate of 5 $mLmin^{-1}$. ^{1}H NMR spectra were recorded on a

Varian 400 MHz spectrometer. Proton chemical shifts are reported in ppm (δ) relative to the solvent reference relative to tetramethylsilane (TMS) (d6-DMSO, d 2.50). Data are reported as follows: chemical shift (multiplicity [singlet (s), doublet (d), triplet (t), quartet (q) and multiplet (m)], coupling constants [Hz], integration). Carbon NMR spectra were recorded on a Varian 500 (125 MHz) spectrometer with complete proton decoupling. Carbon chemical shifts were reported in ppm (δ) relative to TMS with the respective solvent resonance as the internal standard (DMSO, 39.5).

LC-MS analyses were performed on a LC-MS Thermo Finnigan with an electrospray source (MSQ) on a Phenomenex Jupiter 5µ C18 (300Å, 150x460 mm) column with a flow rate of 0.8 $mLmin^{-1}$ at room temperature. Fluorescence spectroscopy was performed on a Varian Spectrophotometer.

3.4.1. PNA 5 synthesis

Synthesis was carried out using repetitive cycles of deprotection, coupling and capping at room temperature. To improve the coupling efficiency double couplings were carried out on PNA-guanine monomers. After each of these cycles two flow washes (25s) with DMF performed.

- Deprotection: 20% piperidine in DMF, 7 minutes
- Coupling: 2.5 equivalents of PNA monomer were dissolved in DMF to a concentration of 0.22M; a solution of HOBT in DMF 0.20M (2.5 equivalents) and a solution of HBTU in DMF 0.20M (2.5 equivalents) were added. 25μL of a mixture of NMM 0.2M in pyridine were added. (Pre-activation time: 1 minute- coupling time:20 minutes).
- Capping: acetic anhydride/2,6 Lutidine/DMF (5/6/89 v/v/v/), 5 minutes.

At the end of the synthesis the resin was washed with DMF, DCM, diethyl ether and dried *in vacuo*. The PNA oligomer was cleaved from the resin and deprotected by a treatment with a solution of TFA/m-cresol (80/20) 90 minutes r.t. The filtrate was flushed by a stream of nitrogen to remove the most of TFA and the PNA oligomer was precipitated by addition of cold diethyl ether, washed three times with diethyl ether and dried *in vacuo* and lyophilized .

PNA 5 purification was carried out by semi-preparative RP-HPLC applying a linear gradient of acetonitrile (0.1% TFA) from 5% to50% in 30 min. 5 mL/min. PNA 5 purity and identity were confirmed by LC-MS system previously described; A gradient of solvent B (0.05% TFA in CH_3CN) from solvent A (0.05% TFA in H_2O) of 5% to 50% was applied over 30 min. and it was identified by electrospray mass analysis.

- PNA 5 (Da): Calculated: 2814.6; $[M+2H]^{2+}$: 1408.3; $[M+3H]^{3+}$: 939.2; $[M+4H]^{4+}$: 704.6.

  Found: 2815.0; $[M+2H]^{2+}$: 1408.5; $[M+3H]^{3+}$: 939.3; $[M+4H]^{4+}$: 704.7.

3.4.2. Peptide Synthesis

All peptides were synthesized by solid phase peptide synthesis as C-terminally amidated and N-terminally derivatives following standard Fmoc chemistry protocol on on a Fmoc-PAL-PEG-PS resin (0.18mmol/g).
Cycles of coupling for each amino acid involves the following steps:

- Deprotection of the N-terminal function (2 step by 5 min) with a solution to a 30% Piperidine in DMF;
- Coupling of 2.5 equivalents of Fmoc-AA, 2.49 equivalents of HOBT/HBTU (0.45 M solution in DMF) and 3.5 equivalents of NMM compared with 0.05 mmol scale synthesis. The reaction time for each pair was 40 min;
- Acetylation two treatments of 5 min with the appropriate volume of a solution of Acetic anhydride (2M)/DIPEA (0.55M)/ DMF).

After each module were performed three washes with DMF for 1min. Cleavage from the solid support was performed by treatment with a TFA/TIS/water (95:2,5:2,5, v/v/v) mixture for 3 hours at R.T.

Crude peptides were analyzed by analytical reverse phase HPLC applying a linear gradient of acetonitrile (0.1% TFA) from 5% to 50% in 30 min. at 0.8 mL/min. Peptide identities were confirmed by LC-MS system previ-

ously described. A gradient of solvent B (0.05% TFA in CH_3CN) from solvent A (0.05% TFA in H_2O) of 5% to 50% was applied over 30 min.

3.4.3. PNA-Peptide conjugates synthesis

The synthesis of PNA-peptide conjugates was carried out in solid phase. The PNA oligomer was increased on PAL-PEG resin (0.18 mmol/g) functionalized with the peptide, employing the same protocol described for the synthesis of PNA 5 oligomer. The conjugates were cleaved by treatment with a solution of 78% TFA, m-cresol 20%, 2% TIS for 3 hours at room temperature.

The *PNA 5- TAT* conjugate was analyzed by analytical RP-HPLC, applying a linear gradient of acetonitrile (0.1% TFA) (0.1% TFA) in water (0.1% TFA) from 5 to 50% in 30 minutes at 0.8 mL/min. The conjugate was purified by semi-preparative RP-HPLC, with the same gradient employed for analytical analysis and characterized by LC-MS system previously described. A gradient of solvent B (0.05% TFA in CH_3CN) from solvent A (0.05% TFA in H_2O) of 5% to 50% was applied over 30 min.

- PNA 5-TAT (Da): Calculated: $[M+3H]^{3+}$: 1549.4; $[M+4H]^{4+}$: 1162.2; $[M+5H]^{5+}$: 929.9; $[M+6H]^{6+}$: 775.1;

  Found: $[M+3H]^{3+:}$ 1551.5; $[M+4H]^{4+:}$ 1163.8; $[M+5H]^{5+:}$ 931.3; $[M+6H]^{6+:}$ 776.3.

The *PNA 5- NLS* conjugate was analyzed by analytical RP-HPLC, applying a linear gradient of acetonitrile (0.1% TFA) (0.1% TFA) in water (0.1% TFA)

from 5 to 50% in 30 minutes at 0.8 mL/min. The conjugate was purified by semi-preparative RP-HPLC, with the same gradient employed for analytical analysis and characterized by LC-MS system previously described. A gradient of solvent B (0.05% TFA in CH_3CN) from solvent A (0.05% TFA in H_2O) of 5% to 50% was applied over 30 min.

- PNA 5-NLS (Da): Calculated: $[M+2H]^{2+}$: 1869.8; $[M+3H]^{3+}$: 1246.8; $[M+4H]^{4+}$: 935.4; $[M+5H]^{5+}$: 748.5; $[M+6H]^{6+}$: 624.0;

  Found: $[M+2H]^{2+}$: 1874.7; $[M+3H]^{3+}$: 1251.3; $[M+4H]^{4+}$: 938.5; $[M+5H]^{5+}$: 751.2; $[M+6H]^{6+}$: 626.1

The *NLS-PNA5- TAT* conjugate was analyzed by analytical RP-HPLC, applying a linear gradient of acetonitrile (0.1% TFA) (0.1% TFA) in water (0.1% TFA) from 5 to 50% in 30 minutes at 0.8 mL/min. The conjugate was purified by semi-preparative RP-HPLC, with the same gradient employed for analytical analysis and characterized by LC-MS system previously described.

A gradient of solvent B (0.05% TFA in CH_3CN) from solvent A (0.05% TFA in H_2O) of 5% to 50% was applied over 30 min.

- NLS-PNA5-TAT (Da): Calculated: $[M+3H]^{3+}$: 1837.9; $[M+4H]^{4+}$: 1378.7; $[M+5H]^{5+}$: 1103.2; $[M+6H]^{6+}$: 919.1; $[M+7H]^{7+}$: 788.2; $[M+8H]^{8+}$: 689.8.

  Found: $[M+3H]^{3+}$: 1839.2; $[M+4H]^{4+}$: 1379.6; $[M+5H]^{5+}$: 1103.9; $[M+6H]^{6+}$: 920.1; $[M+7H]^{7+}$: 788.8; $[M+8H]^{8+}$: 690.3.

PNA 6- Bi-NLS conjugate was analyzed by analytical RP-HPLC, applying a linear gradient of acetonitrile (0.1% TFA) (0.1% TFA) in water (0.1% TFA)

from 5 to 50% in 30 minutes at 0.8 mL/min. The conjugate was purified by semi-preparative RP-HPLC, with the same gradient employed for analytical analysis and characterized by LC-MS system previously described. A gradient of solvent B (0.05% TFA in CH_3CN) from solvent A (0.05% TFA in H_2O) of 5% to 50% was applied over 30 min.

- PNA 6- Bi-NLS (Da): Calculated: $[M+3H]^{3+}$: 1968.0; $[M+4H]^{4+}$: 1476.3; $[M+5H]^{5+}$: 1181.2; $[M+6H]^{6+}$: 984.5; $[M+7H]^{7+}$: 844.0; $[M+8H]^{8+}$: 738.6; $[M+9H]^{9+}$: 656.7; $[M+10H]^{10+}$: 591.1;

  Found: $[M+3H]^{3+}$: 1968.6; $[M+4H]^{4+}$: 1476.7; $[M+5H]^{5+}$: 1181.6; $[M+6H]^{6+}$: 984.8; $[M+7H]^{7+}$: 844.3; $[M+8H]^{8+}$: 738.9; $[M+9H]^{9+}$: 657.0; $[M+10H]^{10+}$: 591.4;

3.4.4. PNA 5-TAT-NLS synthesis

The synthesis of PNA 5-TAT conjugate was carried out in solid phase. The PNA oligomer was increased on PAL-PEG (0.18 mmol/g) resin functionalized with the peptide, employing the same protocol described for the synthesis of PNA oligomer unconjugated.

Mtt group was removed employing several (15-20) short acidic treatment with a solution of DCM/TFA/ TIS (96.5/1/2.5 v/v/v) for 3 minutes. After each treatment washes with DMF for 25s were performed. A treatment with a solution to a 20% DIPEA in DMF for 5 min allowed the anchorage on TAT's side chain of the first amino acid of NLS peptide.

NLS was increased on PNA 5-TAT's side chain, employing the same protocol described for the peptides synthesis. The conjugate was cleaved by

treatment with a solution of 78% TFA, m-cresol 20%, 2% TIS for 3 hours at room temperature.

The *PNA5- TAT-NLS* conjugate was analyzed by analytical RP-HPLC, applying a linear gradient of acetonitrile (0.1% TFA) (0.1% TFA) in water (0.1% TFA) from 5 to 50% in 30 minutes at 0.8 mL/min. The conjugate was purified by semi-preparative RP-HPLC, with the same gradient employed for analytical analysis and characterized by MALDI-TOF Mass Spectrocopy.

- PNA 5-TAT-NLS (Da): Calculated: $[M+H]^+$= 5550.02 m/z;
  Found: $[M+H]^+$= 5456,25 m/z;

3.4.5. *FITC-PNA-Peptide conjugates synthesis*

The synthesis of PNAs-Peptide conjugates was carried out in solid phase. The PNA oligomer was increased on PAL-PEG (0.18 mmol/g) resin functionalized with the peptide, employing the same protocol described for the synthesis of PNA oligomer unconjugated.

The introduction of the linker was carried out in solid phase. Fmoc-HAx-OH was added on PAL-PEG resin functionalized with the PNA-peptide conjugates, employing the same protocol described for the peptide synthesis, involving the following steps:

- Deprotection of the N-terminal function (2 step by 5 min) with a solution to a 30% Piperidine in DMF;
- Coupling of 2.5 equivalents of Fmoc-Hax-OH, 2.49 equivalents of HOBT/HBTU (0.45 M solution in DMF) and 3.5 equivalents of NMM compared with 0.05 mmol scale synthesis. The reaction time for each pair was 40 min;

- Acetylation two treatments of 5 min with the appropriate volume of a solution of Acetic anhydride (2M)/DIPEA (0.55M)/ DMF).

Finally, after deprotection of N-terminal function with a solution to a 30% Piperidine in DMF, 5 equivalents of FITC were added employing 7 equivalents of NMM and time reactions of 1h for each coupling steps. To improve the coupling efficiency double couplings were carried out on each reagents. Conjugates were cleaved by treatment with a solution of 78% TFA, m-cresol 20%, 2% TIS for 3 hours at room temperature.

The *FITC-PNA 5-TAT* conjugate was analyzed by analytical RP-HPLC, applying a linear gradient of acetonitrile (0.1% TFA) (0.1% TFA) in water (0.1% TFA) from 5 to 50% in 30 minutes at 0.8 mL/min. The conjugate was purified by semi-preparative RP-HPLC, with the same gradient employed for analytical analysis and characterized by LC-MS system previously described. A gradient of solvent B (0.05% TFA in CH_3CN) from solvent A (0.05% TFA in H_2O) of 5% to 50% was applied over 30 min.

- FITC-PNA5-TAT (Da): Calculated: $[M+3H]^{3+}$: 1716.1; $[M+4H]^{4+}$: 1287.3; $[M+5H]^{5+}$: 1030.0; $[M+6H]^{6+}$: 858.5; $[M+7H]^{7+}$: 736.1; $[M+8H]^{8+}$: 644.1. $[M+9]^{9+}$: 572.7; $[M+10]^{10+}$: 515.5.

  Found: $[M+3H]^{3+}$: 1709.8; $[M+4H]^{4+}$: 1282,6; $[M+5H]^{5+}$: 1026.7; $[M+6H]^{6+}$: 855.6; $[M+7H]^{7+}$: 733.0; $[M+8H]^{8+}$: 642.0. $[M+9]^{9+}$: 570.3; $[M+10]^{10+}$: 513.7.

The *FITC-PNA 6-Bi-NLS* conjugate was analyzed by analytical RP-HPLC, applying a linear gradient of acetonitrile (0.1% TFA) (0.1% TFA) in water

(0.1% TFA) from 5 to 50% in 30 minutes at 0.8 mL/min. The conjugate was purified by semi-preparative RP-HPLC, with the same gradient employed for analytical analysis and characterized by LC-MS system previously described. A gradient of solvent B (0.05% TFA in CH_3CN) from solvent A (0.05% TFA in H_2O) of 5% to 50% was applied over 30 min.

- FITC-PNA 6-Bi-NLS (Da): Calculated: $[M+4H]^{4+}$:1604.6; $[M+5H]^{5+}$: 1281.5; $[M+6H]^{6+}$: 1068.1; $[M+7H]^{7+}$: 915.7; $[M+8H]^{8+}$: 801.3; $[M+9H]^{9+}$: 712.7

  Found: $[M+4H]^{4+}$:1601.6; $[M+5H]^{5+}$: 1282.1; $[M+6H]^{6+}$: 1068.6; $[M+7H]^{7+}$: 916.1; $[M+8H]^{8+}$: 801.3; $[M+9H]^{9+}$: 712.4;

The ***FITC-NLS-PNA5-TAT*** conjugate was analyzed by analytical RP-HPLC, applying a linear gradient of acetonitrile (0.1% TFA) (0.1% TFA) in water (0.1% TFA) from 5 to 50% in 30 minutes at 0.8 mL/min. The conjugate was purified by semi-preparative RP-HPLC, with the same gradient employed for analytical analysis and characterized by LC-MS system previously described. A gradient of solvent B (0.05% TFA in CH_3CN) from solvent A (0.05% TFA in H_2O) of 5% to 50% was applied over 30 min.

- FITC-NLS-PNA 5-TAT (Da): Calculated: $[M+4H]^{4+}$: 1504.6; $[M+5H]^{5+}$: 1203.4; $[M+6H]^{6+}$: 1003.1; $[M+7H]^{7+}$: 859.9; $[M+8H]^{8+}$: 752.5; $[M+9]^{+9}$: 669.0; $[M+10H]^{10+}$: 602.2; $[M+11H]^{11+}$: 547.6; $[M+12H]^{12+}$: 502.0; $[M+13]^{13+}$: 463.4.

  Found: : $[M+4H]^{4+}$: 1498.0; $[M+5H]^{5+}$: 1198.5; $[M+6H]^{6+}$: 997.6; $[M+7H]^{7+}$: 856.4; $[M+8H]^{8+}$: 749.0; $[M+9]^{+9}$: 665.7; $[M+10H]^{10+}$: 599.0; $[M+11H]^{11+}$: 544.3; $[M+12H]^{12+}$: 499.7; $[M+13]^{13+}$: 461.0.

3.4.6. Synthesis of TO-PNA 5-TAT conjugate

3.3.6.a *Preparation of compound 1 (Figure 29)*

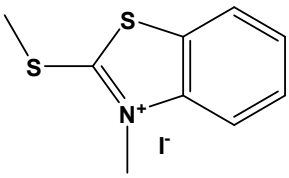

3-methylbenzothiazole-2-thione (2.00 g, 11.0 mmol, 1.00 equiv.) and methyl iodide (3.00 g, 21.1 mmol, 1.92 equiv.) were combined in a 50 mL round bottom flask sealed with a rubber septa and heated to 45 °C for 5 hours. The reaction mixture became a white solid. After cooling to 25 °C, the solid was resuspended in 100 mL methanol. Diethyl ether (75 ml) was added to ensure that the product had fully precipitated. The precipitate was collected by vacuum filtration and dried under reduced pressure to yield 2.74 g (77%) of a white solid. **UV-Vis**: λ_{max} (H_2O): 226 nm (ε= 24,700 $M^{-1}cm^{-1}$), 306 nm (ε= 17,200 $M^{-1}cm^{-1}$); **^{1}H NMR** (400 MHz, DMSO) d 3.13 (s, 3H, SCH_3), 4.12 (s, 3H, NCH_3), 7.73 (m, 1H, Ar), 7.85 (m, 1H, Ar), 8.20 (d, J= 8.42 Hz, 1H, Ar), 8.40 (d, J= 8.42 Hz, 1H, Ar);

3.3.6.b *Preparation of compound 2 (Figure 29)*

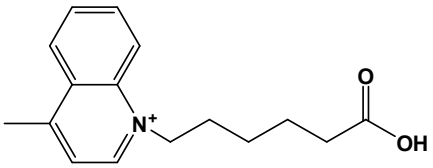

Lepidine (2.21 g, 15.5 mmol, 1.00 equiv.) and 6-bromohexanoic acid (3.29 g, 16.9 mmol, 1.09 equiv.) were combined in a 100 mL round bottom flask sealed with a rubber septa and heated at 125 °C for 5 hours.

The resulting brown residue was dissolved in 28 mL of methylene chloride and the product was precipitated upon addition of 16 mL of acetone. The precipitate was collected by vacuum filtration and dried under reduced pressure to yield 2.87 g (55%) of a tan solid. **UV-Vis**: λ_{max} (H_2O) 234 nm (ε= 33,200 $M^{-1}cm^{-1}$), 314 nm (ε= 8,300 $M^{-1}cm^{-1}$); **^{1}H NMR** (400 MHz, DMSO) d

1.40 (m, 2H, CH_2), 1.56 (m, 2H, CH_2), 1.96 (m, 2H, CH_2), 2.23 (t, J= 7.2 Hz, 2H, CH_2), 3.01 (s, 3H, CH_3), 5.01 (t, J= 7.5 Hz, 2H, NCH_2), 8.07 (m, 2H, Ar), 8.27 (m, 1H, Ar), 8.58 (m, 2H, Ar), 9.42 (d, J= 5.85 Hz, 1H, Ar);

3.3.6.c *Preparation of compound 3 (Figure 29)*

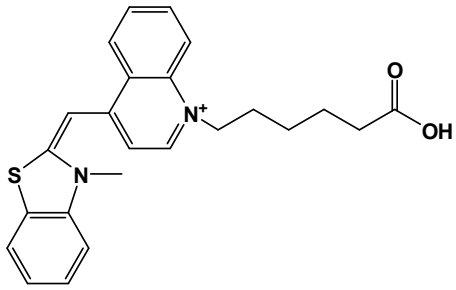

Compound **1** (1.21 g, 3.58 mmol, 1.00 equiv.) and compound **2** (1.16 g, 3.58 mmol, 1.00 equiv.) were suspended in 36 mL of ethanol and heated to 70 °C for 1 hour to dissolve.

Triethylamine (1.10 mL, 7.82 mmol, 2.18 equiv.) was then added and the reaction was cooled to 50 OC. After 3 hours, the slurry was allowed to cool to 25 °C, and diethyl ether (107 mL) was added to fully precipitate a red solid. The crude solid was suspended in acetone (70 mL)/ ether (100 mL) for 1 hour, collected by vacuum filtration and dried under reduced pressure to yield 1.06 g (56%) of a red solid. **UV-Vis**: λ_{max} (H_2O) 502 nm (ε= 66400 $M^{-1}cm^{-1}$); **^{1}H NMR** (400 MHz, DMSO) d 1.38 (m, 2H, CH_2), 1.56 (m, 2H, CH_2), 1.86 (m, 2H, CH_2), 2.21 (t, J= 7.2 Hz, 2H, CH_2), 4.03 (s, 3H, NCH_3), 4.61 (t, J= 7.2 Hz, 2H, NCH_2), 6.94 (s, 1H, CH), 7.40 (m, 2H, Ar), 7.62 (m, 1H, Ar), 7.77 (m, 2H, Ar), 8.00 (m, 1H, Ar), 8.07 (d, J= 4 7.69 Hz, 1H, Ar), 8.15 (d, J= 9.16 Hz, 1H, Ar), 8.65 (d, J= 6.96 Hz, 1H, Ar), 8.81 (d, J= 8.62 Hz, 1H, Ar); **^{13}C NMR** (125 MHz, DMSO): d 175.6, 161.2, 149.7, 145.6, 141.7, 138.2, 134.5, 129.4, 128.0, 127.0, 126.0, 125.4, 125.1, 124.1, 119.3, 114.2, 109.0, 89.3, 55.2, 35.1, 34.9, 29.8, 26.7, 25.3;

3.3.6.d *Preparation of TO-peptide conjugates (Figure 29)*

TO-PNA5-TAT conjugate was synthesized on solid support using commercially available Fmoc-PAL-PEG-PS (0.18 mmol/g). The TO was increased on PAL-PEG (0.18 mmol/g) resin functionalized with the PNA 5-TAT conjugate, employing the following protocol:

- Deprotection of the N-terminal function (2 step by 5 min) with a solution to a 30% Piperidine in DMF;
- Coupling of 2.5 equivalents of TO, 2.49 equivalents of HOBT/HBTU (0.45 M solution in DMF) and 3.5 equivalents of NMM compared with 2 μmol scale synthesis. The reaction time for each pair was 1h;
- Acetylation two treatments of 5 min with the appropriate volume of a solution of Acetic anhydride (2M)/DIPEA (0.55M)/ DMF).

The conjugates were cleaved by treatment with a solution of 78% TFA, m-cresol 20%, 2% TIS for 3 hours at room temperature.

TO-PNA5-TAT purification was carried out by semi-preparative RP-HPLC applying a linear gradient of acetonitrile (0.1% TFA) from 5% to50% in 30 min. 5 mL/min. PNA 5 purity and identity were confirmed by LC-MS system previously described; A gradient of solvent B (0.05% TFA in CH_3CN) from solvent A (0.05% TFA in H_2O) of 5% to 70% was applied over 30 min. and it was identified by electrospray mass analysis.

- TO-PNA5-TAT (Da): Calculated: $[M+3H]^{3+}$: 1678.3; $[M+4H]^{4+}$: 1259.1; $[M+5H]^{5+}$: 1007.6; $[M+6H]^{6+}$: 839.6; $[M+7H]^{7+}$: 719.8; $[M+8H]^{8+}$: 630.1; $[M+9H]^{9+}$: 560.1.

- Found: : $[M+3H]^{3+}$: 1676.2; $[M+4H]^{4+}$: 1257.4; $[M+5H]^{5+}$: 1006.2; $[M+6H]^{6+}$: 838.6; $[M+7H]^{7+}$: 718.9; $[M+8H]^{8+}$: 629.6; $[M+9H]^{9+}$: 559.7.

3.4.7. TO-PNA 5-TAT strand invasion and fluorescence measurement

DNA5-DNA5c duplex was obtained employing 1μM of DNA 5 and 1μM of DNA 5c in buffered solution (100 mM NaCl, 10 mM NaH_2PO_4, pH 7.0). After annealing reaction (90° C 5 min, 4°C over night), strand invasion experiments using TO-PNA 5-TAT were performed, adding : a) 1μM of probe to duplex solution (TO-PNA 5-TAT: DNA5/DNA5c ratios was 1:1); b) 2μM of probe to duplex solution (TO-PNA 5-TAT: DNA5/DNA5c ratios was 2:1);

Fluorescence measurements were carried out in buffered solution (100 mM NaCl, 10 mM NaH_2PO_4, pH 7.0), employing 1μM oligos and probes in a final volume of 2.5 mL (λ_{ex}=470 nm, $slit_{ex}$ = 2.5, $slit_{em}$= 10.0).

The DNA sequences were:

5-CAGGGCAGCCCCTGCCCACCGCACACTGCGCTGCACGTACGT-3' (DNA5) and 5'-CCAGACCCACTGTGCGTGTGACAGCGGCTGATCTG-3' (DNA5c).

CHAPTER 4

4. *SECOND GENERATION PNA*

The success of PNAs unveiled that oligonucleotide analogs could be obtained with drastic changes from the natural structure, provided that some important structural features were preserved. The PNAs scaffold has served as a model for the design of new compounds able to perform DNA recognition[117].

Synthetic organic chemistry has played a fundamental role in the achievement of these goals, by allowing to obtain new structures for the PNA monomers, and by developing novel strategies for oligomer synthesis (Figure 37). Since their discovery many modifications of PNA structures have been proposed, in order to improve their performances in term of affinity and specificity towards complementary oligonucleotides. A modification introduced in the PNAs structure can improve its pharmacological potential generally in three different ways: i) improving DNA binding affinity; ii) improving sequence specificity, in particular for directional preference (antiparallel vs parallel) and mismatch recognition[118]; iii) improving bioavailability (cell internalization, pharmacokinetics, etc.).

This area of research has been particularly active and the recent literature is full of publications that describe the synthesis and properties of new analogues of PNA[119].

Modified nucleotide bases can be used to interfere in the processes of hybridization (Figure 38).

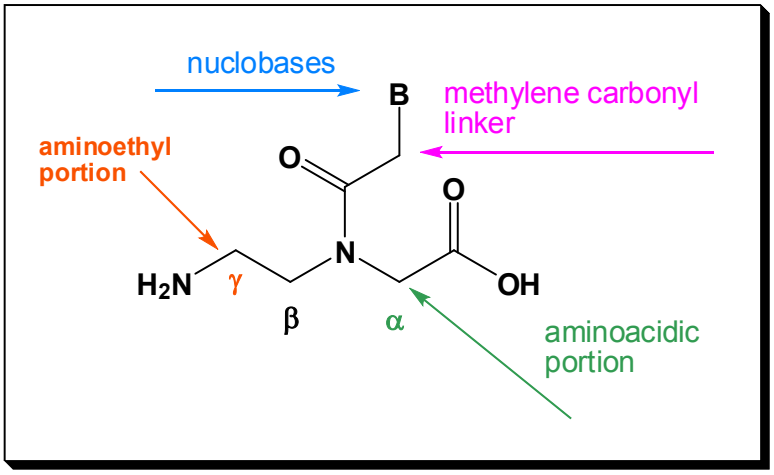

Figure 37: PNA structural modifications

For example, a N4-benzoyl cytosine (1) is able to inhibit the formation of the triplex $(PNA)_2$/DNA as it creates steric hindrance reason[120]. The base pair 2-thiouracil (2) and 2.6-diamminopurina (3) acts on the recognition between PNA and DNA with a peculiar mechanism known as double-duplex invasion leading to the formation of the complex with stoichiometry $(PNA)_2$-$(DNA)_2$[121]. The replacement of cytosine with 5-methylcytosine (4) in a PNA-DNA chimera increases the stability of the duplex, while the replacement of thymine with 5 - bromouracil (5) has no effect in terms of increased or decreased stability. Instead, the simultaneous introduction of two modified bases 4 and 5 in a PNA-DNA chimera causes a destabilization of the triple helix $(DNA)_2$/PNA-DNA, if compared to a DNA triplex[122].

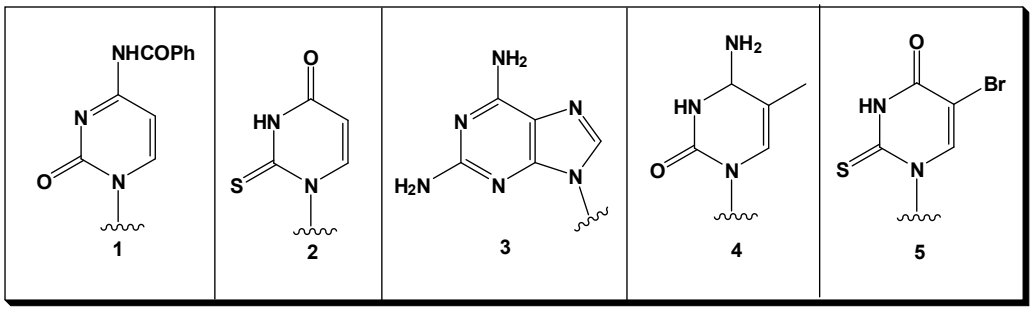

Figure 38: Examples of modified nucleobases.

Modifications in the linker have underlined the importance of the methylene carbonyl group for the structural organization of a PNA oligomer and the hybridization process. In fact, the replacement of these with both rigid and flexible linker led always to a duplex destabilization. A devastating effect on the binding properties of PNA was observed with the conversion of the tertiary amide bond in the corresponding tertiary amine[76] (Figure 39).

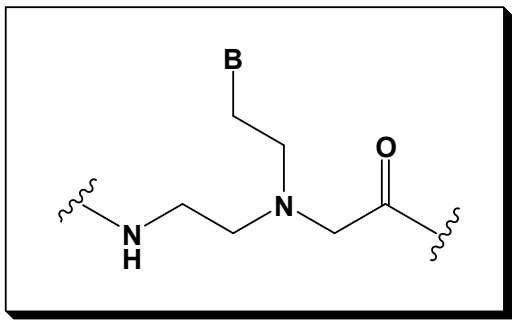

Figure 39: Replacement of the methylene carbonyl linker with a more flexible ethylene linker

4.1. CHEMICAL MODIFICATION OF PNA BACKBONE

Introduction of different functional groups with different charges/ flexibility/polarity in the backbone have been described[119a,123-124] and these study showed that a "constrained flexibility" is necessary to have a good DNA binding. On the basis of these studies, modified PNAs have been constantly improved during the years, using the concept of "preorganization", i.e. the ability of adopt a conformation suitable for DNA binding, thus minimizing the entropy loss of the binding process.

Figure 40 shows the main strategies used to achieve this goal. Preorganization was obtained either by cyclization of the PNA backbone (in the aminoethyl side or in glycine side), by adding substituents in the C_2 (α position)

or C_5 (γ position) carbon of the monomer or by inserting the aminoethyl group in cyclic structures[125].

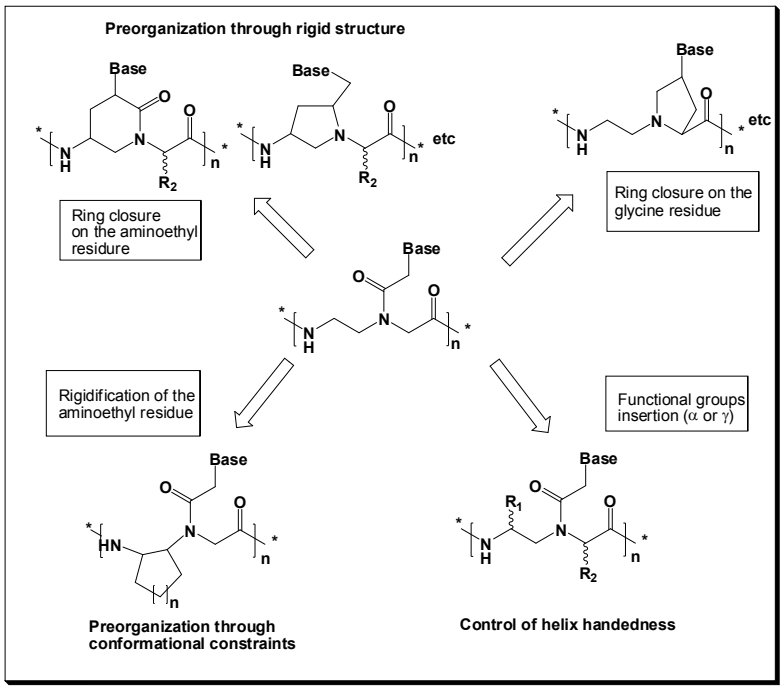

Figure 40: Strategies for inducing preorganization in the PNA monomers.

The two classes of PNA with conformationally constrained backbones which have shown improved properties are acyclic PNAs with functional backbones and cyclic PNAs, in which preorganization is achieved through conformational constraint or through rigidification of the backbone.
In the following paragraphs the classes of acyclic PNAs will be discussed in details.

4.1.1. ACYCLIC PNAS WITH CONSTRAINED STRUCTURES

In 1994, Nielsen and co-workers showed how the insertion of a methylene group in any position of the PNA backbone or in the linker between the backbone and the nucleobase resulted in a net loss of DNA binding properties. This fact was subsequently explained in terms of "constrained flexibil-

ity" of PNAs: in order to be a good DNA binding molecule, a modified oligonucleotide should not be too flexible, nor too rigid.

Using the linear *N*-(2-aminoethyl)glycine as starting point, several PNA derivatives were obtained by insertion of side chain either at the C_α or C_γ carbon atoms[126]. These modifications could modulate the conformational properties of PNA. Nielsen at al., starting from L-amino acid synthons, synthesized Cα-substituted chiral PNAs and showed that the insertion of an amino acid derived side chain slightly destabilized antiparallel PNA-DNA duplexes. Chiral PNAs derived from alanine or from arginine and lysine side chains showed the best affinity for DNA, on account, respectively, of the small steric hindrance and of the electrostatic interaction with the negatively charged DNA strand. Instead PNAs bearing side chains derived from bulky apolar amino acids (valine, tryptophan or phenylalanine) displayed a bad affinity for DNA. These data clearly showed that the steric hindrance is responsible for the destabilization of PNA / DNA duplexes.

The affinity of chiral PNAs for complementary DNA was found to be also influenced by the enantioselectivity. In absence of any stereogenic centers, two achiral complementary PNAs will form an equimolar mixtures of left-handed and right-handed helices. Instead, the addition of some stereogenic centers in one of the PNA strands, leads to the predominance of an orientation of the helices[127].

On the basis of such premises, Sforza and colleagues have synthesized PNAs containing a chiral D-lysine and by X-ray diffraction they showed that D-configuration allows the lysine side chains to be placed in an optimal position to fit in right-handed helix, whereas the L-lysine side chains would have given strong intra-strand steric clashes[128].

These studies were further confirmed by Nielsen and colleagues (creating PNA monomers substituted in α position by D lysine) and by Ly and co-workers (they developed cell-penetrating arginine PNAs).

In conclusion the use of several C_α-substituited lysine-based monomers inserted in a PNA strand allows to prevent self-aggregation of complementary PNA sequences, while increasing the affinity for negatively charged DNA[129]. However only a few such modifications showed improvements in the hybridization properties, many of which require either elaborate synthesis or the use of relatively expensive D-amino acids as starting materials (because L-configuration in α position does not allow to bind to DNA or RNA).

For these reasons gamma Peptide Nucleic Acid have been recently investigated. A detailed study was performed by Sforza et al. by comparing chiral PNAs substituted with L- or D-lysine at either α and γ position or at both position simultaneously[130]. They confirmed that γPNAs derived from L-amino acids adopted a right-handed helix and they are able to hybridize to DNA and RNA with high affinity and sequence selectivity[128]. Starting from these considerations, modifications at γ position seems to be the most promising because of the simplicity and flexibility in synthesis and the benefits that they confer on the hybridization properties of PNA. Several analogues have been explored so far, having methyl, hydroxymethyl, thiomethyl, aminobutyl and guanidinium groups[131, 132] (Figure 41).

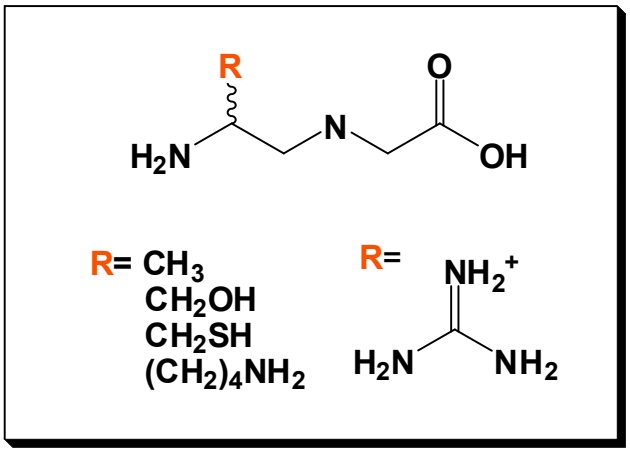

Figure 41: γ-modified PNA analogues

The introduction of a side chain in the position γ does not compromise DNA binding. For example, functionalization of the position with a γ butylamino group, such to mimic the lysine side chain, not only does not affect the formation of PNA/DNA duplex, but also leads to a slight increase in thermal stability of the complex formed. Moreover, these features are preserved even if the amino group of the lysine side chain is further functionalized with quite bulky molecules, such as fluorophores[133].

Rapireddy et al. showed that GPNA, PNA analogues with a guanidine group on the α position of the backbone, designed to target the transcriptional start-site of the E-cadherin gene were demonstrated to effectively inhibit protein translation, showing low toxicity and high cell permeability[119a]. These analogues were found unable to inhibit gene transcription, probably due to electrostatic interactions with the phosphates of nucleic acids which slow down the diffusion of the molecules in the cytoplasm and in the nucleus. Sahu and colleagues have proposed instead a second generation of GPNA arising from L-amino acids and in which the guanidinium group is located in gamma position[134]. These derivatives have shown favorable properties of hybridization as well as cellular uptake.

Recently Crawford et al. have shown that the substitution at the γ-position of a number of amino acid side chains with varying degree of steric hindrance (valine, isoleucine, phenylalanine, alanine) does not affect the hybridization properties of PNAs[135].

Studies on γ PNA oligomers demonstrated that preorganization is a requisite to increase the affinity of binding toward complementary nucleic acids while the presence of positive charges on the backbone increases their cellular uptake. CD studies on PNA oligomers containing γ hydroxymethyl have shown that these oligomers are structurally preorganized[131c]; The secondary structure of the oligomers depends on the position of the chiral moiety and is induced when the chiral moiety is at the C-terminus. Recently the crystal

structure of a γ PNA/DNA duplex has been solved; these studies revealed that the helix is induced by the steric clash between the γ carbon and the nitrogen of the tertiary amide of the backbone and is stabilized by the sequential base stacking[136].

Interestingly the stability of the hybrids is not influenced by the spacing between the chiral units. Furthermore γ PNA are the only analogue discovered so far having the ability to invade a mixed sequence DNA double helix[131d, 137]. The ease and flexibility of synthesis, along with superior hybridization properties and enzymatic stability, make γPNAs an attractive nucleic acid platform for various biological and medical applications- as molecular tools as well as therapeutic and diagnostic reagents.

4.2. *RESULTS AND DISCUSSION*

4.2.1. SYNTHESIS AND CHARACTERIZATION OF γ SULPHATE PNAS

Encouraged by these results reported in the literature on γ PNA and with the aim to develop a new PNA analogue more DNA-like in terms of polarity, charge and solubility we undertook studies on γ PNAs having a sulphate moiety in the gamma position of the backbone. Studies on γ sulphate PNA add a new brick to our knowledge on the effect of charge on the secondary structure, stability of the hybrids and potential of the modified oligomer to be biologically active.

The sulphate group is, in fact, very similar to the phosphate of DNA, in geometry, steric hindrance, polarity; furthermore a sulphate monoester has the same charge as the phosphate diester present in oligonucleotides. The sulphate PNA should in principle keeps the advantages of standard PNA (stability to degradation and binding affinity) and also should be more soluble, less prone to aggregation. Two more advantages of this negatively charged analogue are: 1) the possibility to increase its uptake employing the tools commonly used for DNA transfection[138] . In fact PNA and PNA analogues (with the only exception of γ guanidine PNA[134]), although showing high binding affinity towards natural nucleic acids and high stability to enzymatic degradation, do not easily cross the cell membrane and consequently show weak biological activity (the delivery of PNA by lipofectamine or other cationic lipids employed for the common DNA delivery has been demonstrated only for PNA complexed to DNA or PNA conjugated to negatively charged peptides[77, 139]). 2) the lack of unspecific interactions with nucleic acids, which instead may occur with positively charged PNA analogues, as the guanidine PNA.

In this work γ sulphate PNAs were investigated, setting up protocols for the synthesis of γ sulphate PNA monomers and oligomers. PNA γ sulphate monomers were obtained after derivatization of γ-hydroxymethyl monomers, synthesized employing a modified version of the protocol reported in the literature for γ Ser PNA starting from L-Fmoc-Ser(OtBu)-OH[131c] (Figure 42).

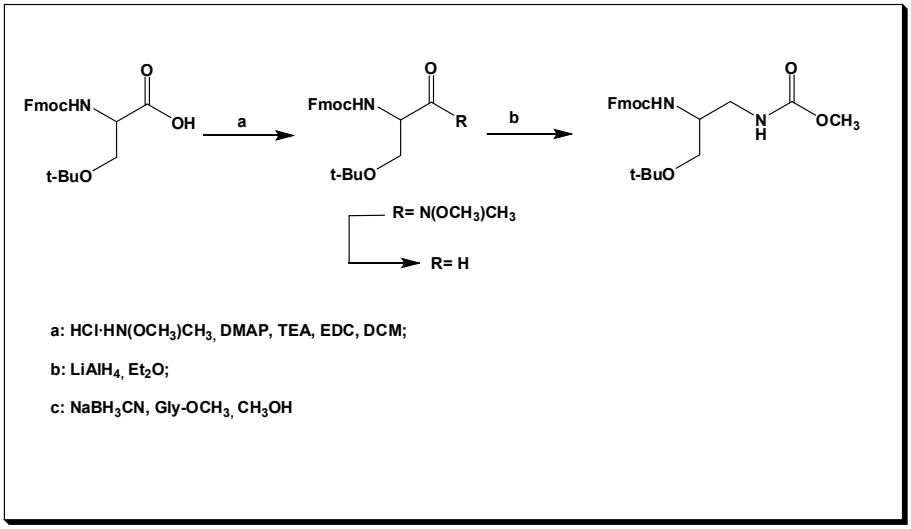

Figure 42: Strategy for γ functionalized backbone synthesis

The amino acid was converted into the corresponding amide by reaction with N,O-dimethylhydroxylamine hydrochloride, in presence of DMAP, TEA, and EDC as activator. The product was purified by extraction with HCl, $NaHCO_3$ acq. and 10% H_2O and finally chromatographed on silica gel. The reaction proceeds with high yields. The reduction of the amide function with lithium aluminum hydride in Et_2O gives the corresponding aldehyde, isolated after extraction with ethyl ether and water with a quantitative yield. Finally, the aldehyde was subjected to reductive amination with glycine methyl ester and DIPEA, thus generating the γ modified backbone.

The functionalization of the bases, involved the anchorage to N 1 of the pyrimidines (C, T) or the N 9 of purines (G, A) of a methylene carbonyl group, essential in order to react with the amino group in α position of glycine .

First of all the bases that possess the exocyclic NH_2 should be properly protected; the choice of protecting groups for exocyclic amino functions and the terminal amino function of the backbone falls to orthogonal protecting groups. In the monomers the exocyclic amines of the nucleobases A, C and G are protected with base labile groups (benzoyl for A and C, isobutyryl for G, Figure 43)[140].

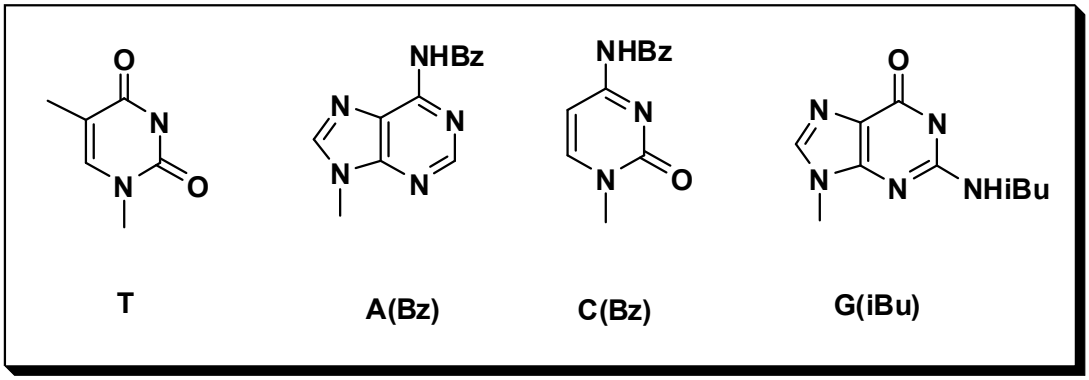

Figure 43: Protected Bases

The functionalization of the four nucleobases has been achieved through a strategy described in the literature that involves the introduction of the methylene carbonyl linker employing methyl-bromoacetate in DMF for thymine and guanine, tert-butyl-bromoacetate in DMF for adenine and benzyl bromoacetate for cytosine.

The products were purified by filtration or liquid chromatography on silica gel. The modified backbone was used for the coupling reaction with the derivatized bases (Figure 44) employing DMAP and EDC.

In order to use these modified monomers in the solid-phase synthesis, it was necessary to remove the ester function on the carboxyl group by a very strong basic hydrolysis, which caused also the removal of the Fmoc protecting group, successively reintroduced employing Fmoc-OSu and sodium bicarbonate.

Finally, after removing under mild acid condition tert-butyl group on γ-hydroxymethyl function, the sulphate was installed on the hydroxyl after reaction with the DMF·SO_3 complex and treatment with TBA/$NaHCO_3$.

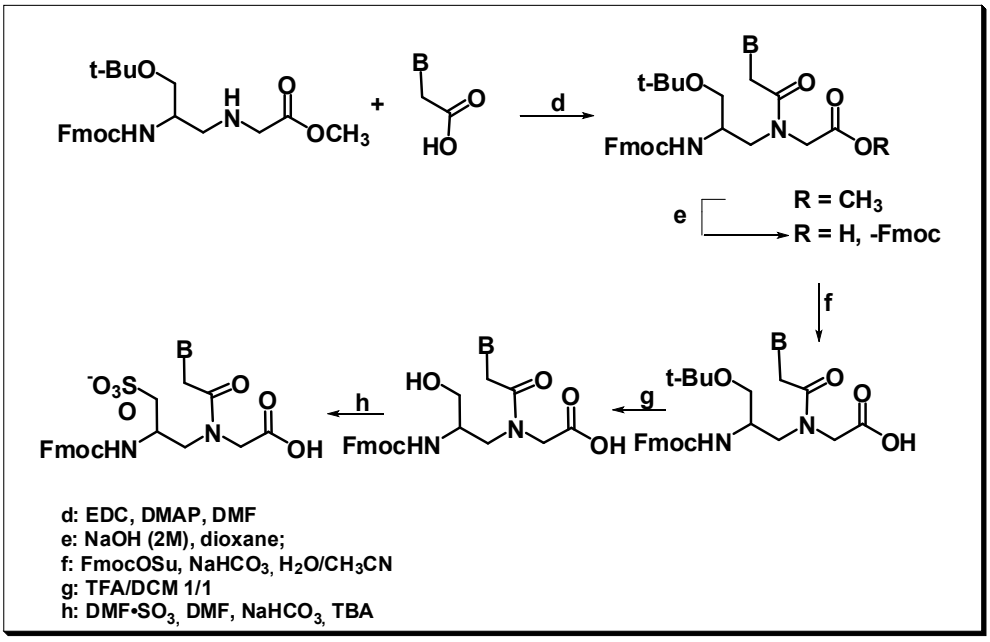

Figure 44: strategy for γ sulfate monomers

TBA acts as a counterion to stabilize the sulfate group, which otherwise would be acid labile, thus making this molecule not compatible with the reaction conditions used in solid-phase synthesis. The stability of the sulphate to both acidic and basic conditions was verified in two separate experiments carried out treating the t^S monomer with the cleavage and deprotection solutions, respectively a concentrated TFA solution for 2 hours at room temperature and a concentrated ammonia solution at 50°C for 16 hours[141] (data not shown). The reactions were monitored by LC-MS; except for the removal of the Fmoc group occurring in basic conditions, no other reaction was observed, demonstrating thus that the TBA counterion is sufficient to stabilize the sulphate group. All monomers were characterized by electrospray mass analysis and NMR (Figure 45).

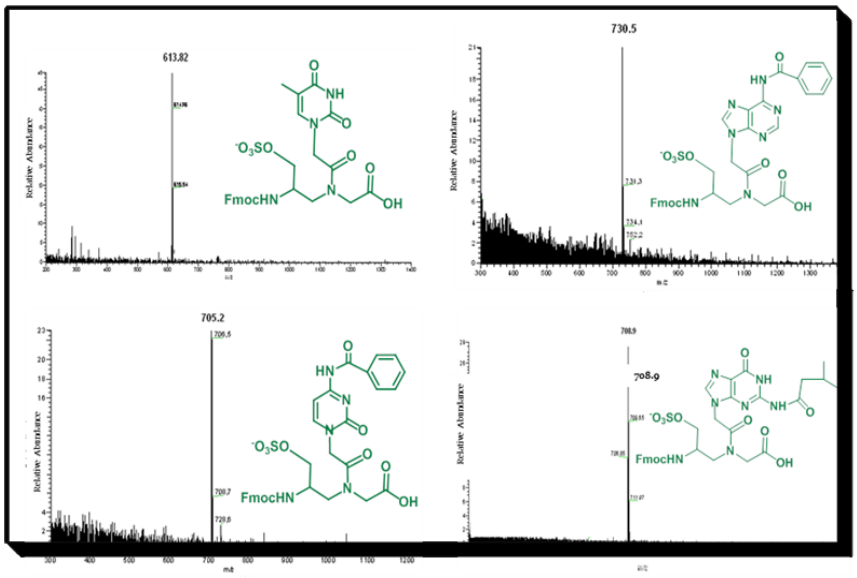

Figure 45: mass spectra of modified monomers

We performed NMR experiments on Fmoc-PNA ^{OH} and Fmoc- PNA^{S} monomers dissolved in DMSO[142]. The discussion is limited to the guanine monomer but the spectral features described were also observed for the other monomers. An expansion of the backbone region of the 2D-TOCSY[143] for the two guanine monomers (g^{OH} in red and g^{S} in blue) is reported in Figure 46.

NMR studies reveal that all monomers exist as a mixture of two rotamers, due to the rotation around the C7-N4 bond, with rotamer **A** being the most abundant.

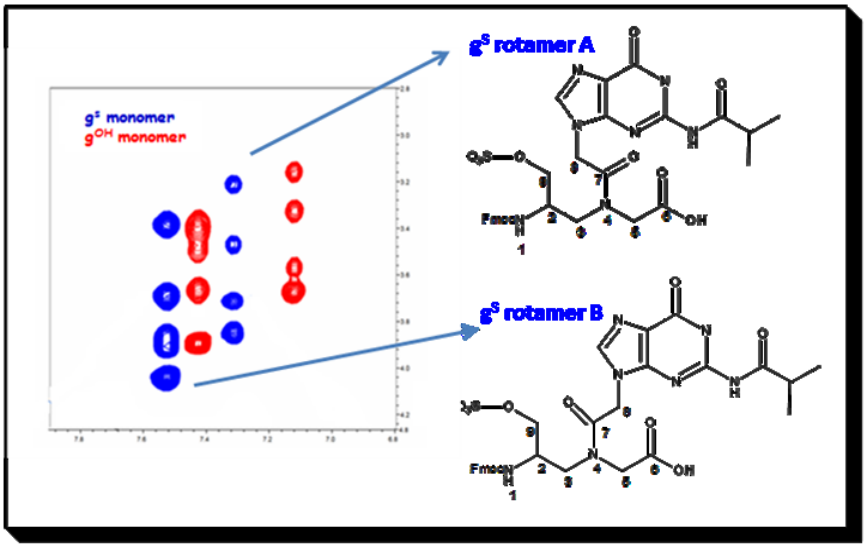

Figure 46: superimposition of the 2D-TOCSY , expansion of the backbone region, for the g^S and g^{OH} monomers.

As expected ^1H NMR signals of the backbone shift downfield upon introduction of the sulphate on the C_2 hydroxymethyl (Table 5).

protons	g^S rotamer A	g^S rotamer B	g^{OH} rotamer A	g^{OH} rotamer B
1	7.53	7.32	7.43	7.12
2	4.04	3.85	3.90	3.67
3a	3.69	3.47	3.49	3.33
3b	3.39	3.21	3.37	3.16
9	3.87	3.71	3.67	3.57

Table 5: ^1H chemical shift for the g^S and g^{OH} backbone protons.

The NOESY spectrum has been used to determine the geometry of the tertiary amide bond: a NOE[144] cross-correlation peak between H-8 and H-3 is found in the conformation where the carbonyl C-7 points toward the C terminus (rotamer A), while a NOE cross-correlation peak between H-8 and H-5 where C-7 carbonyl group points toward the N terminus (rotamer B) (Figure 47). A clear difference is evident between the two monomers: the signals for rotamer A and B of the Fmoc- g^{OH}-OH monomer have a comparable intensity while in the Fmoc-g^{S}-OH monomer the signals of rotamer A have about two times the intensity of those of rotamer B.

This indicates that in the Fmoc-g^{S}-OH monomer the conformation in which the C-7 carbonyl group points toward the C-terminus is slightly favoured. γ modified PNA monomers show different conformational preferences depending on the steric hindrance of the substituent on C_2. To gain details on the structural preferences of sulphate PNA monomers, studies were performed to identify and evaluate the coupling pattern of the spin system composed of H-2, H-3a, H-3b by a DQ-COSY experiment carried out on the sulphate guanine monomer (g^{s}). The signal of H-3a for rotamer A appears as doublet of doublets with coupling constants of ~15 and ~10 Hz, while H-3b appears as a doublet of doublets with coupling constants of ~15 and ~5 Hz. (Figure 47).

This suggests the presence of a preferred conformation in solution that involves one trans diaxial interaction (180°) between H-2 and H-3a (J of ~10 Hz) and one axial to equatorial interaction (+60°) between H-2 and H-3b (J of ~5 Hz).

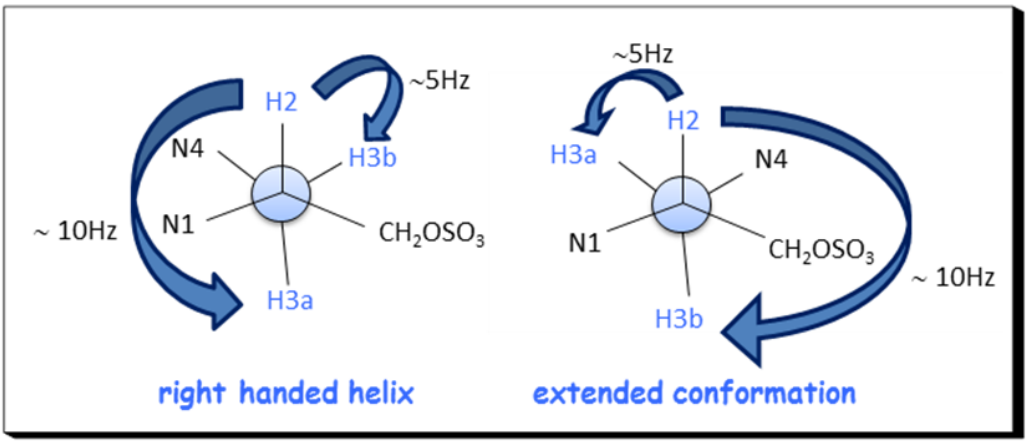

Figure 47 : the two hypothesized conformations for the g^S monomers.

The ~15 Hz coupling constant corresponds to the geminal coupling (J_2) between H-3a and H-3b. For rotamer B we observe a ~10 Hz coupling constant between H-3b and H-2 corresponding to a trans diaxial relationship, and a ~5 Hz coupling constant between H-3a and H-2 corresponding to an equatorial to axial relationship (Figure 48). Being R the absolute configuration at C-2, the conformation that produces the relative spatial arrangement of protons H-2, H-3a, and H-3b in rotamer A corresponds to that observed in PNA monomers when they are in oligomers forming a right-handed helix.

The conformation of rotamer B corresponds to an extended conformation. These data suggest that the introduction of a sulphate in the gamma position of the backbone partially modifies the conformational preferences of γ modified hindered monomers. Interestingly, the conformation of rotamer A reproduces the situation observed in valine and isoleucine γ modified monomers[136]. The restricted rotation around C2-C3 forces the monomer in a specific conformation, corresponding to the one adopted in a right handed helix. On the other hand, rotamer B, assumes a more extended conformation, as demonstrated by the inversion in the pattern of coupling constants.

The next step was to set up experimental conditions for the solid phase coupling for all four monomers. A series of mixtures of activator and bases were tested. The best coupling conditions result to be the following.
For Fmoc- t^S-OH: 50 µL of a 0.3M solution (7.9 eq.) in an. DMF of monomer, 50 µL of HBTU (0.2M) (5.2 eq.) in DMF, 50 µL MDCH (0.8M) in pyridine, 30 minutes. For Fmoc- c^S (Bz)-OH, Fmoc-a^S (Bz)-OH, Fmoc g^S (iBu)-OH: 50 µL of a 0.3M solution (7.9 eq.) in an. DMF of monomer, 50 µL of HBTU (0.2M) (5.2 eq.) in DMF, NMM 0.2M, 50 µL of pyridine 0.2M in DMF , 30 minutes.
To target the *ErbB2* gene promoter, the sequence CTCCTCCTC, encompassing tract from -220 to -228 upstream of the first codon, was chosen[141a-146].

In the sequence all T were inserted as sulphate T (t^S). Studies were focused on a homopyrimidine oligomer designed to interfere with the transcription of the gene ErbB2, a cell membrane surface-bound receptor tyrosine kinase normally involved in the signal transduction pathways leading to cell growth and differentiation. ErbB2 is encoded within the genome by Her2/neu, a known proto-oncogene of great importance for its involvement in breast cancer development and its correlation to increased chemoresistance of the cancer cells[145, 146].

The oligomer $ct^Scct^Scct^Sc$ (PNA7 S) was assembled on a PAL-PEG resin using standard conditions for the standard monomers[147] and the conditions described earlier for the t^S building blocks. The oligomer was cleaved in standard conditions, purified by RP-HPLC and characterized by LC-MS (Figure 48).

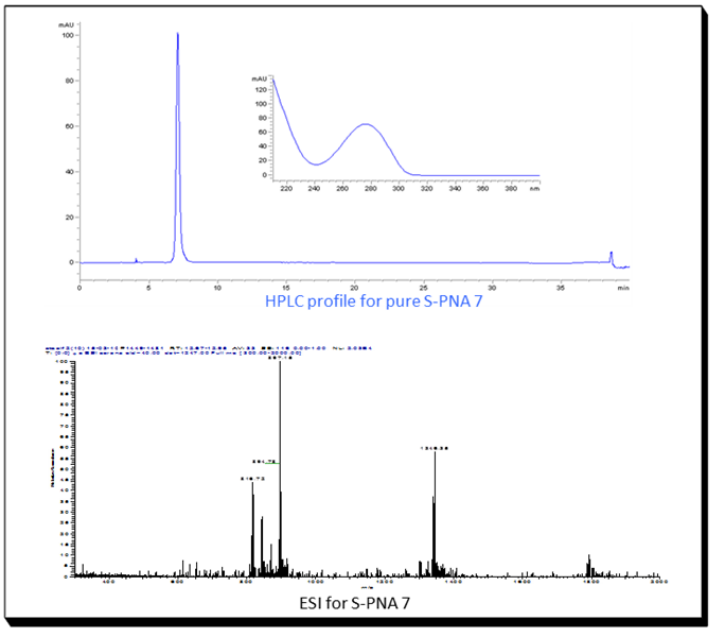

Figure 48: HPLC profile and ESI for PNA7 S.

The unmodified PNA ctcctcctc (PNA 7) was obtained using the previously showed protocols [116], purified by RP-HPLC, characterized by electrospray and used in the control experiments.

The oligomer containing hydroxymethyl modified γ PNA T monomer (t^{OH}), c $t^{OH}cct^{OH}cct^{OH}c$ (PNA7 OH) was obtained as the $ct^{S}cct^{S}cct^{S}c$, the t^{OH} monomer was coupled as the t^{S} monomer and used in the control experiments.

Studies on the secondary structure of a polypirimidine oligomer were carried out by **CD**.

CD spectra of the oligomer $ct^{S}cct^{S}cct^{S}c$ (PNA7 S) were recorded at different concentrations. A very weak signal appears when the oligomer has a 10μM concentration; the CD spectrum shows a deep minimum at 267 nm and a very shallow minimum at 238 nm. The CD spectrum of PNA7 S was compared to that of PNA7 OH, the analogue oligomer containing t^{OH} monomers (Figure 49).

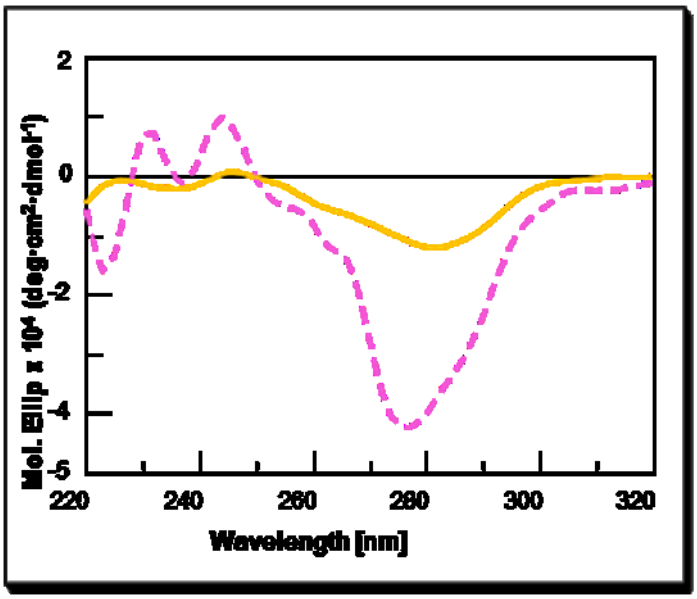

Figure 49: CD spectra of PNA7 S (_) and PNA7 OH (---) in 10mM Phosphate buffer, pH 7 at 10mM strand concentration.

It is reported in the literature that PNA oligomers containing gamma hydroxymethyl monomers adopt the structure of a right handed helix[131c]. The spectra recorded for PNA7 S and PNA7 OH show bands in the same position, with the bands in PNA7 S spectrum being far less intense. This result suggests that the PNA7 S oligomer has a lower content of secondary structure as compared to the PNA7 OH oligomer. Likely this reflects the presence of a population of monomers which assume an extended conformation, as assessed by NMR, and do not induce any secondary structure in the oligomer.

Furthermore it is also reasonable to hypothesize that the electrostatic repulsions between the negative charges and the steric hindrance of sulphates in the backbone contribute to the helix unwinding in PNA7 S. Polypirimidine PNA sequences are known to hybridize DNA forming triplexes of stoichiometry PNA_2/DNA.

In order to determine the stoichiometry of the polypirimidine PNA7S/DNA_c complex (DNAc, complementary sequence, GTGGTGGTG), the continuous variation method was employed. The absorbance at 260 nm of

PNA7 S (and PNA7) and DNAc solutions at different PNA7 S (PNA7)/DNAc ratios was measured. The plots of the absorbance *vs* the molar fraction of the PNA7 S (PNA7) show in both cases a minimum around 0.7, which suggests a stoichiometry 2:1 PNA7 S (PNA7):DNAc (Figure 50).

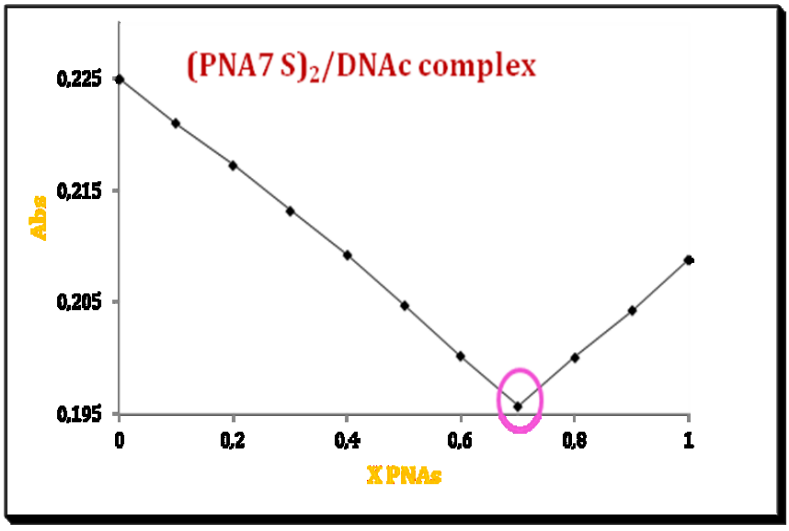

Figure 50: Job Plot for stoirchiometric determination of $(PNA7\ S)_2$/DNAc complex .

The presence of sulphates in the side chain of the oligomer PNA7 S does not hamper the formation of hybrids with complementary DNAc; the stoichiometry of the hybrid suggests that PNA7 S follows the same hybridization rule as standard PNA7.

The structure of the triplexes formed by PNA7 S with complementary DNAc was also investigated by CD and compared to the structure of a triplex formed by the unmodified PNA7 oligomer. CD spectra for the two hybrids are superimposable, showing two maxima at 270 and 225 nm and one minimum at 250 nm (Figure 51). The spectrum recorded for the DNA triplex, as expected, is different. PNA7 S forms a triple helix having the features of the P-helix formed by standard PNA[148].

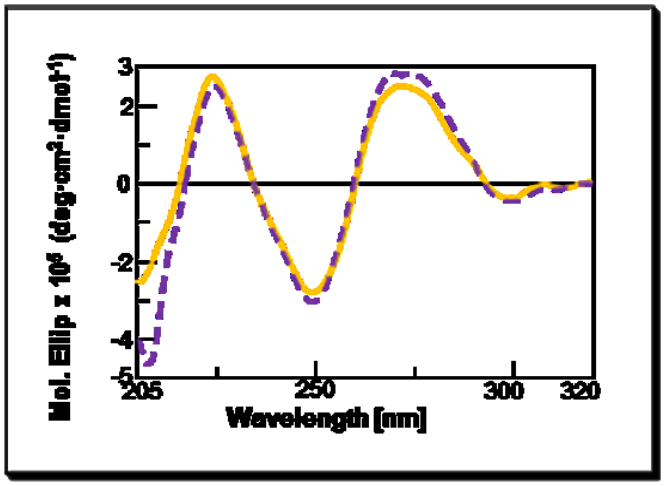

Figure 51: CD spectra of $(PNA7\ S)_2$/DNAc (_), and $(PNA\ 7)_2$/DNAc (--) in 10mM Na buffer, 100mM NaCl, 5mM $MgCl_2$, Ph 7 at 3µM triplex concentration.

The stability of the hybrid was investigated by melting experiments followed by CD. Melting curves were recorded for the $(PNA7\ S)_2$DNAc and, as a control, for the $(PNA7)_2$DNAc and for the $(DNA)_2$DNAc triplexes (see Table 6 for the sequences of the oligomers).

Name	sequence	number
PNA7 S	$ct^{S}c\ ct^{S}c\ ct^{S}c$	1
PNA7	ctcctcctc	2
PNA7 OH	$ct^{OH}c\ ct^{OH}c\ ct^{OH}c$	3
DNA	CTCCTCCTC	4
DNAc	GAGGAGGAG	5
DNA c mis	GAG**C**AGGAG	6
DNA c mis S	GAGG**T**GGAG	7

Table 6 : Oligomers sequences. PNA bases are indicated with lower case letters, DNA bases with upper case letters.

In all cases a single transition was observed. The Tm_s were estimated to be 52.2 °C for $(PNA7)_2DNAc$, 46.6°C for $(PNA7\ S)_2DNAc$ and 42.2 for $(DNA)_2DNAc$ (Table 7).

triplex	$(1)_25$	$(1)_26$	$(1)_27$	$(2)_25$	$(2)_27$	$(4)_25$	$(4)_27$	$(1)_25$ *
Tm	46.6	29.6	24.2	52.2	32,5	42.2	26.8	50,8

Table 7: melting temperature of the triplexes recorded in 10mM Na Phosphate buffer, 100mM NaCl, 5mM $MgCl_2$, pH 7 ; * higher ionic strenght: 10mM Na Phosphate buffer, 200mM NaCl, 10mM $MgCl_2$, pH 7.

The PNA7 S triplex is thermally more stable than the DNA triplex. However a destabilization with respect to the standard PNA7 hybrid is observed, which can be explained considering the electrostatic repulsion between the negatively charged phosphate of DNA and sulphate of PNA7 S. The effect of the introduction of one mismatch in the complementary DNA strand on the melting temperature of the hybrids was investigated in two cases: when the mismatched base is complementary to a PNA monomer in PNA7 S (DNA mis: GAGCAGGAG) and when the mismatched base is complementary to a t^S monomer (DNAc mis S: GAGGTGGAG).

A significant decrease in the melting temperature of the triplex was observed in both cases, being larger (-22.4°C) for the latter, demonstrating thus the high selectivity in the binding of sulphate modified PNAs. In parallel the same effect was investigated on hybrids formed by PNA7 and DNA oligomers measuring their melting temperature. The triplexes $(DNA)_2DNA$ mis S and $(PNA7)_2DNA$ mis S have a melting temperature respectively 15.4 °C and 19.7°C lower than the perfectly matched hybrid. The effect of a single mismatch on the melting temperature of the hybrid formed by PNA7 S suggests it has the highest selectivity in the binding of DNA as compared to PNA7 and DNA. Furthermore, as the thermal stability of DNA hybrids depends on the ionic strength, unlike that of hybrids formed by standard

PNA7[149], being increased at high ionic strength, we investigated the effect of the ionic strength on the stability of the PNA7 S hybrid. The melting temperature of (PNA7 S)$_2$ DNA was found dependent by the ionic strength, being increased of about 4°C when the concentrations of NaCl and $MgCl_2$ are doubled.

To evaluate the effect of sulphate PNA on gene expression, the *ErbB2* gene targeting was chosen as model. *ErbB2* is a known proto-oncogene localized on the long arm of chromosome 17 (17q11-21). Its over-expression has been reported in numerous cancers, including breast and ovarian tumors and is correlated to increased chemoresistance of the cancer cells[146].

ErbB2 encodes a protein member of the EGFR/erbB protein family, more commonly known as the epidermal growth factor receptor family. ErbB2 is a cell membrane surface-bound receptor tyrosine kinase which is normally involved in the signal transduction pathways leading to cell growth and differentiation[145]. EGFR signaling is activated by non specific ligand binding to the extracellular domain of the receptor. This determines receptor homo-/hetero-dimerization and a subsequent autophosphorylation by the intracellular kinase domain, resulting in receptor activation. After activation, phosphorylation of cytoplasmic substrates occurs and a signaling cascade drives many cellular responses, which include changes in gene expression, cytoskeletal rearrangement, anti-apoptosis and increased cell proliferation[150].

4.2.2. CYTOTOXICITY ASSAY

A cytotoxicity assay on SKBR3 with increasing concentrations of PNA7 S was performed. Results showed no significant difference on cell survival with respect to SKBR3 grown in the absence of the oligonucleotide ana-

logues (data not shown). Thus, these data demonstrates that there is no intrinsic toxicity of the sulphate-PNA on our cellular model.

4.2.3. FLOW CYTOMETRIC ANALYSIS

The ability of PNA7 S to recognize a specific DNA sequences was determined by analyzing its effect on the reduction of the amount of ErbB2 receptor on cell surface of SKBR3 cells overexpressing ErbB2 by flow cytometric assays. In particular, SKBR3 were transfected with PNA7 S in the presence of lipofectamine at different concentration of the compound. The cells, harvested after 48 h, were incubated in the presence of Herceptin as primary antibody. The signal, indicating the binding of Herceptin to the receptor on SKBR3 cell surface, significantly decreases in the presence of increasing amount of PNA7 S. Differently, there was no signal change when cells were transfected with PNA in the same conditions. This experiment suggests that the PNA7 S, unlike PNA7, is able to inhibit the expression of the receptor in a dose-response manner (Figure 52).

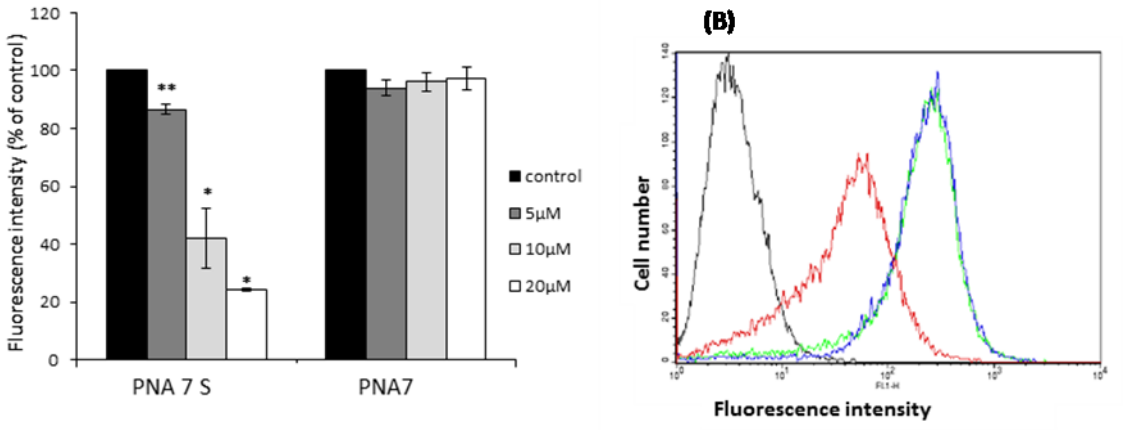

Figure52: Flow cytometric analysis of ErbB2 expression on SKBR3 cells. (**A**) Histograms were obtained from at least three independent experiments. Data are expressed as percentage of decrease *vs* control (cells not transfected and treated with an anti-ErbB2 antibody) ± SE. Statistical significance was carried out by means of the two tailed, paired, Student's t test, **p<0.01, *p<0.05. (**B**) Single result representative of three similar experiments. Not transfected cells (black curve), not transfected and treated cells with an anti-ErbB2 antibody (green curve), transfected with 10 mM PNA7 S and treated with an anti-ErbB2 antibody (red curve) and transfected with 10 mM PNA7 and treated with an anti-ErbB2 antibody (blue curve).

4.2.4. qPCR.

A quantitative analysis of *ErbB2* expression was obtained by qPCR. In detail, SKBR3 cells were transfected for 48 h with different amounts of PNA7 S or PNA7 in the presence of lipofectamine and then total RNA was extracted from cells. Following the reverse transcription, performed using random primers and MMLV reverse-transcriptase, a qPCR reaction was carried out using specific primers for glyceraldehyde-3-phosphate dehydrogenase (GAPDH, a housekeeping gene, used as reference gene) and *ErbB2*.

Data from this analysis showed that the PNA7 S was able to reproducibly down-regulate *ErbB2* expression at all concentrations tested. The expression of *ErbB2* in the presence of 10 μM was significantly lower than that at 5 μM (C_T: 13.7 and 12.0, respectively). In contrast, treatment with PNA does not reduce ErbB2 gene expression (Table 8).

	ErbB2		GAPDH	
Antigene oligonucleotides	**Threshold Cycle (C_T)**	**SD**	**Threshold Cycle (C_T)**	**SD**
Control	11.5	0.00	11.9	0.08
PNA S 5 μM	12.0*	0.14	11.7	0.18
PNA S 10 μM	13.7**	0.09	11.8	0.05
PNA 5 μM	11.5	0.08	10.9	0.21
PNA 10 μM	11.0	0.16	10.4	0.19

Table 8 : qPCR of *ErbB2* and GAPDH genes. RNA was obtained after transfection of SKBR3 cells with PNA S and PNA at 5 and 10 μM concentration. The experiments were performed in triplicate and repeated at least 3 times. Data are expressed as medium C_T ± SD. Statistical significance was carried out by means of Student's t test, (* p= 0.02; **p= 0.0006).

qPCR and FACS analyses demonstrate that a treatment of SKBR3 cells with PNA S determines a significant decrease both in gene expression and in the amount of receptor on SKBR3 cell surface. These results suggest that

PNA7 S binds to the *ErbB2* promoter, likely forming a triplex, and acts as an antigéne. One of the major challenges in the design of an antigéne molecule is the optimization of its DNA binding, which is achieved in several ways, for example conjugating to the PNA intercalating, chelating and alkylating agents, or using bis PNA[65,141a, 151, 152].

Interestingly PNA7 S forms triplexes less stable than the standard PNA, but it exhibits a biological activity unlike PNA7. In this case it may be hypothesized that the differences between PNA7 and PNA7 S are due to the different uptake of the two molecules: the negatively charged PNA7 S reasonably binds strongly the cationic lipids used for the delivery, being able to reach the nucleus in a sufficient amount to determine the antigéne effect, unlike PNA7 which, lacking of charge, is not efficiently delivered to the nucleus and therefore does not display any biological activity.

Our hypothesis is consistent with results recently published, in which an efficient delivery, although measured on an antisense PNA7, was achieved attaching to the PNA7 a phosphonate or a bis phosphonate peptide[153] and underlines how critical is the efficiency in the uptake to achieve biological activity.

4.3. CONCLUSIONS

PNA7 S is the first example reported so far of antigéne γ PNA bearing a negative charge. The introduction of the sulphate group in the γ position of the backbone positively influences the binding properties and the biological activity of the oligomer. The PNA7 S shows a strong binding selectivity toward DNA, a potent antigéne activity and lack of toxicity.

The ability to act as antigéne suggests how the biological activity of PNA based molecules strictly depends on their ability to be taken up by cells. γ sulphate PNAs represent therefore a potent tool in strategies aimed at interfering in gene expression.

4.4. *MATERIALS AND METHODS*

Reagents for the synthesis and solvents were purchased at Sigma-Aldrich. Activators (HBTU and HOBt) and amino acids were purchased at Novabiochem. DIPEA, DMF, DCM were from Romil and piperidine from Biosolve. Fmoc-PAL-PEG-PS resin was from Applied Biosystems. Fmoc-T-OH and Fmoc-C(Bhoc)-OH PNA monomers were purchased at Link Technologies. Analytical RP-HPLC runs were carried out on a HP Agilent Series 1200 apparatus using a Phenomenex Jupiter 5µ C18 300Å, 250x4.6 mm column with a flow rate of 1.0 mL min^{-1}. LCMS analyses were run on a Thermo Finnigan instrument equipped with a MSQ ES source using a Phenomenex Jupiter 5µ C18 300Å , 150x4.6 mm column with a flow rate of 0.8 mL min-1.

Preparative RP-HPLC was carried out on a Shimadzu 8A apparatus equipped with an UV Shimadzu detector using a Phenomenex Jupiter 10µ Proteo 90Å, 250x10 mm column.

Circular dichroism spectra were recorded on a Jasco J-810 spectropolarimeter equipped with a Peltier thermal controller unity using a 1-cm quartz cell.

Monodimensional ^{1}H- and ^{13}C-NMR spectra were recorded on a Varian Innova instrument (600 MHz) at room temperature. All chemical shifts are expressed in ppm with respect to the signals of the residual protonated solvents ($CDCl_3$ or DMSO-d_6). Bidimensional NMR experiments were performed on a Varian ^{UNITY}*INOVA* 500 spectrometer, equipped with a 5-mm triple resonance probe and triple-axis pulsed-field gradients.

4.4.1. Synthesis of the monomers

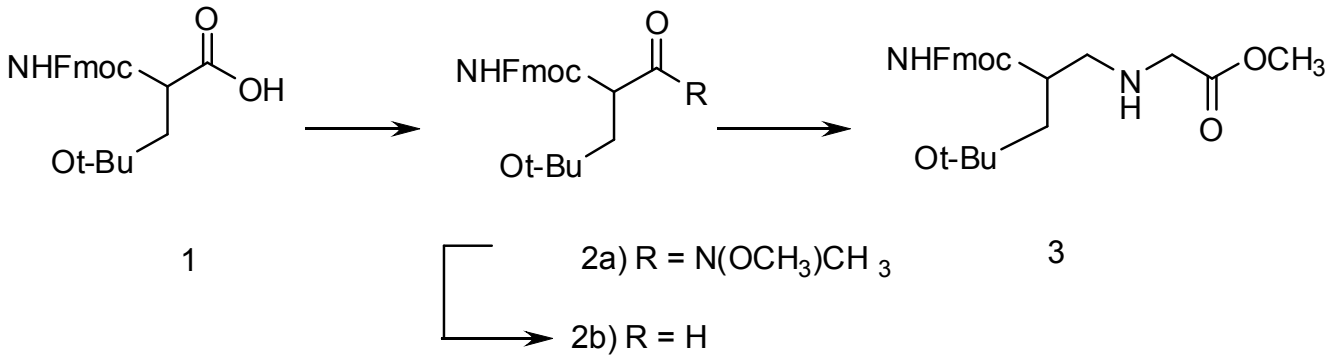

Scheme 1: Synthesis of the backbone

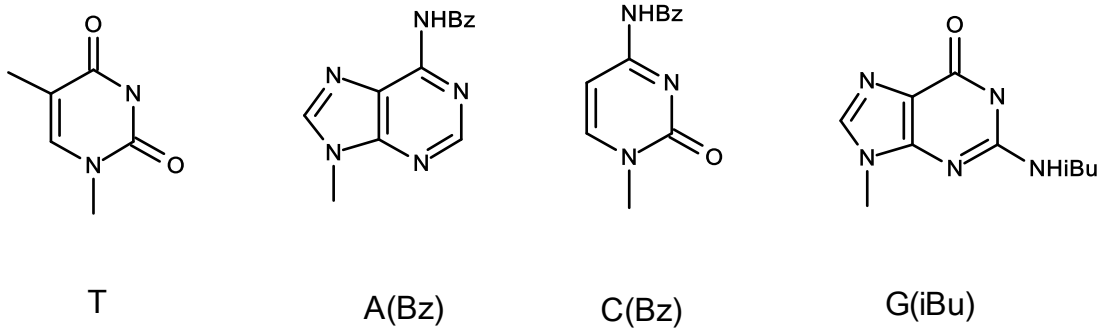

Scheme 2: Protected bases

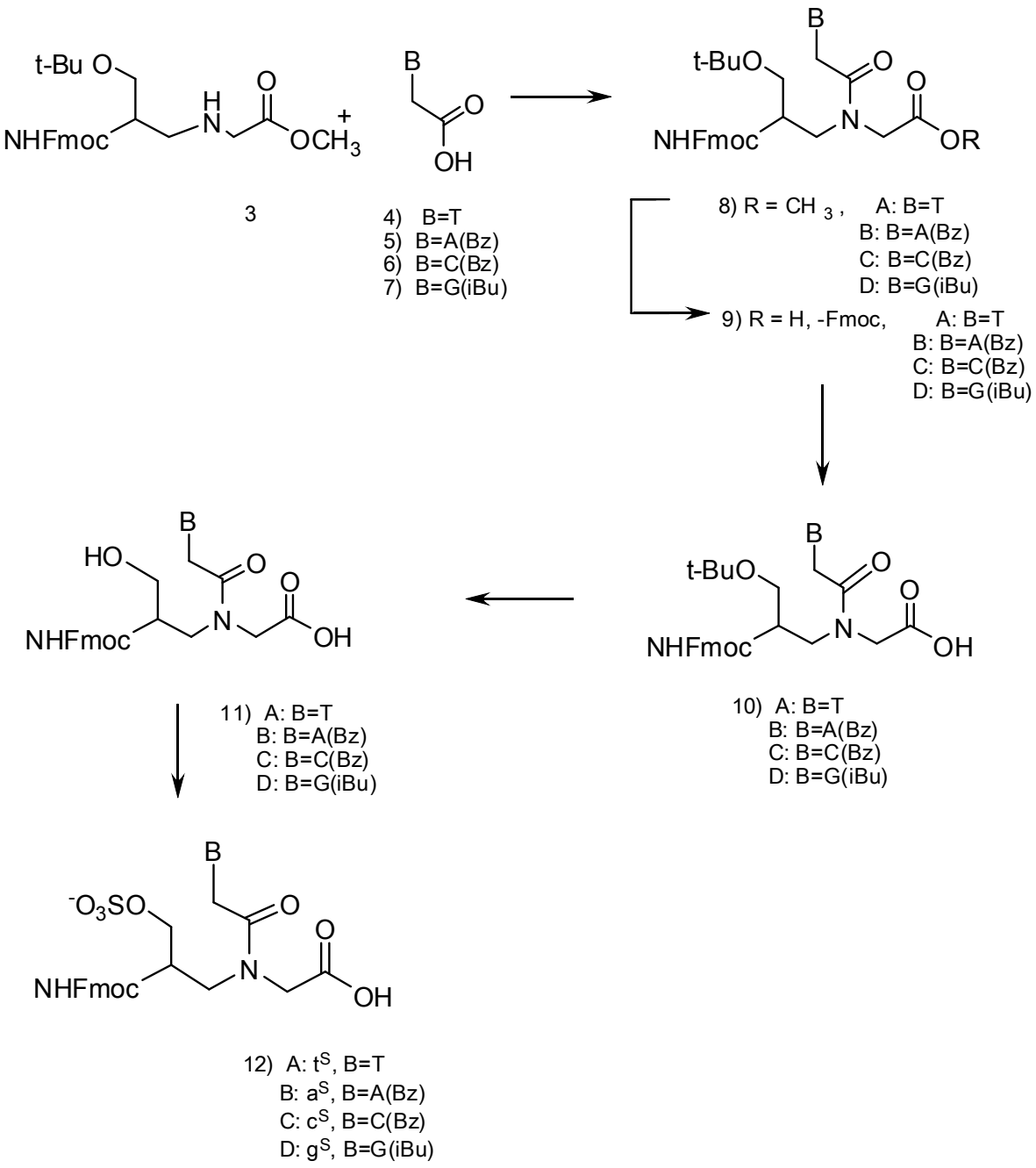

Scheme 3: assembly of the monomers

Fmoc-Ser(tBu)-N(OCH_3)CH_3 (2a)

Fmoc-Ser(tBu)-OH (**1**) (1.5 g, 3.9 mmol) was dissolved in dry CH_2Cl_2 (52 mL). N,O-(dimethyl)-hydroxylamine chloridrate (0.507 mg, 5.2 mmol) and DMAP (47.8 mg, 0.39 mmol) were added and the mixture was cooled at 0°C. Triethylamine (933 µL, 0.678 g) and EDC (0.9 g; 4.69 mmol) were added. The reaction was stirred 1 hour at 0°C and 19 hours at room temperature.

The crude was extracted with HCl 1N first, $NaHCO_3$ aq. 10% and finally with H_2O; the organic layer was treated with Na_2SO_4 an. , filtered and concentrated. The product was isolated after purification by silica gel chromatography, eluted with ethylic ether /petroleum ether 1/1 v/v.
Yield: 90% (1.66 g)

Mass analysis: m/z (ESI), $[M+H]^+$ calculated: 426.4 ; found: 426.5

^{1}H NMR($CDCl_3$): 1.16 (9 H, s, t-butyl-C<u>H</u>$_3$), 3.24 (3H, s, -N-C<u>H</u>$_3$-), 3.60-3.65 (2H, m, -CH-C<u>H</u>$_2$-O-), 3.77 (3H, s, -O-C<u>H</u>$_3$), 4.23 (1H, t, Fmoc-C<u>H</u>-CH_2-), 4.34 (2H, d, Fmoc- C<u>H</u>$_2$-O-), 4.87 (1H, t, -NH-C<u>H</u>-CH_2- O-), 7.21-7.74 (8H, m, Fmoc)

^{13}C NMR ($CDCl_3$): 27.34 (t-butyl-<u>C</u>H_3-), 47.15 (-N-<u>C</u>H_3), 51.80 (Fmoc-<u>C</u>H), 61.48 (-NH-<u>C</u>H-C-), 62.04 (-O-<u>C</u>H_3-), 67.10 (-<u>C</u>H_2-O-Fmoc), 73.58 (t-butyl-<u>C</u>-), 125.23, 125.21, 127.05, 127.66, 141.27, 143.87 (Fmoc), 144.00 (-CH_2-<u>C</u>OO-N), 156.0 (-O-<u>C</u>OO-NH).

Fmoc-Ser(tBu)-OCH_3 (3)

Fmoc-Ser(tBu)N(OCH_3)CH_3 **(2a)** (0.78 g; 1.8 mmol) dissolved in dry diethyl ether (11 mL) was cooled at 0°C under argon. Lithium aluminum hydride (3.5 mL; 3.5mmol) was added dropwise and the reaction was stirred at 0°C, 1 hour. The reaction was quenched with a solution of $KHSO_4$ (0.2 M); the crude was extracted with H_2O. The organic layer containing the aldehyde

Fmoc-Ser(tBu)-H (2b) was treated with Na_2SO_4 an. , filtered and concentrated.

Fmoc-Ser(tBu)-H(**2b**) (0.58 g; 1.5 mmol) dissolved in anhydrous CH_3OH (16 mL) was cooled at 0°C under nitrogen. In a separate flask glycine methylester chlorhydrate (0.4 g; 3.1 mmol) was dissolved in CH_3OH (2 mL) and DIPEA (500 μL). The two solutions were mixed and the reaction was stirred at 4°C, 4hours . Acetic acid (290 μL) and sodium cianoborhydride (152 mg; 2.41 mmol) were then added and the mixture was stirred 30 minutes. The reaction was quenched with a solution of $NaHCO_3$ 10%; the crude was extracted with ethyl acetate. The organic layer was treated with Na_2SO_4 an. , filtered and concentrated. Product **3** was purified by silica gel chromatography eluted in ethyl acetate/hexane7/3 v/v.

Yield: 60 % (0.41g)

Mass analysis: m/z (ESI), $[M+H]^+$ calculated : 443.0 ; found :443.1

^{1}H NMR ($CDCl_3$): 1.17 (9H, s, t-butyl-C<u>H</u>$_3$), 2.11 (1H, s, -CH_2- N<u>H</u>-CH_2-), 2.74 (2H, dd, -CH-C<u>H</u>$_2$-N-), 3.44 (2H, bs, NH-C<u>H</u>$_2$-COO), 3.47 (2H, br s, -CH-C<u>H</u>$_2$-O-), 3.70 (3H, s, -O-C<u>H</u>$_3$), 3.88 (1H, br s, -NH-C<u>H</u>-CH_2-), 4.23 (1H, m, Fmoc- C<u>H</u>-CH_2), 4.40 (2H, m, Fmoc-C<u>H</u>$_2$-O), 7.28-7.76 (8H, m, Fmoc).

^{13}C NMR($CDCl_3$): 27.62 (t-butyl-<u>C</u>H_3-), 47.42 (Fmoc-<u>C</u>H-CH_2), 50.92 (-CH-<u>C</u>H_2-N-), 51.06 (-NH-<u>C</u>H_2-CO), 52.15 (-O-<u>C</u>H_3), 62.25 (NH-<u>C</u>H-CH_2-), 67.10 (Fmoc-<u>C</u>H_2-O-), 73.36 (CH-CH_2-O-), 125.33, 127.25, 127.85 (Fmoc), 144.10, 144.24 (Fmoc), 156.85 (-O-<u>C</u>O-N-) , 173.75 (<u>C</u>OOCH_3)

<u>Fmoc-Ser(tBu)-A(Bz)-OCH_3 (8B)</u>

0.17 g of Fmoc-Ser(tBu)-OCH_3 **(3)**(0.37 mmol) are dissolved in 3.7 mL of anhydrous DMF; A(Bz)-CH_2COOH (224 mg, 0.75 mmol)(prepared following

the protocol reported by Finn, PJ et al. *Nucleic Acids Research* **(**1996)) EDC (144.3mg, 0.75 mmol) and DMAP (4.6 mg, 0.04 mmol) are added. After 12 hours stirring the solvent is evaporated; the residue is dissolved in $CHCl_3$ and washed with $NaHCO_{3\ aq.}$ The organic layer is treated with Na_2SO_4 and the solvent evaporated. The product is purified by silica gel chromatography eluted in ethyl acetate/hexane 9/1 v/v.

Yield: 85% (225 mg)

Mass analysis: m/z (ESI), $[M+H]^+$ calculated 698.0; found 698.2

^{1}H NMR($CDCl_3$): 1.26 (9H, s, t-butyl-C<u>H</u>$_3$), 3.41–3.70 (4H, m, -CH–C<u>H</u>$_2$–O-N-CH-C<u>H</u>$_2$), 3.72 (3H, s, OC<u>H</u>$_3$), 3.82 (2H, s, CO-C<u>H</u>$_2$-adenine), 3.97-4.20 (3H, m, NH-C<u>H</u>-CH$_2$, NH-C<u>H</u>$_2$-COOCH$_3$), 4.28 (1H, t, CH-Fmoc), 4.40-4.41 (2H, d, CH$_2$-Fmoc), 7.28-7.75 (8H, m, Fmoc and 5H, m, Bz), 8.12 (1H, s, H(2)-adenine), 8.68 (1H, s, H, (8)-adenine).

^{13}C NMR ($CDCl_3$): 27.90 (t-butyl-<u>C</u>H$_3$), 44.22 (N-<u>C</u>H$_2$-COO), 47.71 (Fmoc-<u>C</u>H-), 49.26 (CH-<u>C</u>H$_2$-N), 49.98 (-NH-<u>C</u>H-CH$_2$), 52.84 (OCH_3), 60.55 (-CO-CH$_2$-adenine), 67.20 (-Fmoc -<u>C</u>H$_2$-), 67.43 (CH-<u>C</u>H$_2$-O), 74.58 (t-butyl-<u>C</u>), 120.52 (C(5)-adenine), 125.32, 127.55, 128.31, 129.34, 133.19, 134.30, 141.81, 144.14 (Fmoc), 144.64 (C(8)-adenine), 149.87 (C(4)-adenine), 153.17 (C(2)-adenine), 155.00 (<u>C</u>O-Fmoc), 165.00 (<u>C</u>O-Bz), 169.83 (-<u>C</u>O-CH$_2$-adenine), 173.06 (<u>C</u>OOCH$_3$).

<u>Fmoc Ser(tBu)-A(Bz)-OH (10 B)</u>

224 mg of Fmoc-Ser(tBu)-A(Bz)-OCH_3 (**8B**)(0.32 mmol) are dissolved in dioxane (4 mL) and treated with NaOH 2M (802 µL, 1.6mol). The mixture is stirred at r.t. and 0 °C, 2 hours; HCl 1N is added until the pH of the solution is 5. The product is extracted with ethyl acetate and dried. The resulting NH_2-Ser(tBu)-A(Bz)OH (156 mg, 0.32 mmol) is dissolved in 2.5 mL of H_2O/CH_3CN 1/1, FmocONSu (216.6 mg, 0.64 mmol) and $NaHCO_3$ are added

(54 mg, 0.64 mmol). The reaction is carried out at pH=8, 2 hours. The reaction is quenched with HCl 2M up to neutralization. The crude is washed with $CHCl_3$, the organic layer is dried. The product is purified by by silica gel chromatography eluted in ethyl acetate/methanol 9/1 v/v.

Yield: 63% (143mg)

Mass analysis: m/z (ESI), [M+H]+ calculated: 707.0; found: 707.2

^{1}H NMR (DMSO-d_6): 1.21 (9H, s, t-butyl-C$\underline{H}_3$), 3.14-4.14 (7H, m, -CH-C$\underline{H}_2$-O, NH-CH-C$\underline{H}_2$, NH-C$\underline{H}$-CH_2, CO-C$\underline{H}_2$-adenine), 4.19-4.41 (5H, m, C$\underline{H}$-Fmoc, C$\underline{H}_2$-Fmoc, NH-C$\underline{H}_2$-COOH), 7.28-8.05 (8H, m, Fmoc and 5H, m, Bz), 8.30 (1H, s, H(2) adenine), 8.62 (1H, s, H(8) adenine).

^{13}C NMR (DMSO-d_6): 31.02 (t-butyl-$\underline{C}H_3$), 47.90 (Fmoc-$\underline{C}$H), 50.73 ($COCH_2$-adenine), 52.15 (NH-$\underline{C}H_2$-COOH), 53.36 (CH-$\underline{C}H_2$-N), 54.72 (NH-$\underline{C}$H-CH_2), 69.00 (Fmoc-$\underline{C}H_2$-), 69.47 (CH-$\underline{C}H_2$-O), 76.82 (t-butyl-$\underline{C}$), 124.09 (C(5)-adenine), 129.17, 130.99, 131.59, 132.42, 136.36 , 144.71 (Fmoc, Bz), 137.41 (C(8)-adenine), 144.71 (C(4)-adenine), 149.50 (C(6)-adenine), 153.90 (C(2)-adenine), 156.73 (COO-Fmoc), 169.64 ($\underline{C}$O-Bz), 170.80 ($\underline{C}$O-CH_2-adenine), 174.08 ($\underline{C}$OOH).

Fmoc Ser(OH)-A(Bz)-OH (11B)

Fmoc Ser(tBu)-A(Bz)-OH (**10B**) (143 mg) is suspended in TFA/DCM 1/1 (3 mL); the solution is stirred 2 hours. The solvent is evaporated and the crude is lyophilized. Yield: 100% (131.5 mg)

Mass analysis: m/z (ESI), $[M+H]^+$ calculated :650.0; found: 650.3

^{1}H NMR: (DMSO-d_6): 3.19 - 3.36 (2H, m, CH-C$\underline{H}_2$-N, rotamer B), 3.57-3.49 (2H, m, CH-C$\underline{H}_2$-N, rotamer A), 3.60 (2H, m, CH-C$\underline{H}_2$-O, rotamer B), 3.70 (1H,

m, NH-C<u>H</u>-CH_2 rotamer B), 3.72 (2H, m, CH-C<u>H_2</u>-O, rotamer A), 3.88 (1H, m, NH-C<u>H</u>-CH_2 rotamer A), 3.96-4.08 (2H, d, N-C<u>H_2</u>-COOH), 4.24-4.34 (3H, m, C<u>H</u>-Fmoc, C<u>H_2</u>-Fmoc), 5.20-5.26 (2H, d, CO-C<u>H_2</u>-adenine, rotamer B), 5.42-5.50 (2H, d, CO-C<u>H_2</u>-adenine, rotamer A), 7.12 (1H, d, N<u>H</u>-CH-CH_2 rotamer B), 7.25-8.10 (8H, m, Fmoc and 5H, m, Bz), 8.48 (1H, s, H(2)adenine), 8.68 (1H, s, H(8)adenine). 7.41 (1H, d, N<u>H</u>-CH-CH_2 rotamer A).

^{13}C NMR (DMSO-d_6): 47.70 (<u>C</u>H-Fmoc), 50.00 (CO-<u>C</u>H_2-adenine), 52.05 (NH-<u>C</u>H_2-CO), 53.20 (CH-<u>C</u>H_2-N), 54.78 (NH-<u>C</u>H-CH_2), 66.53 (CH-<u>C</u>H_2-O), 69.40 (CH_2-Fmoc), 121.08 (C(5)-adenine), 132.42, 129.44, 128.59, 128.00, 126.16 (Fmoc, Bz), 134.32 (C(8)-adenine), 144.79, 141.69 (Fmoc), 150.71 (C(4)-adenine), 152.41 (C(6)-adenine), 153.62 (C(2)-adenine), 156.83 (CO-Fmoc), 166.76 (CO-Bz), 167.71 (CO-CH_2-adenine), 171.64 (COOH).

<u>Fmoc Ser(OSO$_3$)-A(Bz)-OH (12 B)</u>

Fmoc Ser(OH)-A(Bz)-OH (**11B**) (143mg, 0.22mmol) is dissolved in 1.2mL of DMF and stirred under argon 10 minutes. DMF·SO_3 (134.8 mg, 0.88 mmol) is added and the reaction is carried out 2 hours under argon at r.t.. The solvent is evaporated. Separately a solution of $NaHCO_3$ sat.(2.86mL) and tetrabutylammonium bisulfate (154.4 mg) is prepared and cooled at 0°C; this solution is added to the reaction mixture and and reacted under stirring 5 minutes. The pH of the solution is then adjusted to 5 with a 10% solution of citric acid. The crude is extracted 4 times with $CHCl_3$, the organic layer is dried under vacuum.

Yield: 95%

Mass analysis: m/z (ESI), $[M+H]^+$ calculated: 729.3; found: 729.4

^{1}H NMR (DMSO-d_6): 3.28 - 3.49 (2H, m, CH-C<u>H</u>$_2$-N, rotamer B), 3.50-3.74 (2H, m, CH-C<u>H</u>$_2$-N, rotamer A), 3.73 (2H, m, CH-C<u>H</u>$_2$-O, rotamer B), 3.86 (1H, m, NH-C<u>H</u>-CH$_2$ rotamer B), 3.90 (2H, m, CH-C<u>H</u>$_2$-O, rotamer A), 3.92-4.04 (2H, d, N-C<u>H</u>$_2$-COOH), 4.08 (1H, m, NH-C<u>H</u>-CH$_2$ rotamer A), 4.24-4.34 (3H, m, C<u>H</u>-Fmoc, C<u>H</u>$_2$-Fmoc), 5.11 (2H, sd, CO-C<u>H</u>$_2$-adenine, rotamer B), 5.50-5.58 (2H, d, CO-C<u>H</u>$_2$-adenine, rotamer A), 7.28-8.10 (8H, m, Fmoc and 5H,m, Bz), 7.35 (1H, d, N<u>H</u>-CH-CH$_2$ rotamer B),7.62 (1H, d, N<u>H</u>-CH-CH$_2$ rotamer A), 8.46 (1H, bs, H(2)adenine), 8.66 (1H, bs, H(8)adenine).

All other monomers are prepared following the same procedure described for the adenine monomer. Bases with the methylene carbonyl linker were prepared according to procedures described in the literature[87, 140a].

<u>Fmoc-Ser(tBu)-T-OCH$_3$ (8A)</u>

Yield: 89% (185.2 mg)

Mass analysis: m/z (ESI), $[M+H]^+$ calculated 609 ; found 609.2

^{1}H NMR ($CDCl_3$): 1.21 (9H, s, t-butyl-C<u>H</u>$_3$), 1.67-1.68 (3H, s, C<u>H</u>$_3$-thymine), 3.42-3.90 (4H, m, -CH-C<u>H</u>$_2$-O-), 3.72 (3H, s, O-C<u>H</u>$_3$), 3.79 (2H, dd, N-C<u>H</u>$_2$-COOCH$_3$), 4.19-4.23 (1H, m, -NH-C<u>H</u>-CH$_2$), 4.29 (1H, t, Fmoc-C<u>H</u>-CH$_2$-), 4.41 (2H, d, Fmoc-C<u>H</u>$_2$-O-), 4.54-4.81 (2H, s, CO-C<u>H</u>$_2$- thymine), 6.96-6.98 (1H, s, H(6)- thymine), 7.29-7.77 (8H, m, Fmoc), 8.02 (1H, s, N<u>H</u>- thymine), 8.24 (1H, s, Fmoc-N<u>H</u>)

^{13}C NMR ($CDCl_3$): 12.33 (C<u>H</u>$_3$- thymine), 27.50 (t-butil-<u>C</u>H$_3$), 47.27 (N-<u>C</u>H$_2$-CO), 47.56 (Fmoc-<u>C</u>H-CH$_2$), 48.87 (CH-CH$_2$-N), 49.60 (NH-<u>C</u>H-CH$_2$-), 49.98 (-CO-<u>C</u>H$_2$- thymine), 52.35 (-O-CH$_3$), 66.74 (Fmoc-<u>C</u>H$_2$-O), 66.96 (-CH-<u>C</u>H$_2$-O-), 73.94 (t-butyl-<u>C</u>), 110.5 (C(5)- thymine), 125.00, 127.09, 127.80, 140.92,

141.18, 143.76 (Fmoc), 141.18 (C(6)- thymine), 150.75 (C(2)- thymine), 163.83 (C(4)- thymine), 167.75 (-CO-CH_2- thymine), 169.51 ($\underline{C}OOCH_3$).

Fmoc Ser(tBu)-T-OH (10 A)

Yield: 63% (223 mg)

Mass analysis: m/z (ESI), $[M+H]^+$ calculated: 595.0; found: 595.2

^{1}H NMR ($DMSO-d_6$): 1.21 (9H, s, t-butyl-$C\underline{H}_3$), 1.67-1.68 (3H, s, $C\underline{H}_3$-thymine), 3.45-3.80 (4H, m,-CH-$C\underline{H}_2$-O, NH-CH-$C\underline{H}_2$), 3.82-3.98 (2H, s, NH-$C\underline{H}_2$-COOH), 4.21-4.45 (5H, m, $C\underline{H}$-Fmoc, $C\underline{H}_2$-Fmoc, CO-$C\underline{H}_2$- thymine), 7.21 (1H, s, H(6)- thymine), 7.29-7.72 (8H, m, Fmoc).

^{13}C NMR ($CDCl_3$): 11.48 ($\underline{C}H_3$- thymine), 26.75 (t-butyl-$\underline{C}H_3$), 46.27 (N-$\underline{C}H_2$-COOH), 47.24 ($\underline{C}$H-Fmoc), 48.09 (CH-$\underline{C}H_2$-N), 49.67 (NH-$\underline{C}$H-CH_2-), 50.21 (CO-CH_2- thymine), 65.00 (Fmoc-$\underline{C}H_2$-O), 71.98 (CH-$\underline{C}H_2$-O), 75.73 (t-butyl-$\underline{C}$), 107.56 (C(5)- thymine), 124.77, 126.59, 127.20, 141.62, 143.32 (Fmoc), 140.23 (C(6)- thymine), 150.54 (C(2)- thymine), 163.93 (C(4)- thymine), 167.75 (-$\underline{C}$O-CH_2- thymine), 170.54 ($\underline{C}$OOH).

Fmoc Ser(OH)-T-OH (11 A)

Yield: 86% (174mg)

Mass analysis: m/z (ESI), $[M+H]^+$ calculated: 538.0 ; found: 538.2

^{1}H NMR ($DMSO-d_6$): 1.67 (3H, s, $C\underline{H}_3$-thymine), 3.13 -3.34 (2H, m, CH-$C\underline{H}_2$-N, rotamer B), 3.33 -3.49 (2H, m, CH-$C\underline{H}_2$-N, rotamer A), 3.56 (2H, m, CH-$C\underline{H}_2$-O, rotamer B), 3.57 (2H, m, CH-$C\underline{H}_2$-O, rotamer A), 3.67 (1H, m, NH-$C\underline{H}$-CH_2 rotamer B), 3.78 (1H, m, NH-$C\underline{H}$-CH_2 rotamer A), 3.92-3.99 (2H, d, N-$C\underline{H}_2$-

COOH), 4.21-4.40 (3H, m, CH-Fmoc, CH_2-Fmoc) , 4.65-4.73 (2H, d, CO-CH_2-thymine), 7.10 (1H, d, NH-CH-CH_2 rotamer B),7.26 (1H, bs, H(6)-thymine), 7.29-7.90 (8H, m, Fmoc), 7.31 (1H, d, NH-CH-CH_2 rotamer A)

^{13}C NMR (DMSO-d_6): 15.91 (CH_3-C5), 50.77 (CH-Fmoc), 51.79 (CO-CH_2-thymine), 53.24 (NH-CH_2-COOH), 55.55 (NH-CH-CH_2), 55.89 (CH-CH_2-N), 66.77 (CH_2-Fmoc), 69.22 (CH-CH_2-O-), 112.13 (C(5)- thymine), 124.15, 129.26, 131.10, 131.67 (Fmoc), 144.76, 147.88 (C_q Fmoc), 146.07 (C(6)-thymine), 155.01 (C(2)- thymine), 159.98 (COO-Fmoc), 168.43 (C(4)-thymine), 171.55 (CO-CH_2- thymine), 174.28 (COOH)

Fmoc Ser(OSO_3)-T-OH (12 A)

Mass analysis: m/z (ESI), $[M+H]^+$ calculated: 617.0 ; found: 618.0

^{1}H NMR (DMSO-d_6): 1.69 (3H, s, CH_3-thymine), 3.32-3.47 (2H, m, CH-CH_2-N, rotamer B), 3.40 - 3.58 (2H, m, CH-CH_2-N, rotamer A), 3.55 (2H, m, CH-CH_2-O, rotamer B), 3.77 (1H, m, NH-CH-CH_2 rotamer B), 3.94-3.96 (2H, d, N-CH_2-COOH), 3.97 (2H, m, CH-CH_2-O, rotamer A), 4.08 (1H, m, NH-CH-CH_2 rotamer A), 4.18-4.32 (3H, m, CH-Fmoc, CH_2-Fmoc) , 4.45 (2H, d, CO-CH_2-thymine, rotamer B) , 4.65-4.73 (2H, d, CO-CH_2-thymine, rotamer A), 7.26-7.90 (8H, m, Fmoc), 7.31 (1H, bs, H(6)-thymine), 7.33 (1H, d, NH-CH-CH_2 rotamer B), 7.52 (1H, d, NH-CH-CH_2 rotamer A).

Fmoc Ser(tBu)-C(Bz)-OCH_3 (8C)

Mass analysis: m/z (ESI), $[M+H]^+$ calculated: 698.0 ; found: 698.2

^{1}H NMR ($CDCl_3$): 1.22 (9H, s, t-butyl-CH_3), 3.30-3.40 (2H, m, CH-CH_2-O), 3.45-3.54 (2H, m, CH-CH_2-O), 3.71 (3H, s, OCH_3), 3.78 (2H, s, CO-CH_2-

cytosine), 3.95-4.65 (7H, m, NH-CH-CH_2, C<u>H</u>-Fmoc, C<u>H_2</u>-Fmoc, N-C<u>H_2</u>-$COOCH_3$, H(5)-cytosine), 7.38 (1H, d, H(6)-cytosine), 7.38-7.90 (8H,m, Fmoc and 5H,m, Bz).

^{13}C NMR ($CDCl_3$): 47.75 (Fmoc-<u>C</u>H), 49.37 (N-<u>C</u>H_2-CO), 50.03 (CH-<u>C</u>H_2-N), 50.42 (NH-<u>C</u>H-CH_2), 52.79 (CO-CH_2-cytosine), 67.18 (<u>C</u>H_2-Fmoc), 67.46 (CH-<u>C</u>H_2-O), 73.94 (t-butyl, Cq), 97.11 (C(5)-cytosine), 125.63, 127.58, 127.75, 128.12, 128.23, 129.17, 129.47 (Fmoc, Bz), 133.61(C_q-Bz), 141.77, 144.26 (C_q-Fmoc), 144.98 (C(6)-cytosine), 150.95 (C(2)-cytosine), 156.75 (COO-Fmoc), 163.18 (<u>C</u>O-CH_2-cytosine), 168.05 (COO-Bz), 170.09 (<u>C</u>OO-OCH_3).

<u>Fmoc Ser(tBu)-C(Bz)-OH (10 C)</u>

Yield: 80% (130 mg)

Mass analysis: m/z (ESI), $[M+H]^+$ calculated : 684.0; found :684.2

^{1}H NMR (DMSO-d_6): 1.21 (9H, s, t-butyl-C<u>H_3</u>), 3.20-4.15 (7H, m, -CH-C<u>H_2</u>-O, NH-CH-C<u>H_2</u>, NH-C<u>H</u>-CH_2, CO-C<u>H_2</u>-cytosine), 4.21-4.40 (6H, m, C<u>H</u>-Fmoc, C<u>H_2</u>-Fmoc, NH-C<u>H_2</u>-COOH, H(5)cytosine), 7.38 (1H, d,H(6)-cytosine), 7.38-8.05 (8H, m, Fmoc, 5H, m, Bz).

^{13}C NMR (DMSO-d_6): 31.22 (t-butyl-<u>C</u>H_3), 50.73 (<u>C</u>H-Fmoc), 52.07 (CO-<u>C</u>H_2-cytosine), 53.65 (NH-<u>C</u>H_2-COOH), 54.23 (NH-<u>C</u>H-CH_2), 54.90 (NH-<u>C</u>H_2-CH), 69.45 (<u>C</u>H_2-Fmoc), 69.59 (CH-<u>C</u>H_2-O), 76.47 (t-butil-<u>C</u>), 99.72 (C(5)-cytosine), 129.23, 131.05, 131.61, 132.43 (Fmoc, Bz), 136.67 (C_q-Bz), 147.30, 147.83 (C_q-Fmoc), 147.90 (C(6)-cytosine), 155.08 (C(2)-cytosine), 159.08 (<u>C</u>OO-Fmoc), 159.91 (C(4)-cytosine), 167.34 (<u>C</u>OO-CH_2-cytosine), 171.31 (COO-Bz), 174.27 (COOH).

Fmoc Ser(OH)-C(Bz)-OH (11 C)

Mass analysis: m/z (ESI), $[M+H]^+$ calculated: 628.0 ; found: 628.1

^{1}H NMR ($DMSO-d_6$)**:** 3.18 - 3.36 (2H, m, CH-C$\underline{H}_2$-N, rotamer B), 3.38 -3.52 (2H, m, CH-C$\underline{H}_2$-N, rotamer A), 3.56 (2H, m, CH-C$\underline{H}_2$-O, rotamer B), 3.61 (2H, m, CH-C$\underline{H}_2$-O, rotamer A), 3.67 (1H, m, NH-C$\underline{H}$-CH_2 rotamer B), 3.79 (1H, m, NH-C$\underline{H}$-CH_2 rotamer A),3.88-4.08 (2H, d, N-C$\underline{H}_2$-COOH), 4.18-4.35 (3H, m, C$\underline{H}$-Fmoc, C$\underline{H}_2$-Fmoc), 4.67 (2H, bs, CO-C$\underline{H}_2$-cytosine, rotamer B), 4.88-4.94 (2H, d, CO-C$\underline{H}_2$-cytosine, rotamer A), 6.05 (1H, d, H(5)cytosine), 7.10 (1H, d, N$\underline{H}$-CH-CH_2 rotamer B), 7.23-8.05 (8H, m, Fmoc and 5H, m, Bz), 7.31 (1H, d, N$\underline{H}$-CH-CH_2 rotamer A), 7.80 (1H, d,H(6)-cytosine)

^{13}C NMR (DMSO): 50.70 (C$\underline{H}$-Fmoc), 51.75 (CO-C$\underline{H}_2$-citosina), 53.68 (NH-C$\underline{H}_2$-COOH), 55.49 (NH-C$\underline{H}$-CH_2), 55.96 (CH-C$\underline{H}_2$-N), 66.77 (CH-C$\underline{H}_2$-O), 69.53 (C$\underline{H}_2$-Fmoc), 99.74 (C(5)-citosina), 129.21, 131.06, 131.60, 132.42 (Fmoc, Bz), 136.67 (C_q, Bz), 144.71, 147.85 (C_q Fmoc), 147.90 (C(6)-cytosine), 155.07 (C(2)-cytosine), 159.02 (C$\underline{O}$-Fmoc), 162.06 (C(4)-cytosine), 167.01 (C$\underline{O}$-CH_2-cytosine), 171.31 (COO-Bz), 174.22 (C$\underline{O}$OH).

Fmoc Ser(OSO_3)-C(Bz)-OH (12 C)

Yield: 91%

Mass analysis: m/z (ESI), $[M+H]^+$ calculated ;706.7; found : 706.7

^{1}H NMR ($DMSO-d_6$): 3.30 - 3.49 (2H, m, CH-C$\underline{H}_2$-N, rotamer B), 3.42 – 3.63 (2H, m, CH-C$\underline{H}_2$-N, rotamer A), 3.74 (2H, m, CH-C$\underline{H}_2$-O, rotamer B), 3.83 (2H, m, CH-C$\underline{H}_2$-O, rotamer A), 3.86 (1H, m, NH-C$\underline{H}$-CH_2 rotamer B), 3.88-4.05 (2H, d, N-C$\underline{H}_2$-COOH), 4.00 (1H, m, NH-C$\underline{H}$-CH_2 rotamer A), 4.28 (3H, m, C$\underline{H}$-Fmoc, C$\underline{H}_2$-Fmoc), 4.74- 4.67 (2H, d, CO-C$\underline{H}_2$-cytosine, rotamer B), 4.82 - 5.02 (2H, d, CO-C$\underline{H}_2$-cytosine, rotamer A), 6.10 (1H, d, H(5)cytosine), 7.25-8.02

(8H, m, Fmoc and 5H, m, Bz), 7.32 (1H, d, N<u>H</u>-CH-CH_2 rotamer B),7.56 (1H, d, N<u>H</u>-CH-CH_2 rotamer A), 7.80 (1H, d,H(6)-cytosine)

<u>FmocSer(tBu)-G(iBu)-OCH_3 (8 D)</u>

Yield: 67% (366 mg)

Mass analysis: m/z (ESI), $[M+H]^+$ calculated: 704.9 ; found: 705.0

^{1}H NMR ($CDCl_3$): 1.14 (6H, d, C<u>H</u>$_3$-isobutiryl), 1.17 (9H, s, t-butyl-CH_3), 2.55-2.75 (1H, m, -C<u>H</u>-$(CH_3)_2$), 3.10-3.32 (2H, m, CH-C<u>H</u>$_2$-O), 3.40- 3.58 (2H, m, -CH-C<u>H</u>$_2$-N), 3.69 (3H, s, OCH_2), 3.79 (CO-C<u>H</u>$_2$-guanine), 4.18-4.30 (1H, m, NH-C<u>H</u>-CH_2), 4.38 (1H, m, CH-Fmoc), 4.70-4.80 (m, 5H, C<u>H</u>$_2$-Fmoc, N-C<u>H</u>$_2$-COO-OCH_3, CH-Fmoc), 7.24-7.74 (1H, s, CH-guanine).

^{13}C NMR ($CDCl_3$)**:** 19.28 (<u>C</u>H$_3$-isobutiryl), 27.95 (<u>C</u>H$_3$-t-butyl), 36.44 (CH-$(CH_3)_2$-isobutiryl), 47.50 (<u>C</u>H-Fmoc), 47.83 (N-<u>C</u>H$_2$-CO), 48.55 (CH-<u>C</u>H$_2$-N), 50.01 (NH-<u>C</u>H-CH_2), 52.78 (O<u>C</u>H$_3$), 67.35 (<u>C</u>H$_2$-Fmoc), 74.24 (C-t-butyl), 120.53 (C(5)-guanine), 125.33,127.25, 127.84 (Fmoc), 140.28 (C(8)-guanina), 141.78, 144.00 (C_q Fmoc), 148.40 (C(2)-guanine), 148.80 (C(8)-guanine), 149.22 (C(4)-guanine), 156.26 (<u>C</u>O-Fmoc), 157.13 (<u>C</u>(6)-guanine), 167.62 (<u>C</u>O-CH_2-guanine), 170.05 (<u>C</u>OOCH_3), 179.80 (<u>C</u>O-isobutiryl).

<u>Fmoc Ser(tBu)-G(iBu)-OH (10 D)</u>

Yield: 81% (290 mg)

Mass analysis: m/z (ESI), $[M+H]^+$ calculated : 690.8 ; found: 690.9

^{1}H NMR (DMSO-d_6): 1.13 (6H, d, C<u>H</u>$_3$-isobutiryl), 1.19 (9H, s, t-butyl-CH_3), 2.72-2.80 (1H, m, C<u>H</u>-$(CH_3)_2$), 3.10-3.50 (5H, m, CH-C<u>H</u>$_2$-O, CH-C<u>H</u>$_2$-N, NH-C<u>H</u>-CH_2), 4.08 (2H, s, CO-C<u>H</u>$_2$-guanine), 4.27- 4.28 (5H, m, C<u>H</u>-Fmoc, CH_2-Fmoc, N-C<u>H</u>$_2$-CO), 7.33-7.87 (8H, m, Fmoc), 7.92 (1H, d, H(8)-guanine).

^{13}C NMR (DMSO-d_6): 22.75 (CH_3-isobutiryl), 31.20 (CH_3-t-butyl), 38.69 (CH-$(CH_3)_2$-isobutiryl), 47.99 (CH-Fmoc), 50.72 (CO-CH_2-guanine), 52.05 (NH-CH2-CO), 54.32 (CH-CH_2-N), 55.11 (NH-CH-CH_2), 69.37 (CH_2-Fmoc), 69.53 (CH-CH_2-O), 76.49 (CO-t-butyl), 124.127 (C(6)-guanine), 129.08, 129.17, 131.00, 131.68 (Fmoc), 144.73, 147.75 (C_q-Fmoc), 147.89 (C(8)-guanine), 151.86 (C(2)-guanine), 153.22 (C(4)-guanine), 158.85 (CO-Fmoc), 159.83 (CO-C(6)-guanine), 171.32 (CO-CH_2-guanine), 174.72 (COOH), 184 (CO-isobutiryl).

Fmoc Ser(OH)-G(iBu)-OH (11 D)

Yield **:** 100%

Mass analysis: m/z (ESI), $[M+H]^+$ calculated: 634.9 ; found: 635.2

^{1}H NMR (DMSO-d_6)**:** 1.08 (6H, d, CH_3-isobutiryl), 2.70 (3H, m, CH-$(CH_3)_2$, CH_2- CH-$(CH_3)_2$), 3.16 - 3.33 (2H, m, CH-CH_2-N, rotamer B), 3.37- 3.49 (2H, m, CH-CH_2-N, rotamer A), 3.57 (2H, m, CH-CH_2-O, rotamer B), 3.67 (2H, m, CH-CH_2-O, rotamer A), 3.67 (1H, m, NH-CH-CH_2, rotamer B), 3.90 (1H, m, NH-CH-CH_2, rotamer A), 3.98-4.07 (2H, d, N-CH_2-COOH), 4.20- 4.33 (3H, m, CH-Fmoc, CH_2-Fmoc), 4.95 (2H, bs, CO-CH_2-guanine, rotamer B), 5.12-5.21 (2H, d, CO-CH_2-guanine, rotamer A), 7.12 (1H, d, NH-CH-CH_2 rotamer B), 7.24-7.90 (8H, m, Fmoc), 7.43 (1H, d, NH-CH-CH_2 rotamer A) , 7.89 (1H, d, H(8)-guanine)

^{13}C NMR (DMSO): 22.89 (CH_3- isobutiryl), 38.70 (CH-$(CH_3)_2$- isobutiryl), 47.99 (CH-Fmoc), 50.69 (CO-CH_2-guanine), 52.02 (NH-CH_2-COOH), 53.55 (CH-CH_2-N), 56.06 (NH-CH-CH_2), 69.59 (CH_2-Fmoc), 70.35 (CH-CH_2-O), 123.30 (C(5)-guanine), 129.14, 131.03, 131.63 (Fmoc), 144.72 (C_q-Fmoc), 147.81 (C(8)-guanine), 151.95 (C(2)-guanine), 153.22 (C(4)-guanine),

158.76 (CO-Fmoc), 162.42 (CO-C(6)-guanine), 170.73 (CO-CH_2-guanine), 174.26 (CH-CH_2-COOH), 184.06 (CO- isobutiryl).

Fmoc Ser(OSO_3)-G(iBu)-OH (12 D)

Yield **:** 100%

Mass analysis: m/z (ESI), $[M+H]^+$ calculated: 714.9 ; found : 713.9

^{1}H NMR (DMSO-d_6): 1.08 (6H, d, CH_3-isobutiryl), 2.74 (3H, m, CH-$(CH_3)_2$, CH_2- CH-$(CH_3)_2$), 3.21 -3.47 (2H, m, CH-CH_2-N, rotamer B), 3.39 -3.69 (2H, m, CH-CH_2-N, rotamer A),3.71 (2H, m, CH-CH_2-O, rotamer B), 3.85 (1H, m, NH-CH-CH_2, rotamer B),3.87 (2H, m, CH-CH_2-O, rotamer A), 3.96-4.02 (2H, d, N-CH_2-COOH), 4.04 (1H, m, NH-CH-CH_2, rotamer A), 4.22- 4.33 (3H, m, CH-Fmoc, CH_2-Fmoc), 4.95 (2H, d, CO-CH_2-guanine, rotamer B),5.14-5.22 (2H, d, CO-CH_2-guanine, rotamer A), 7.25-7.89 (8H, m, Fmoc), 7.32 (1H, d, NH-CH-CH_2 rotamer B), 7.53 (1H, d, NH-CH-CH_2 rotamer A), 7.92 (1H, d, H(8)-guanine) .

4.4.2. Solid phase conditions for coupling of PNA7 S monomers

Fmoc Ser(OSO_3)-T-OH: 50 µL of a 0.3M solution (7.9 eq.) in an. DMF of monomer, 50 µL of HBTU (0.2M) (5.2 eq.) in DMF, 50 µL MDCH (0.8M) in pyridine, 30 minutes.

Fmoc Ser(OSO_3)-C (Bz)-OH, Fmoc Ser(OSO_3)-A (Bz)-OH, Fmoc Ser(OSO_3)-G (iBu)-OH: 50 µL of a 0.3M solution (7.9 eq.) in an. DMF of monomer, 50 µL of HBTU (0.2M) (5.2 eq.) in DMF, NMM 0.2M, 50 µL of pyridine 0.2M in DMF , 30 minutes.

4.4.3. Solid phase synthesis of PNA7 , PNA7 S and PNA7 OH

Oligomers were obtained by solid phase synthesis on the Fmoc-PAL-PEG-PS resin (0.19 mmol/g) using a 2 μmol scale. The synthesis is carried out by repetitive cycles of deprotection, coupling and capping.

Deprotection: 20% piperidine in DMF, 7 minutes

Capping: Acetic anhydride 5%, 2,6 lutidine 6% in DMF, 5 minutes.

Coupling for PNA7 S and PNA7 OH:

Fmoc-C(Bhoc)-OH: 50 μL of a monomer 0.2M solution in an. DMF (5 eq.), 50 μL of HATU 0.18M in DMF (4 eq.), and 50 μL of DIPEA(0.2 M)/ 2,6 lutidine (0.3M) in DMF 30 minutes.

Fmoc Ser(OSO_3)-(T)OH (12 A) and Fmoc Ser(OtBu)-(T)OH (10 A): 50 μL of a monomer 0.3M solution (7.9 eq.) in an. DMF, 50 μL of HBTU (0.2M) (5.2 eq.) in DMF, 50 μL MDCH (0.8M) in pyridine, 30 minutes. Modified monomers are always double coupled.

Coupling for PNA 7: the protocol described in chapter 2 followed.

At the end of the synthesis the oligomer is cleaved off the resin and deprotected by treatment with TFA/m-cresol 80/20, 90 min. , r.t.. The TFA is concentrated and the PNA is precipitated with cold diethyl ether. The sample is lyophilized and purified by RP-HPLC using a gradient of acetonitrile (0.1% TFA) in H_2O (0.1% TFA) from 5 to 25% in 30 minutes.

ESI analysis for PNA7 S: calculated: $[M+H]^+$= 2694.44 m/z ; $[M + 2H]^{2+}$ = 1348.2 m/z, $[M + 3H]^{3+}$= 899.1 m/z

found: $[M + 2H]^{2+}$ = 1346.35 m/z, $[M + 3H]^{3+}$ = 897.15 m/z

ESI analysis for <u>PNA7</u>: calculated: $[M+H]^{+}$= 2323.26 m/z; $[M + 2H]^{2+}$ = 1162.63 m/z; $[M + 3H]^{3+}$ = 775.42 m/z

found: $[M + 2H]^{2+}$ = 1163.9 m/z; $[M + 3H]^{3+}$ = 775.96 m/z

ESI analysis for <u>PNA7 OH</u>: calculated: $[M+H]^{+}$= 2415.44 m/z; $[M + 2H]^{2+}$ = 1208.22 m/z; $[M + 3H]^{3+}$ = 805.74; ; $[M + 4H]^{4+}$= 604.61 m/z; ; $[M + 5H]^{5+}$= 483.88

found: $[M + 3H]^{3+}$ = 804.28 m/z; $[M + 4H]^{4+}$ = 603.20 m/z; $[M + 5H]^{5+}$= 483.90

~~4.4.4.~~ <u>NMR spectroscopy</u>

The 2D spectra were acquired using the TPPI (time-proportional phase-incrementation) method to obtain complex data points in the t_1 dimension. A standard set of 2D experiments DQF-COSY,[26] TOCSY[27] and NOESY[25] were acquired at 25°C[142a]. The TOCSY experiments were recorded using a MLEV17 mixing scheme of 70 ms with 9 kHz spin-lock field strength; the NOESY spectra were carried out with a mixing time of 150 ms. Chemical shifts were referenced to external TMS (tetramethylsylane) (δ=0 ppm). For data processing and spectral analysis the programs VNMR 6.1B and CARA were used (Bartels C et al 1995). All samples were purified by HPLC before analysis.

4.4.5. *Determination of the stoichiometry of the complex by Job Plot*

Concentrations of the single strands was determined by UV at 260nm, using for S-PNA and PNA ε = 64.5 $Lmol^{-1}cm^{-1}$ and for DNA ε = 101.6 $Lmol^{-1}cm^{-1}$.

3 μM solutions of PNA7 S, PNA7 and DNAc in Phosphate buffer 10mM, 100mM NaCl, pH = 7 were prepared. Solutions at different molar fraction of PNA7 S (or PNA7) and DNAc were prepared, keeping constant the (PNA7 S or PNA 7 + DNA) total concentrations .

Samples were annealed, warming up at 90°C and slowly cooling down to 4°C. UV spectra were recorded on a Jasco spectrophotometer at 25°C. Plotting the molar fraction (X) of PNA7 S or PNA7 vs the Absorbance at 260nm, a minimum around 0.7 X PNA7 is found, which indicates the stoichiometry of the complexes is (PNA7 S and PNA) 2: DNAc 1. The experiment was performed in duplicate.

4.4.6. *CD analyses*

CD spectra were recorded at 5°C in the 320-200 nm range and are the results of 6 scans. Single strands and triplexes were dissolved in Phosphate buffer 10mM, 100mM NaCl, 5mM $MgCl_2$ pH = 7. Triplexes were annealed by warming up at 90°C and slowly cooling down to 4°C.

Thermic denaturation experiments were carried out using 3 μM triplexes at a 0.5°C/min scan speed, recording at 225 nm for PNA7 S and PNA7 and at 266 nm for DNA triplexes.

4.4.7. Biological Assays

Cell culture.

SKBR3 cells (ATCC, U.S.) were grown in DMEM supplemented with 10% fetal bovin serum (FBS), 1% glutamine, 100 U/mL penicillin and 100 μg/mL streptomycin (Invitrogen, U.S.), at 37 °C and 5% CO_2.

Citotoxicity assay.

For the evaluation of the cytotoxic effect of compounds, the exponentially growing cells were seeded at a density of 5.0 $x10^3$/well in 96-well flat bottom tissue culture microplates, and incubated with 1, 5 and 10 μM of PNA7 S at 37°C for 72 hours. Cell number was evaluated with crystal violet, which correlates optical density with cell number, according to the procedure described by Gilles et al.

SKBR3 Binding Assay by Fluorescence Activated Cell Sorting (FACS).

$7.5x10^4$ cells/well were plated in 24-well plates, allowed to adhere for 24 h, and then transfected using Lipofectamine LTX (Invitrogen, CA, U.S.) according to the manufacturer's instruction, with PNA7 S or PNA7. After 48 h, cells were incubated with 10 nM Herceptin (kindly provided by Dr. S. De Luca , IBB, CNR Italy), then washed with PBS 1X, 0.1% BSA and incubated with a 1:1000 dilution of primary antibody (mouse anti-human, clone HP6017, SIGMA, U.S.). Secondary antibody (goat anti-mouse FITC-conjugate, Santa Cruz, CA, U.S.) was used at 1:200 dilution. Subsequently cells were detached, resuspended in PBS 1X, 0.1% BSA and analyzed by flow cytometer, equipped with a 488 nm argon laser (FACScalibur Becton Dickinson, U.S.).

For each sample 20.000 events were acquired and analyzed using Cell Quest software.

RT-PCR and qPCR.

Total RNA was extracted from lysates of transfected cells by using Tri-reagent™ (Sigma Aldrich, U.S.) according to the manufacturer's instructions. Reverse transcription was performed using 0.5 μg of total RNA, 200 U of MMLV (Finnzymes, Finland) and 250 ng of random primers (Fermentas, Germany). Reaction temperature was set at 42 °C for 1 h. The reaction buffer was: 50 mM Tris HCl pH 8.3; 75 mM KCl; 3 mM $MgCl_2$; 5 mM DTT.

After reverse transcription, qPCR assay was carried out using the following primers, GAPDH: forward primer, 5'-ATGGGGAAGGTGAAGGTC-3', reverse primer 5'-GTCATGGATGACCTTGGC-3' (purchased by Sigma-Genosys Ltd); ErbB2: forward primer, 5'-GGGAAGAATGGGGTCGTCAAA-3', reverse primer 5'-CTCCTCCCTGGGGTGTCAAGT-3'.

The amplification reactions were run at least in triplicate. Reactions were performed in Rotor-gene Q (Qiagen) and contained 2 μL cDNA, 3 μL of primers (final primer concentration of 10 μM each), and 10 μL of SYBR Premix Ex Taq II (Takara, Japan), in a final volume of 25 μL. The qPCR protocol was as follows: 2 minutes at 95 °C followed by 45 cycles of 1 minute at 95 °C, 1 min at 60 °C and 1 min at 72 °C.

REFERENCES

1. Kim, V. N., Small RNAs: classification, biogenesis, and function. *Mol Cells* **2005,** *19* (1), 1-15.

2. Orphanides, G.; Reinberg, D., A unified theory of gene expression. *Cell* **2002,** *108* (4), 439-51.

3. Maniatis, T.; Reed, R., An extensive network of coupling among gene expression machines. *Nature* **2002,** *416* (6880), 499-506.

4. Harbison, C. T.; Gordon, D. B.; Lee, T. I.; Rinaldi, N. J.; Macisaac, K. D.; Danford, T. W.; Hannett, N. M.; Tagne, J. B.; Reynolds, D. B.; Yoo, J.; Jennings, E. G.; Zeitlinger, J.; Pokholok, D. K.; Kellis, M.; Rolfe, P. A.; Takusagawa, K. T.; Lander, E. S.; Gifford, D. K.; Fraenkel, E.; Young, R. A., Transcriptional regulatory code of a eukaryotic genome. *Nature* **2004,** *431* (7004), 99-104.

5. Brockmann, R.; Beyer, A.; Heinisch, J. J.; Wilhelm, T., Posttranscriptional expression regulation: what determines translation rates? *PLoS Comput Biol* **2007,** *3* (3), e57.

6. Mata, J.; Marguerat, S.; Bahler, J., Post-transcriptional control of gene expression: a genome-wide perspective. *Trends Biochem Sci* **2005,** *30* (9), 506-14.

7. Day, D. A.; Tuite, M. F., Post-transcriptional gene regulatory mechanisms in eukaryotes: an overview. *J Endocrinol* **1998,** *157* (3), 361-71.

8. (a) Dreyfuss, G.; Kim, V. N.; Kataoka, N., Messenger-RNA-binding proteins and the messages they carry. *Nat Rev Mol Cell Biol* **2002,** *3* (3), 195-205; (b) Moore, M. J., From birth to death: the complex lives of eukaryotic mRNAs. *Science* **2005,** *309* (5740), 1514-8.

9. St Johnston, D., Moving messages: the intracellular localization of mRNAs. *Nat Rev Mol Cell Biol* **2005,** *6* (5), 363-75.

10. Gebauer, F.; Hentze, M. W., Molecular mechanisms of translational control. *Nat Rev Mol Cell Biol* **2004,** *5* (10), 827-35.

11. Parker, R.; Song, H., The enzymes and control of eukaryotic mRNA turnover. *Nat Struct Mol Biol* **2004,** *11* (2), 121-7.

12. Keene, J. D., RNA regulons: coordination of post-transcriptional events. *Nat Rev Genet* **2007,** *8* (7), 533-43.

13. Djuranovic, S.; Nahvi, A.; Green, R., A parsimonious model for gene regulation by miRNAs. *Science* **2011,** *331* (6017), 550-3.

14. Grewal, S. I.; Elgin, S. C., Transcription and RNA interference in the formation of heterochromatin. *Nature* **2007,** *447* (7143), 399-406.

15. Farazi, T. A.; Juranek, S. A.; Tuschl, T., The growing catalog of small RNAs and their association with distinct Argonaute/Piwi family members. *Development* **2008,** *135* (7), 1201-14.

16. Jinek, M.; Doudna, J. A., A three-dimensional view of the molecular machinery of RNA interference. *Nature* **2009,** *457* (7228), 405-12.

17. (a) Brennecke, J.; Aravin, A. A.; Stark, A.; Dus, M.; Kellis, M.; Sachidanandam, R.; Hannon, G. J., Discrete small RNA-generating loci as master regulators of transposon activity in Drosophila. *Cell* **2007,** *128* (6), 1089-103; (b) Gunawardane, L. S.; Saito, K.; Nishida, K. M.; Miyoshi, K.; Kawamura, Y.; Nagami, T.; Siomi, H.; Siomi, M. C., A slicer-mediated mechanism for repeat-associated siRNA 5' end formation in Drosophila. *Science* **2007,** *315* (5818), 1587-90.

18. Bartel, D. P., MicroRNAs: target recognition and regulatory functions. *Cell* **2009,** *136* (2), 215-33.

19. Bartel, D. P.; Chen, C. Z., Micromanagers of gene expression: the potentially widespread influence of metazoan microRNAs. *Nat Rev Genet* **2004,** *5* (5), 396-400.

20. Carthew, R. W.; Sontheimer, E. J., Origins and Mechanisms of miRNAs and siRNAs. *Cell* **2009,** *136* (4), 642-55.

21. Baek, D.; Villen, J.; Shin, C.; Camargo, F. D.; Gygi, S. P.; Bartel, D. P., The impact of microRNAs on protein output. *Nature* **2008,** *455* (7209), 64-71.

22. (a) Lee, R. C.; Feinbaum, R. L.; Ambros, V., The C. elegans heterochronic gene lin-4 encodes small RNAs with antisense

complementarity to lin-14. *Cell* **1993,** *75* (5), 843-54; (b) Wightman, B.; Ha, I.; Ruvkun, G., Posttranscriptional regulation of the heterochronic gene lin-14 by lin-4 mediates temporal pattern formation in C. elegans. *Cell* **1993,** *75* (5), 855-62.

23. Pasquinelli, A. E.; Reinhart, B. J.; Slack, F.; Martindale, M. Q.; Kuroda, M. I.; Maller, B.; Hayward, D. C.; Ball, E. E.; Degnan, B.; Muller, P.; Spring, J.; Srinivasan, A.; Fishman, M.; Finnerty, J.; Corbo, J.; Levine, M.; Leahy, P.; Davidson, E.; Ruvkun, G., Conservation of the sequence and temporal expression of let-7 heterochronic regulatory RNA. *Nature* **2000,** *408* (6808), 86-9.

24. (a) Lai, E. C.; Tomancak, P.; Williams, R. W.; Rubin, G. M., Computational identification of Drosophila microRNA genes. *Genome Biol* **2003,** *4* (7), R42; (b) Lim, L. P.; Lau, N. C.; Weinstein, E. G.; Abdelhakim, A.; Yekta, S.; Rhoades, M. W.; Burge, C. B.; Bartel, D. P., The microRNAs of Caenorhabditis elegans. *Genes Dev* **2003,** *17* (8), 991-1008.

25. Sharp, P. A., RNA interference--2001. *Genes Dev* **2001,** *15* (5), 485-90.

26. Lim, L. P.; Glasner, M. E.; Yekta, S.; Burge, C. B.; Bartel, D. P., Vertebrate microRNA genes. *Science* **2003,** *299* (5612), 1540.

27. Grosshans, H.; Slack, F. J., Micro-RNAs: small is plentiful. *J Cell Biol* **2002,** *156* (1), 17-21.

28. Kim, V. N., MicroRNA biogenesis: coordinated cropping and dicing. *Nat Rev Mol Cell Biol* **2005,** *6* (5), 376-85.

29. Reinhart, B. J.; Slack, F. J.; Basson, M.; Pasquinelli, A. E.; Bettinger, J. C.; Rougvie, A. E.; Horvitz, H. R.; Ruvkun, G., The 21-nucleotide let-7 RNA regulates developmental timing in Caenorhabditis elegans. *Nature* **2000,** *403* (6772), 901-6.

30. Chen, C. Z.; Li, L.; Lodish, H. F.; Bartel, D. P., MicroRNAs modulate hematopoietic lineage differentiation. *Science* **2004,** *303* (5654), 83-6.

31. Yekta, S.; Shih, I. H.; Bartel, D. P., MicroRNA-directed cleavage of HOXB8 mRNA. *Science* **2004,** *304* (5670), 594-6.

32. Brennecke, J.; Hipfner, D. R.; Stark, A.; Russell, R. B.; Cohen, S. M., bantam encodes a developmentally regulated microRNA that controls cell

proliferation and regulates the proapoptotic gene hid in Drosophila. *Cell* **2003,** *113* (1), 25-36.

33. Johnston, R. J.; Hobert, O., A microRNA controlling left/right neuronal asymmetry in Caenorhabditis elegans. *Nature* **2003,** *426* (6968), 845-9.

34. Poy, M. N.; Eliasson, L.; Krutzfeldt, J.; Kuwajima, S.; Ma, X.; Macdonald, P. E.; Pfeffer, S.; Tuschl, T.; Rajewsky, N.; Rorsman, P.; Stoffel, M., A pancreatic islet-specific microRNA regulates insulin secretion. *Nature* **2004,** *432* (7014), 226-30.

35. Esau, C.; Kang, X.; Peralta, E.; Hanson, E.; Marcusson, E. G.; Ravichandran, L. V.; Sun, Y.; Koo, S.; Perera, R. J.; Jain, R.; Dean, N. M.; Freier, S. M.; Bennett, C. F.; Lollo, B.; Griffey, R., MicroRNA-143 regulates adipocyte differentiation. *J Biol Chem* **2004,** *279* (50), 52361-5.

36. Hornstein, E.; Mansfield, J. H.; Yekta, S.; Hu, J. K.; Harfe, B. D.; McManus, M. T.; Baskerville, S.; Bartel, D. P.; Tabin, C. J., The microRNA miR-196 acts upstream of Hoxb8 and Shh in limb development. *Nature* **2005,** *438* (7068), 671-4.

37. Zhao, Y.; Samal, E.; Srivastava, D., Serum response factor regulates a muscle-specific microRNA that targets Hand2 during cardiogenesis. *Nature* **2005,** *436* (7048), 214-20.

38. Cullen, B. R., Viral and cellular messenger RNA targets of viral microRNAs. *Nature* **2009,** *457* (7228), 421-5.

39. Pfeffer, S.; Zavolan, M.; Grasser, F. A.; Chien, M.; Russo, J. J.; Ju, J.; John, B.; Enright, A. J.; Marks, D.; Sander, C.; Tuschl, T., Identification of virus-encoded microRNAs. *Science* **2004,** *304* (5671), 734-6.

40. Cai, X.; Lu, S.; Zhang, Z.; Gonzalez, C. M.; Damania, B.; Cullen, B. R., Kaposi's sarcoma-associated herpesvirus expresses an array of viral microRNAs in latently infected cells. *Proc Natl Acad Sci U S A* **2005,** *102* (15), 5570-5.

41. Calin, G. A.; Dumitru, C. D.; Shimizu, M.; Bichi, R.; Zupo, S.; Noch, E.; Aldler, H.; Rattan, S.; Keating, M.; Rai, K.; Rassenti, L.; Kipps, T.; Negrini, M.; Bullrich, F.; Croce, C. M., Frequent deletions and down-regulation of micro-RNA genes miR15 and miR16 at 13q14 in chronic lymphocytic leukemia. *Proc Natl Acad Sci U S A* **2002,** *99* (24), 15524-9.

42. Cimmino, A.; Calin, G. A.; Fabbri, M.; Iorio, M. V.; Ferracin, M.; Shimizu, M.; Wojcik, S. E.; Aqeilan, R. I.; Zupo, S.; Dono, M.; Rassenti, L.; Alder, H.; Volinia, S.; Liu, C. G.; Kipps, T. J.; Negrini, M.; Croce, C. M., miR-15 and miR-16 induce apoptosis by targeting BCL2. *Proc Natl Acad Sci U S A* **2005,** *102* (39), 13944-9.

43. Michael, M. Z.; SM, O. C.; van Holst Pellekaan, N. G.; Young, G. P.; James, R. J., Reduced accumulation of specific microRNAs in colorectal neoplasia. *Mol Cancer Res* **2003,** *1* (12), 882-91.

44. Braasch, D. A.; Corey, D. R., Novel antisense and peptide nucleic acid strategies for controlling gene expression. *Biochemistry-Us* **2002,** *41* (14), 4503-10.

45. Zeng, Y.; Wagner, E. J.; Cullen, B. R., Both natural and designed micro RNAs can inhibit the expression of cognate mRNAs when expressed in human cells. *Mol Cell* **2002,** *9* (6), 1327-33.

46. Chan, J. A.; Krichevsky, A. M.; Kosik, K. S., MicroRNA-21 is an antiapoptotic factor in human glioblastoma cells. *Cancer Res* **2005,** *65* (14), 6029-33.

47. (a) Krutzfeldt, J.; Rajewsky, N.; Braich, R.; Rajeev, K. G.; Tuschl, T.; Manoharan, M.; Stoffel, M., Silencing of microRNAs in vivo with 'antagomirs'. *Nature* **2005,** *438* (7068), 685-9; (b) Krutzfeldt, J.; Kuwajima, S.; Braich, R.; Rajeev, K. G.; Pena, J.; Tuschl, T.; Manoharan, M.; Stoffel, M., Specificity, duplex degradation and subcellular localization of antagomirs. *Nucleic Acids Res* **2007,** *35* (9), 2885-92.

48. Sohail, M.; Southern, E. M., Selecting optimal antisense reagents. *Adv Drug Deliv Rev* **2000,** *44* (1), 23-34.

49. (a) Eckstein, F., Phosphorothioate oligodeoxynucleotides: what is their origin and what is unique about them? *Antisense Nucleic Acid Drug Dev* **2000,** *10* (2), 117-21; (b) Geary, R. S.; Yu, R. Z.; Levin, A. A., Pharmacokinetics of phosphorothioate antisense oligodeoxynucleotides. *Curr Opin Investig Drugs* **2001,** *2* (4), 562-73; (c) Friedman, K. J.; Kole, J.; Cohn, J. A.; Knowles, M. R.; Silverman, L. M.; Kole, R., Correction of aberrant splicing of the cystic fibrosis transmembrane conductance regulator (CFTR) gene by antisense oligonucleotides. *J Biol Chem* **1999,** *274* (51), 36193-9.

50. Friedman, K. J.; Silverman, L. M., Cystic fibrosis syndrome: a new paradigm for inherited disorders and implications for molecular diagnostics. *Clin Chem* **1999,** *45* (7), 929-31.

51. Hutvagner, G.; Simard, M. J.; Mello, C. C.; Zamore, P. D., Sequence-specific inhibition of small RNA function. *PLoS Biol* **2004,** *2* (4), E98.

52. Karras, J. G.; McKay, R. A.; Dean, N. M.; Monia, B. P., Deletion of individual exons and induction of soluble murine interleukin-5 receptor-alpha chain expression through antisense oligonucleotide-mediated redirection of pre-mRNA splicing. *Mol Pharmacol* **2000,** *58* (2), 380-7.

53. Kumar, R.; Singh, S. K.; Koshkin, A. A.; Rajwanshi, V. K.; Meldgaard, M.; Wengel, J., The first analogues of LNA (locked nucleic acids): phosphorothioate-LNA and 2'-thio-LNA. *Bioorg Med Chem Lett* **1998,** *8* (16), 2219-22.

54. Naguibneva, I.; Ameyar-Zazoua, M.; Nonne, N.; Polesskaya, A.; Ait-Si-Ali, S.; Groisman, R.; Souidi, M.; Pritchard, L. L.; Harel-Bellan, A., An LNA-based loss-of-function assay for micro-RNAs. *Biomed Pharmacother* **2006,** *60* (9), 633-8.

55. Ahn, D. G.; Kourakis, M. J.; Rohde, L. A.; Silver, L. M.; Ho, R. K., T-box gene tbx5 is essential for formation of the pectoral limb bud. *Nature* **2002,** *417* (6890), 754-8.

56. Suwanmanee, T.; Sierakowska, H.; Fucharoen, S.; Kole, R., Repair of a splicing defect in erythroid cells from patients with beta-thalassemia/HbE disorder. *Mol Ther* **2002,** *6* (6), 718-26.

57. Kloosterman, W. P.; Lagendijk, A. K.; Ketting, R. F.; Moulton, J. D.; Plasterk, R. H., Targeted inhibition of miRNA maturation with morpholinos reveals a role for miR-375 in pancreatic islet development. *PLoS Biol* **2007,** *5* (8), e203.

58. Nielsen, P. E.; Egholm, M.; Buchardt, O., Peptide nucleic acid (PNA). A DNA mimic with a peptide backbone. *Bioconjug Chem* **1994,** *5* (1), 3-7.

59. Wu, H.; Lima, W. F.; Zhang, H.; Fan, A.; Sun, H.; Crooke, S. T., Determination of the role of the human RNase H1 in the pharmacology of DNA-like antisense drugs. *J Biol Chem* **2004,** *279* (17), 17181-9.

60. Lee, Y. S.; Kim, H. K.; Chung, S.; Kim, K. S.; Dutta, A., Depletion of human micro-RNA miR-125b reveals that it is critical for the proliferation of differentiated cells but not for the down-regulation of putative targets during differentiation. *J Biol Chem* **2005,** *280* (17), 16635-41.

61. Tian, T.; Xu, Y.; Dai, J.; Wu, J.; Shen, H.; Hu, Z., Functional polymorphisms in two pre-microRNAs and cancer risk: a meta-analysis. *Int J Mol Epidemiol Genet* **2010,** *1* (4), 358-66.

62. Hoffman, A. E.; Zheng, T.; Yi, C.; Leaderer, D.; Weidhaas, J.; Slack, F.; Zhang, Y.; Paranjape, T.; Zhu, Y., microRNA miR-196a-2 and breast cancer: a genetic and epigenetic association study and functional analysis. *Cancer Res* **2009,** *69* (14), 5970-7.

63. Jazdzewski, K.; Murray, E. L.; Franssila, K.; Jarzab, B.; Schoenberg, D. R.; de la Chapelle, A., Common SNP in pre-miR-146a decreases mature miR expression and predisposes to papillary thyroid carcinoma. *Proc Natl Acad Sci U S A* **2008,** *105* (20), 7269-74.

64. Hutvagner, G.; McLachlan, J.; Pasquinelli, A. E.; Balint, E.; Tuschl, T.; Zamore, P. D., A cellular function for the RNA-interference enzyme Dicer in the maturation of the let-7 small temporal RNA. *Science* **2001,** *293* (5531), 834-8.

65. Nielsen, P. E.; Egholm, M.; Berg, R. H.; Buchardt, O., Sequence-selective recognition of DNA by strand displacement with a thymine-substituted polyamide. *Science* **1991,** *254* (5037), 1497-500.

66. Jensen, K. K.; Orum, H.; Nielsen, P. E.; Norden, B., Kinetics for hybridization of peptide nucleic acids (PNA) with DNA and RNA studied with the BIAcore technique. *Biochemistry* **1997,** *36* (16), 5072-7.

67. Ray, A.; Norden, B., Peptide nucleic acid (PNA): its medical and biotechnical applications and promise for the future. *Faseb J* **2000,** *14* (9), 1041-60.

68. Christensen, L.; Fitzpatrick, R.; Gildea, B.; Petersen, K. H.; Hansen, H. F.; Koch, T.; Egholm, M.; Buchardt, O.; Nielsen, P. E.; Coull, J.; et al., Solid-phase synthesis of peptide nucleic acids. *J Pept Sci* **1995,** *1* (3), 175-83.

69. Karras, J. G.; Maier, M. A.; Lu, T.; Watt, A.; Manoharan, M., Peptide nucleic acids are potent modulators of endogenous pre-mRNA splicing of the

murine interleukin-5 receptor-alpha chain. *Biochemistry-Us* **2001,** *40* (26), 7853-9.

70. Mologni, L.; Marchesi, E.; Nielsen, P. E.; Gambacorti-Passerini, C., Inhibition of promyelocytic leukemia (PML)/retinoic acid receptor-alpha and PML expression in acute promyelocytic leukemia cells by anti-PML peptide nucleic acid. *Cancer Res* **2001,** *61* (14), 5468-73.

71. (a) Abes, S.; Turner, J. J.; Ivanova, G. D.; Owen, D.; Williams, D.; Arzumanov, A.; Clair, P.; Gait, M. J.; Lebleu, B., Efficient splicing correction by PNA conjugation to an R6-Penetratin delivery peptide. *Nucleic Acids Res* **2007,** *35* (13), 4495-502; (b) Fabani, M. M.; Gait, M. J., miR-122 targeting with LNA/2'-O-methyl oligonucleotide mixmers, peptide nucleic acids (PNA), and PNA-peptide conjugates. *Rna* **2008,** *14* (2), 336-46; (c) Turner, J. J.; Ivanova, G. D.; Verbeure, B.; Williams, D.; Arzumanov, A. A.; Abes, S.; Lebleu, B.; Gait, M. J., Cell-penetrating peptide conjugates of peptide nucleic acids (PNA) as inhibitors of HIV-1 Tat-dependent trans-activation in cells. *Nucleic Acids Res* **2005,** *33* (21), 6837-49.

72. Nielsen, P. E., Peptide nucleic acids: on the road to new gene therapeutic drugs. *Pharmacol Toxicol* **2000,** *86* (1), 3-7.

73. Bentin, T.; Nielsen, P. E., Enhanced peptide nucleic acid binding to supercoiled DNA: possible implications for DNA "breathing" dynamics. *Biochemistry-Us* **1996,** *35* (27), 8863-9.

74. Cutrona, G.; Carpaneto, E. M.; Ulivi, M.; Roncella, S.; Landt, O.; Ferrarini, M.; Boffa, L. C., Effects in live cells of a c-myc anti-gene PNA linked to a nuclear localization signal. *Nat Biotechnol* **2000,** *18* (3), 300-3.

75. Gambari, R., New trends in the development of transcription factor decoy (TFD) pharmacotherapy. *Curr Drug Targets* **2004,** *5* (5), 419-30.

76. Hyrup, B.; Nielsen, P. E., Peptide nucleic acids (PNA): synthesis, properties and potential applications. *Bioorg Med Chem* **1996,** *4* (1), 5-23.

77. Koppelhus, U.; Nielsen, P. E., Cellular delivery of peptide nucleic acid (PNA). *Adv Drug Deliv Rev* **2003,** *55* (2), 267-80.

78. (a) Bergan, R.; Connell, Y.; Fahmy, B.; Neckers, L., Electroporation enhances c-myc antisense oligodeoxynucleotide efficacy. *Nucleic Acids Res* **1993,** *21* (15), 3567-73; (b) Nastruzzi, C.; Cortesi, R.; Esposito, E.; Gambari,

R.; Borgatti, M.; Bianchi, N.; Feriotto, G.; Mischiati, C., Liposomes as carriers for DNA-PNA hybrids. *J Control Release* **2000,** *68* (2), 237-49.

79. Fisher, T. L.; Terhorst, T.; Cao, X.; Wagner, R. W., Intracellular disposition and metabolism of fluorescently-labeled unmodified and modified oligonucleotides microinjected into mammalian cells. *Nucleic Acids Res* **1993,** *21* (16), 3857-65.

80. Lebedeva, I.; Benimetskaya, L.; Stein, C. A.; Vilenchik, M., Cellular delivery of antisense oligonucleotides. *Eur J Pharm Biopharm* **2000,** *50* (1), 101-19.

81. Veldhoen, S.; Laufer, S. D.; Restle, T., Recent developments in peptide-based nucleic acid delivery. *Int J Mol Sci* **2008,** *9* (7), 1276-320.

82. Derossi, D.; Chassaing, G.; Prochiantz, A., Trojan peptides: the penetratin system for intracellular delivery. *Trends Cell Biol* **1998,** *8* (2), 84-7.

83. Vives, E.; Brodin, P.; Lebleu, B., A truncated HIV-1 Tat protein basic domain rapidly translocates through the plasma membrane and accumulates in the cell nucleus. *J Biol Chem* **1997,** *272* (25), 16010-7.

84. Derossi, D.; Calvet, S.; Trembleau, A.; Brunissen, A.; Chassaing, G.; Prochiantz, A., Cell internalization of the third helix of the Antennapedia homeodomain is receptor-independent. *J Biol Chem* **1996,** *271* (30), 18188-93.

85. Derossi, D.; Joliot, A. H.; Chassaing, G.; Prochiantz, A., The third helix of the Antennapedia homeodomain translocates through biological membranes. *J Biol Chem* **1994,** *269* (14), 10444-50.

86. Pooga, M.; Hallbrink, M.; Zorko, M.; Langel, U., Cell penetration by transportan. *Faseb J* **1998,** *12* (1), 67-77.

87. Aldrian-Herrada, G.; Desarmenien, M. G.; Orcel, H.; Boissin-Agasse, L.; Mery, J.; Brugidou, J.; Rabie, A., A peptide nucleic acid (PNA) is more rapidly internalized in cultured neurons when coupled to a retro-inverso delivery peptide. The antisense activity depresses the target mRNA and protein in magnocellular oxytocin neurons. *Nucleic Acids Res* **1998,** *26* (21), 4910-6.

88. Blobel, G., Unidirectional and bidirectional protein traffic across membranes. *Cold Spring Harb Symp Quant Biol* **1995,** *60*, 1-10.

89. (a) Cartier, R.; Reszka, R., Utilization of synthetic peptides containing nuclear localization signals for nonviral gene transfer systems. *Gene Ther* **2002,** *9* (3), 157-67; (b) Macadangdang, B.; Zhang, N.; Lund, P. E.; Marple, A. H.; Okabe, M.; Gottesman, M. M.; Appella, D. H.; Kimchi-Sarfaty, C., Inhibition of multidrug resistance by SV40 pseudovirion delivery of an antigene peptide nucleic acid (PNA) in cultured cells. *PLoS One* **2011,** *6* (3), e17981.

90. Braun, K.; Peschke, P.; Pipkorn, R.; Lampel, S.; Wachsmuth, M.; Waldeck, W.; Friedrich, E.; Debus, J., A biological transporter for the delivery of peptide nucleic acids (PNAs) to the nuclear compartment of living cells. *J Mol Biol* **2002,** *318* (2), 237-43.

91. (a) Wojciechowski, F.; Hudson, R. H., A convenient route to N-[2-(Fmoc)aminoethyl]glycine esters and PNA oligomerization using a Bis-N-Boc nucleobase protecting group strategy. *J Org Chem* **2008,** *73* (10), 3807-16; (b) Debaene, F.; Winssinger, N., Azidopeptide nucleic acid. An alternative strategy for solid-phase peptide nucleic acid (PNA) synthesis. *Org Lett* **2003,** *5* (23), 4445-7; (c) Musumeci, D.; Roviello, G. N.; Valente, M.; Sapio, R.; Pedone, C.; Bucci, E. M., New synthesis of PNA-3'DNA linker monomers, useful building blocks to obtain PNA/DNA chimeras. *Biopolymers* **2004,** *76* (6), 535-42.

92. Husken, N.; Gasser, G.; Koster, S. D.; Metzler-Nolte, N., "Four-potential" ferrocene labeling of PNA oligomers via click chemistry. *Bioconjug Chem* **2009,** *20* (8), 1578-86.

93. (a) Gogoi, K.; Mane, M. V.; Kunte, S. S.; Kumar, V. A., A versatile method for the preparation of conjugates of peptides with DNA/PNA/analog by employing chemo-selective click reaction in water. *Nucleic Acids Res* **2007,** *35* (21), e139; (b) Vernille, J. P.; Kovell, L. C.; Schneider, J. W., Peptide nucleic acid (PNA) amphiphiles: synthesis, self-assembly, and duplex stability. *Bioconjug Chem* **2004,** *15* (6), 1314-21.

94. Le Chevalier Isaad, A.; Papini, A. M.; Chorev, M.; Rovero, P., Side chain-to-side chain cyclization by click reaction. *J Pept Sci* **2009,** *15* (7), 451-4.

95. Chan, S. Y.; Loscalzo, J., MicroRNA-210: a unique and pleiotropic hypoxamir. *Cell Cycle* **2010,** *9* (6), 1072-83.

96. (a) Hu, S.; Huang, M.; Li, Z.; Jia, F.; Ghosh, Z.; Lijkwan, M. A.; Fasanaro, P.; Sun, N.; Wang, X.; Martelli, F.; Robbins, R. C.; Wu, J. C., MicroRNA-210 as a novel therapy for treatment of ischemic heart disease. *Circulation* **2010,** *122* (11 Suppl), S124-31; (b) Fasanaro, P.; D'Alessandra, Y.; Di Stefano, V.; Melchionna, R.; Romani, S.; Pompilio, G.; Capogrossi, M. C.; Martelli, F., MicroRNA-210 modulates endothelial cell response to hypoxia and inhibits the receptor tyrosine kinase ligand Ephrin-A3. *J Biol Chem* **2008,** *283* (23), 15878-83; (c) Kulshreshtha, R.; Ferracin, M.; Wojcik, S. E.; Garzon, R.; Alder, H.; Agosto-Perez, F. J.; Davuluri, R.; Liu, C. G.; Croce, C. M.; Negrini, M.; Calin, G. A.; Ivan, M., A microRNA signature of hypoxia. *Mol Cell Biol* **2007,** *27* (5), 1859-67.

97. (a) Camps, C.; Buffa, F. M.; Colella, S.; Moore, J.; Sotiriou, C.; Sheldon, H.; Harris, A. L.; Gleadle, J. M.; Ragoussis, J., hsa-miR-210 Is induced by hypoxia and is an independent prognostic factor in breast cancer. *Clin Cancer Res* **2008,** *14* (5), 1340-8; (b) Zhang, Z.; Sun, H.; Dai, H.; Walsh, R. M.; Imakura, M.; Schelter, J.; Burchard, J.; Dai, X.; Chang, A. N.; Diaz, R. L.; Marszalek, J. R.; Bartz, S. R.; Carleton, M.; Cleary, M. A.; Linsley, P. S.; Grandori, C., MicroRNA miR-210 modulates cellular response to hypoxia through the MYC antagonist MNT. *Cell Cycle* **2009,** *8* (17), 2756-68.

98. Huang, X.; Ding, L.; Bennewith, K. L.; Tong, R. T.; Welford, S. M.; Ang, K. K.; Story, M.; Le, Q. T.; Giaccia, A. J., Hypoxia-inducible mir-210 regulates normoxic gene expression involved in tumor initiation. *Mol Cell* **2009,** *35* (6), 856-67.

99. Giannakakis, A.; Sandaltzopoulos, R.; Greshock, J.; Liang, S.; Huang, J.; Hasegawa, K.; Li, C.; O'Brien-Jenkins, A.; Katsaros, D.; Weber, B. L.; Simon, C.; Coukos, G.; Zhang, L., miR-210 links hypoxia with cell cycle regulation and is deleted in human epithelial ovarian cancer. *Cancer Biol Ther* **2008,** *7* (2), 255-64.

100. Foekens, J. A.; Sieuwerts, A. M.; Smid, M.; Look, M. P.; de Weerd, V.; Boersma, A. W.; Klijn, J. G.; Wiemer, E. A.; Martens, J. W., Four miRNAs associated with aggressiveness of lymph node-negative, estrogen receptor-positive human breast cancer. *Proc Natl Acad Sci U S A* **2008,** *105* (35), 13021-6.

101. Bianchi, N.; Zuccato, C.; Lampronti, I.; Borgatti, M.; Gambari, R., Expression of miR-210 during erythroid differentiation and induction of gamma-globin gene expression. *BMB Rep* **2009,** *42* (8), 493-9.

102. Rogers, H. M.; Yu, X.; Wen, J.; Smith, R.; Fibach, E.; Noguchi, C. T., Hypoxia alters progression of the erythroid program. *Exp Hematol* **2008,** *36* (1), 17-27.

103. Semenza, G. L., Involvement of oxygen-sensing pathways in physiologic and pathologic erythropoiesis. *Blood* **2009,** *114* (10), 2015-9.

104. Turner, J. J.; Arzumanov, A. A.; Gait, M. J., Synthesis, cellular uptake and HIV-1 Tat-dependent trans-activation inhibition activity of oligonucleotide analogues disulphide-conjugated to cell-penetrating peptides. *Nucleic Acids Res* **2005,** *33* (1), 27-42.

105. Bendifallah, N.; Rasmussen, F. W.; Zachar, V.; Ebbesen, P.; Nielsen, P. E.; Koppelhus, U., Evaluation of cell-penetrating peptides (CPPs) as vehicles for intracellular delivery of antisense peptide nucleic acid (PNA). *Bioconjug Chem* **2006,** *17* (3), 750-8.

106. Diaz-Mochon, J. J.; Bialy, L.; Watson, J.; Sanchez-Martin, R. M.; Bradley, M., Synthesis and cellular uptake of cell delivering PNA-peptide conjugates. *Chem Commun (Camb)* **2005,** (26), 3316-8.

107. Lange, A.; Mills, R. E.; Lange, C. J.; Stewart, M.; Devine, S. E.; Corbett, A. H., Classical nuclear localization signals: definition, function, and interaction with importin alpha. *J Biol Chem* **2007,** *282* (8), 5101-5.

108. (a) Tonelli, R.; Purgato, S.; Camerin, C.; Fronza, R.; Bologna, F.; Alboresi, S.; Franzoni, M.; Corradini, R.; Sforza, S.; Faccini, A.; Shohet, J. M.; Marchelli, R.; Pession, A., Anti-gene peptide nucleic acid specifically inhibits MYCN expression in human neuroblastoma cells leading to cell growth inhibition and apoptosis. *Mol Cancer Ther* **2005,** *4* (5), 779-86; (b) Bremner, K. H.; Seymour, L. W.; Logan, A.; Read, M. L., Factors influencing the ability of nuclear localization sequence peptides to enhance nonviral gene delivery. *Bioconjug Chem* **2004,** *15* (1), 152-61.

109. Kosugi, S.; Hasebe, M.; Matsumura, N.; Takashima, H.; Miyamoto-Sato, E.; Tomita, M.; Yanagawa, H., Six classes of nuclear localization signals specific to different binding grooves of importin alpha. *J Biol Chem* **2009,** *284* (1), 478-85.

110. Li, K.; Liu, B., Conjugated polyelectrolyte amplified thiazole orange emission for label free sequence specific DNA detection with single nucleotide polymorphism selectivity. *Anal Chem* **2009,** *81* (10), 4099-105.

111. Svanvik, N.; Westman, G.; Wang, D.; Kubista, M., Light-up probes: thiazole orange-conjugated peptide nucleic acid for detection of target nucleic acid in homogeneous solution. *Anal Biochem* **2000,** *281* (1), 26-35.

112. Svanvik, N.; Stahlberg, A.; Sehlstedt, U.; Sjoback, R.; Kubista, M., Detection of PCR products in real time using light-up probes. *Anal Biochem* **2000,** *287* (1), 179-82.

113. (a) Berndl, S.; Wagenknecht, H. A., Fluorescent color readout of DNA hybridization with thiazole orange as an artificial DNA base. *Angew Chem Int Ed Engl* **2009,** *48* (13), 2418-21; (b) Kummer, S.; Knoll, A.; Socher, E.; Bethge, L.; Herrmann, A.; Seitz, O., Fluorescence imaging of influenza H1N1 mRNA in living infected cells using single-chromophore FIT-PNA. *Angew Chem Int Ed Engl* **2011,** *50* (8), 1931-4.

114. Tonelli, A.; Tedeschi, T.; Germini, A.; Sforza, S.; Corradini, R.; Medici, M. C.; Chezzi, C.; Marchelli, R., Real time RNA transcription monitoring by Thiazole Orange (TO)-conjugated Peptide Nucleic Acid (PNA) probes: norovirus detection. *Mol Biosyst* **2011,** *7* (5), 1684-92.

115. Robertson, K. L.; Yu, L.; Armitage, B. A.; Lopez, A. J.; Peteanu, L. A., Fluorescent PNA probes as hybridization labels for biological RNA. *Biochemistry-Us* **2006,** *45* (19), 6066-74.

116. Mahon, K. P., Jr.; Ortiz-Meoz, R. F.; Prestwich, E. G.; Kelley, S. O., Photosensitized DNA cleavage promoted by amino acids. *Chem Commun (Camb)* **2003,** (15), 1956-7.

117. Corradini, R.; Sforza, S.; Tedeschi, T.; Totsingan, F.; Manicardi, A.; Marchelli, R., Peptide nucleic acids with a structurally biased backbone. Updated review and emerging challenges. *Curr Top Med Chem* **2011,** *11* (12), 1535-54.

118. Petraccone, L.; Pagano, B.; Esposito, V.; Randazzo, A.; Piccialli, G.; Barone, G.; Mattia, C. A.; Giancola, C., Thermodynamics and kinetics of PNA-DNA quadruplex-forming chimeras. *J Am Chem Soc* **2005,** *127* (46), 16215-23.

119. (a) Dragulescu-Andrasi, A.; Rapireddy, S.; He, G.; Bhattacharya, B.; Hyldig-Nielsen, J. J.; Zon, G.; Ly, D. H., Cell-permeable peptide nucleic acid designed to bind to the 5'-untranslated region of E-cadherin transcript induces potent and sequence-specific antisense effects. *J Am Chem Soc* **2006,**

128 (50), 16104-12; (b) Pensato, S.; Saviano, M.; Romanelli, A., New peptide nucleic acid analogues: synthesis and applications. *Expert Opin Biol Ther* **2007,** *7* (8), 1219-32.

120. Christensen, L.; Hansen, H. F.; Koch, T.; Nielsen, P. E., Inhibition of PNA triplex formation by N4-benzoylated cytosine. *Nucleic Acids Res* **1998,** *26* (11), 2735-9.

121. Lohse, J.; Dahl, O.; Nielsen, P. E., Double duplex invasion by peptide nucleic acid: a general principle for sequence-specific targeting of double-stranded DNA. *Proc Natl Acad Sci U S A* **1999,** *96* (21), 11804-8.

122. Ferrer, E.; Shevchenko, A.; Eritja, R., Synthesis and hybridization properties of DNA-PNA chimeras carrying 5-bromouracil and 5-methylcytosine. *Bioorg Med Chem* **2000,** *8* (2), 291-7.

123. Ishizuka, T.; Yoshida, J.; Yamamoto, Y.; Sumaoka, J.; Tedeschi, T.; Corradini, R.; Sforza, S.; Komiyama, M., Chiral introduction of positive charges to PNA for double-duplex invasion to versatile sequences. *Nucleic Acids Res* **2008,** *36* (5), 1464-71.

124. (a) Kumar, V. A.; Ganesh, K. N., Conformationally constrained PNA analogues: structural evolution toward DNA/RNA binding selectivity. *Acc Chem Res* **2005,** *38* (5), 404-12; (b) Mitra, R.; Ganesh, K. N., PNAs grafted with (alpha/gamma, R/S)-aminomethylene pendants: regio and stereo specific effects on DNA binding and improved cell uptake. *Chem Commun (Camb)* **2011,** *47* (4), 1198-200.

125. Tedeschi, T.; Sforza, S.; Corradini, R.; Marchelli, R., Synthesis of new chiral PNAs bearing a dipeptide-mimic monomer with two lysine-derived stereogenic centres. *Tetrahedron Letters* **2005,** *46*, 8395-8399.

126. (a) Kosynkina, L.; Wang, W.; Liang, T. C., A convenient synthesis of chiral peptide nucleic acid (PNA) monomers. *Tetrahedron Letters* **1994,** *35* (29), 5173–5176; (b) Xu, J. C.; Wu, Y., Synthesis of chiral peptide nucleic acids using Fmoc chemistry. *Tetrahedron* **2001,** *57* (38), 8107-8113; (c) de Koning, M. C.; Petersen, L.; Weterings, J. J.; Overhand, M.; van der Marel, G. A.; Filippov, D. V., Synthesis of thiol-modified peptide nucleic acids designed for post-assembly conjugation reactions. *Tetrahedron* **2006,** *62* (14), 3248-3258.

127. Tedeschi, T.; Sforza, S.; Dossena, A.; Corradini, R.; Marchelli, R., Lysine-based peptide nucleic acids (PNAs) with strong chiral constraint: control of helix handedness and DNA binding by chirality. *Chirality* **2005,** *17 Suppl*, S196-204.

128. Sforza, S.; Tedeschi, T.; Corradini, R.; Marchelli, R., Induction of helical handness and DNA binding properties of peptide Nucleic Acids (PNAs) with two stereogenic centres. *Curr Top Med Chem* **2007**, 5879-5885.

129. Sforza, S.; Tedeschi, T.; Corradini, R.; Dossena, A.; Marchelli, R., Direction control in DNA binding of chiral D-lysine-based peptide nucleic acid (PNA) probed by electrospray mass spectrometry. *Chem Commun (Camb)* **2003,** (9), 1102-3.

130. Sforza, S.; Galaverna, G.; Dossena, A.; Corradini, R.; Marchelli, R., Role of chirality and optical purity in nucleic acid recognition by PNA and PNA analogs. *Chirality* **2002,** *14* (7), 591-8.

131. (a) Englund, E. A.; Appella, D. H., Gamma-substituted peptide nucleic acids constructed from L-lysine are a versatile scaffold for multifunctional display. *Angew Chem Int Ed Engl* **2007,** *46* (9), 1414-8; (b) Pensato, S.; Saviano, M.; Bianchi, N.; Borgatti, M.; Fabbri, E.; Gambari, R.; Romanelli, A., gamma-Hydroxymethyl PNAs: Synthesis, interaction with DNA and inhibition of protein/DNA interactions. *Bioorg Chem* **2010,** *38* (5), 196-201; (c) Dragulescu-Andrasi, A.; Rapireddy, S.; Frezza, B. M.; Gayathri, C.; Gil, R. R.; Ly, D. H., A simple gamma-backbone modification preorganizes peptide nucleic acid into a helical structure. *J Am Chem Soc* **2006,** *128* (31), 10258-67; (d) Rapireddy, S.; Bahal, R.; Ly, D. H., Strand invasion of mixed-sequence, double-helical B-DNA by gamma-peptide nucleic acids containing G-clamp nucleobases under physiological conditions. *Biochemistry* **2011,** *50* (19), 3913-8.

132. Sahu, B.; Sacui, I.; Rapireddy, S.; Zanotti, K. J.; Bahal, R.; Armitage, B. A.; Ly, D. H., Synthesis and characterization of conformationally preorganized, (R)-diethylene glycol-containing gamma-peptide nucleic acids with superior hybridization properties and water solubility. *J Org Chem* **2011,** *76* (14), 5614-27.

133. (a) Dose, C.; Seitz, O., Convergent synthesis of peptide nucleic acids by native chemical ligation. *Org Lett* **2005,** *7* (20), 4365-8; (b) Englund, E. A.; Appella, D. H., Synthesis of gamma-substituted peptide nucleic acids: a new

place to attach fluorophores without affecting DNA binding. *Org Lett* **2005,** *7* (16), 3465-7.

134. Sahu, B.; Chenna, V.; Lathrop, K. L.; Thomas, S. M.; Zon, G.; Livak, K. J.; Ly, D. H., Synthesis of conformationally preorganized and cell-permeable guanidine-based gamma-peptide nucleic acids (gammaGPNAs). *J Org Chem* **2009,** *74* (4), 1509-16.

135. Crawford, M. J.; Rapireddy, S.; Bahal, R.; Sacui, I.; Ly, D. H., Effect of Steric Constraint at the gamma-Backbone Position on the Conformations and Hybridization Properties of PNAs. *J Nucleic Acids* **2011,** *2011*, 652702.

136. Yeh, J. I.; Shivachev, B.; Rapireddy, S.; Crawford, M. J.; Gil, R. R.; Du, S.; Madrid, M.; Ly, D. H., Crystal structure of chiral gammaPNA with complementary DNA strand: insights into the stability and specificity of recognition and conformational preorganization. *J Am Chem Soc* **2010,** *132* (31), 10717-27.

137. He, G.; Rapireddy, S.; Bahal, R.; Sahu, B.; Ly, D. H., Strand invasion of extended, mixed-sequence B-DNA by gammaPNAs. *J Am Chem Soc* **2009,** *131* (34), 12088-90.

138. (a) Koppelhus, U.; Nielsen, P. E., Cellular delivery of peptide nucleic acid (PNA). *Adv Drug Deliv Rev* **2003,** *55* (2), 267-80; (b) Cortesi, R.; Mischiati, C.; Borgatti, M.; Breda, L.; Romanelli, A.; Saviano, M.; Pedone, C.; Gambari, R.; Nastruzzi, C., Formulations for natural and peptide nucleic acids based on cationic polymeric submicron particles. *AAPS PharmSci* **2004,** *6* (1), E2.

139. (a) Hamilton, S. E.; Simmons, C. G.; Kathiriya, I. S.; Corey, D. R., Cellular delivery of peptide nucleic acids and inhibition of human telomerase. *Chem Biol* **1999,** *6* (6), 343-51; (b) Herbert, B.; Pitts, A. E.; Baker, S. I.; Hamilton, S. E.; Wright, W. E.; Shay, J. W.; Corey, D. R., Inhibition of human telomerase in immortal human cells leads to progressive telomere shortening and cell death. *Proc Natl Acad Sci U S A* **1999,** *96* (25), 14276-81; (c) Doyle, D. F.; Braasch, D. A.; Simmons, C. G.; Janowski, B. A.; Corey, D. R., Inhibition of gene expression inside cells by peptide nucleic acids: effect of mRNA target sequence, mismatched bases, and PNA length. *Biochemistry* **2001,** *40* (1), 53-64; (d) Borgatti, M.; Breda, L.; Cortesi, R.; Nastruzzi, C.; Romanelli, A.; Saviano, M.; Bianchi, N.; Mischiati, C.; Pedone, C.; Gambari, R., Cationic liposomes as delivery systems for double-stranded PNA-DNA chimeras

exhibiting decoy activity against NF-kappaB transcription factors. *Biochem Pharmacol* **2002,** *64* (4), 609-16.

140. (a) Finn, P. J.; Gibson, N. J.; Fallon, R.; Hamilton, A.; Brown, T., Synthesis and properties of DNA-PNA chimeric oligomers. *Nucleic Acids Res* **1996,** *24* (17), 3357-63; (b) Aldrian-Herrada, G.; Rabie, A.; Wintersteiger, R.; Brugidou, J., Solid-phase synthesis of peptide nucleic acid (PNA) monomers and their oligomerization using disulphide anchoring linkers. *J Pept Sci* **1998,** *4* (4), 266-81; (c) Timar, Z.; Kovacs, G.; Schmel, Z., Fmoc/acyl protecting groups in the synthesis of polyamide (peptide) nucleic acid monomers. *J Chem Soc Perk T 1* **2000,** (1), 19-26.

141. (a) Zhilina, Z. V.; Ziemba, A. J.; Nielsen, P. E.; Ebbinghaus, S. W., PNA-nitrogen mustard conjugates are effective suppressors of HER-2/neu and biological tools for recognition of PNA/DNA interactions. *Bioconjug Chem* **2006,** *17* (1), 214-22; (b) Vasquez Campos, S.; Miranda, L. P.; Meldal, M., Preparation of novel O-sulfated amino acid building blocks with improved acid stability for Fmoc-based solid-phase peptide synthesis. *J Chem Soc Perk T 1* **2002,** (5), 682-686.

142. (a) Rance, M.; Sorensen, O. W.; Bodenhausen, G.; Wagner, G.; Ernst, R. R.; Wuthrich, K., Improved spectral resolution in cosy 1H NMR spectra of proteins via double quantum filtering. *Biochem Biophys Res Commun* **1983,** *117* (2), 479-85; (b) Bartels, C.; Xia, T.; Billeter, M.; Gunthert, P.; Wüthrich, K., The program XEASY for computer-supported NMR spectral analysis of biological macromolecules. *J Biomol NMR* **1995,** *6*, 1-10.

143. Griesinger, C.; Otting, G.; Wüthrich, K.; Ernst, R. R., Clean TOCSY for proton spin system identification in macromolecules. *J Am Chem Soc* **1988,** *110* (23), 7870-7872.

144. Kumar, A.; Ernst, R. R.; Wuthrich, K., A two-dimensional nuclear Overhauser enhancement (2D NOE) experiment for the elucidation of complete proton-proton cross-relaxation networks in biological macromolecules. *Biochem Biophys Res Commun* **1980,** *95* (1), 1-6.

145. Roskoski, R., Jr., The ErbB/HER receptor protein-tyrosine kinases and cancer. *Biochem Biophys Res Commun* **2004,** *319* (1), 1-11.

146. Harari, D.; Yarden, Y., Molecular mechanisms underlying ErbB2/HER2 action in breast cancer. *Oncogene* **2000,** *19* (53), 6102-14.

147. Avitabile, C.; Moggio, L.; D'Andrea, L. D.; Pedone, C.; Romanelli, A., Development of an efficient and low-cost protocol for the manual PNA synthesis by Fmoc chemistry. *Tetrahedron Letters* **2010,** *51* (29), 3716-3718.

148. Betts, L.; Josey, J. A.; Veal, J. M.; Jordan, S. R., A nucleic acid triple helix formed by a peptide nucleic acid-DNA complex. *Science* **1995,** *270* (5243), 1838-41.

149. Tomac, S.; Sarkar, M.; Ratilainen, T.; Wittung, P.; Nielsen, P. E.; Norden, B.; Graslund, A., Ionic effects on the stability and conformation of peptide nucleic acid complexes. *J Am Chem Soc* **1996,** *118* (24), 5544-5552.

150. Yarden, Y.; Sliwkowski, M. X., Untangling the ErbB signalling network. *Nat Rev Mol Cell Biol* **2001,** *2* (2), 127-37.

151. (a) Armitage, B.; Koch, T.; Frydenlund, H.; Orum, H.; Batz, H. G.; Schuster, G. B., Peptide nucleic acid-anthraquinone conjugates: strand invasion and photoinduced cleavage of duplex DNA. *Nucleic Acids Res* **1997,** *25* (22), 4674-8; (b) Kaihatsu, K.; Shah, R. H.; Zhao, X.; Corey, D. R., Extending recognition by peptide nucleic acids (PNAs): binding to duplex DNA and inhibition of transcription by tail-clamp PNA-peptide conjugates. *Biochemistry* **2003,** *42* (47), 13996-4003.

152. Bentin, T.; Nielsen, P. E., Superior duplex DNA strand invasion by acridine conjugated peptide nucleic acids. *J Am Chem Soc* **2003,** *125* (21), 6378-9.

153. (a) Roviello, G. N.; Musumeci, D.; De Cristofaro, A.; Capasso, D.; Di Gaetano, S.; Bucci, E. M.; Pedone, C., Alternate dab-aegPNAs: synthesis, nucleic acid binding studies and biological activity. *Mol Biosyst* **2010,** *6* (1), 199-205; (b) Shiraishi, T.; Hamzavi, R.; Nielsen, P. E., Subnanomolar antisense activity of phosphonate-peptide nucleic acid (PNA) conjugates delivered by cationic lipids to HeLa cells. *Nucleic Acids Res* **2008,** *36* (13), 4424-32.